

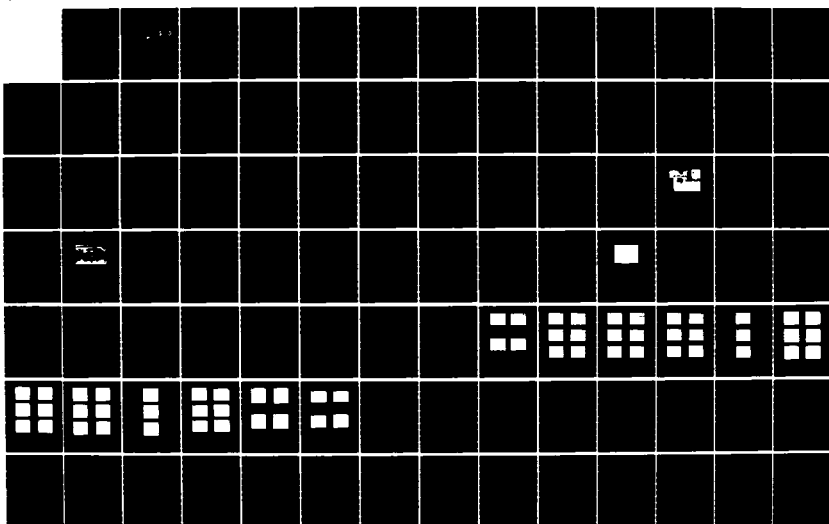
AD-R165 589

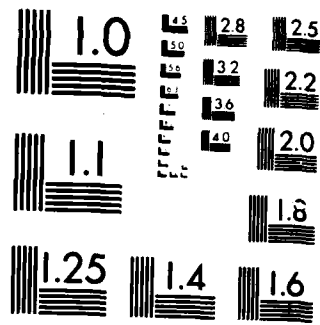
ELECTRON INDUCED CONDUCTIVITY OF AL203 RS PERTAINING TO 1/2
THERMIONIC INTEGRATED CIRCUITS(U) NAVAL POSTGRADUATE
SCHOOL MONTEREY CA P J PETERSON DEC 85

UNCLASSIFIED

F/G 9/5

NL





MICROCOPY RESOLUTION TEST CHART
NATIONAL BUREAU OF STANDARDS 1963-A

(2)

NAVAL POSTGRADUATE SCHOOL

Monterey, California

AD-A165 589



DTIC
ELECTED
MAR 24 1986
S D
D

THESIS

ELECTRON INDUCED CONDUCTIVITY OF Al₂O₃
AS PERTAINING TO THERMIONIC INTEGRATED CIRCUITS

by

Peter J. Peterson

December 1985

Thesis Advisor:

F. R. Buskirk

Approved for public release; distribution is unlimited.

DTIC FILE COPY
2013

86 3 21 027

UNCLASSIFIED

SECURITY CLASSIFICATION OF THIS PAGE

AIA-5509

REPORT DOCUMENTATION PAGE

1a. REPORT SECURITY CLASSIFICATION UNCLASSIFIED		1b. RESTRICTIVE MARKINGS	
2a. SECURITY CLASSIFICATION AUTHORITY		3. DISTRIBUTION/AVAILABILITY OF REPORT Approved for public release; distribution is unlimited.	
2b. DECLASSIFICATION/DOWNGRADING SCHEDULE			
4 PERFORMING ORGANIZATION REPORT NUMBER(S)		5. MONITORING ORGANIZATION REPORT NUMBER(S)	
6a. NAME OF PERFORMING ORGANIZATION Naval Postgraduate School	6b. OFFICE SYMBOL (if applicable) Code 54	7a. NAME OF MONITORING ORGANIZATION Naval Postgraduate School	
6c. ADDRESS (City, State, and ZIP Code) Monterey, California 93943-5100		7b. ADDRESS (City, State, and ZIP Code) Monterey, California 93943-5100	
8a. NAME OF FUNDING/SPONSORING ORGANIZATION	8b. OFFICE SYMBOL (if applicable)	9. PROCUREMENT INSTRUMENT IDENTIFICATION NUMBER	
8c. ADDRESS (City, State, and ZIP Code)		10. SOURCE OF FUNDING NUMBERS	
		PROGRAM ELEMENT NO	PROJECT NO
		TASK NO	WORK UNIT ACCESSION NO.
11. TITLE (Include Security Classification) ELECTRON INDUCED CONDUCTIVITY OF Al_2O_3 AS PERTAINING TO THERMIONIC INTEGRATED CIRCUITS			
12. PERSONAL AUTHOR(S) Peterson, Peter J.			
13a. TYPE OF REPORT Master's Thesis	13b. TIME COVERED FROM _____ TO _____	14. DATE OF REPORT (Year, Month, Day) 1985 December	15. PAGE COUNT 109
16. SUPPLEMENTARY NOTATION			
17. COSATI CODES		18. SUBJECT TERMS (Continue on reverse if necessary and identify by block number) Thermionic Integrated Circuit (TIC); Electron Induced Conductivity (EIC); Aluminum Oxide (Al_2O_3); Radiation Induced Conductivity (RIC)	
19. ABSTRACT (Continue on reverse if necessary and identify by block number) Experiments were conducted to measure the electron induced conductivity (EIC) of single crystal sapphire (Al_2O_3) and poly-crystalline alumina (Al_2O_3). The EIC is generated when the samples are bombarded with high energy electrons, utilizing the Naval Postgraduate School's S-Band Linear Accelerator (LINAC). The EIC was measured at dose rates up to 6×10^6 rad (Si)/sec. The EIC for alumina was an order of magnitude smaller than the value for sapphire. The value calculated for alumina was 10^{-4} ($\Omega\text{-cm}$) $^{-1}$ and 10^{-3} ($\Omega\text{-cm}$) $^{-1}$ for sapphire. The response of EIC to a given dose rate did not change as the dose accumulated. Surface flashover problems during electron irradiation were observed and are discussed.			
20. DISTRIBUTION/AVAILABILITY OF ABSTRACT <input checked="" type="checkbox"/> UNCLASSIFIED/UNLIMITED <input type="checkbox"/> SAME AS RPT. <input type="checkbox"/> DTIC USERS		21. ABSTRACT SECURITY CLASSIFICATION Unclassified	
22a. NAME OF RESPONSIBLE INDIVIDUAL F. R. Buskirk		22b. TELEPHONE (Include Area Code) (408) 646-2765	22c. OFFICE SYMBOL 61 Bs

Approved for public release; distribution is unlimited.

Electron Induced Conductivity of Al₂O₃ as pertaining to
Thermionic Integrated Circuits

by

Peter J. Peterson
Lieutenant, United States Navy
B.S., UW River Falls, 1973

Submitted in partial fulfillment of the
requirements for the degree of

MASTER OF SCIENCE IN PHYSICS

from the

NAVAL POSTGRADUATE SCHOOL
December 1985

Author: Peter J. Peterson
Peter J. Peterson

Approved by: Fred R Buskirk
F. R. Buskirk, Thesis Advisor

J. R. Neighbours
J. R. Neighbours, Second Reader

G. E. Schacher
G. E. Schacher, Chairman,
Department of Physics

J. N. Dyer
J. N. Dyer,
Dean of Science and Engineering

ABSTRACT

Experiments were conducted to measure the electron induced conductivity (EIC) of single crystal sapphire (Al_2O_3) and poly-crystalline alumina (Al_2O_3). The EIC is generated when the samples are bombarded with high energy electrons, utilizing the Naval Postgraduate School's S-band linear accelerator (LINAC). The EIC was measured at dose rates up to 6×10^7 rad (Si)/sec. The EIC for alumina was an order of magnitude smaller than the value for sapphire. The value calculated for alumina was 10^{-4} ($\Omega\text{-cm}$) $^{-1}$ and 10^{-3} ($\Omega\text{-cm}$) $^{-1}$ for sapphire. The response of EIC to a given dose rate did not change as the dose accumulated. Surface flashover problems during electron irradiation were observed and are discussed.

10/10/85

Accession For	
NTIS	CRA&I <input checked="" type="checkbox"/>
DTIC	TAB <input type="checkbox"/>
Unannounced <input type="checkbox"/>	
Justification	
By	
Distribution /	
Availability Codes	
Dist	Avail and/or Special
A-1	



TABLE OF CONTENTS

I.	INTRODUCTION	7
	A. OVERVIEW	7
II.	THEORY	11
	A. GENERAL MECHANISMS	11
	1. Energy Levels in Crystalline Insulators	11
	2. Traps	13
	3. Recombination Centers	14
	B. ELECTRON INTERACTION WITH MATTER	15
	1. Collision Stopping Power	17
	2. Radiative Stopping Power	22
	3. Dose Measurement	23
	C. RADIATION EFFECTS OF ELECTRONS IN INSULATORS	24
	1. Displacement Damage	25
	2. Ionization	28
	3. Pair Production	30
	4. Electron Excitation	30
	D. CONDUCTIVITY	31
	1. Electrical Conductivity of Al_2O_3	31
	2. Electron Induced Conductivity (EIC) of Al_2O_3	32
III.	EXPERIMENT	35
	A. SAMPLE FABRICATION	35

B. PRE-IRRADIATION AND POST-IRRADIATION MEASUREMENTS	36
C. NPS LINAC	36
D. TEST PROCEDURE	40
IV. DATA AND RESULTS	44
A. STEADY STATE RESISTIVITY AND CONDUCTIVITY	44
B. TRANSIENT EIC	49
C. DOSE RATE CALCULATIONS	51
V. DISCUSSION OF RESULTS	55
VI. CONCLUSIONS	59
APPENDIX A: EIC PHOTOGRAPHS	61
APPENDIX B: EQUIPMENT LIST	74
APPENDIX C: INPUT PROGRAM FOR ELECTRON PHOTON TRANSPORT ACCEPT CODE - CYLTRAN	75
LIST OF REFERENCES	106
INITIAL DISTRIBUTION LIST	108

ACKNOWLEDGEMENT

I wish to thank my thesis co-advisors, Professor F. R. Buskirk and Professor J. R. Neighbours for their patience, encouragement, insight and willing assistance.

Thanks are also extended to Don Snyder for his expertise and invaluable help at the LINAC control station.

A special gratification to Dr. Dave Lynn and his co-workers at Los Alamos National Laboratory for providing the EIC samples used in the research and for all of their valuable time and assistance.

I. INTRODUCTION

A. OVERVIEW

Today the United States with its sophisticated weaponry, complex electronic components and internetting communication systems is dependent upon the semiconductor integrated circuit. These electronic systems must be able to perform in hostile radiation environments both natural and man-made. Typical radiation sources include natural space environments, interplanetary and planetary environments for space probes, the cosmic ray environments, nuclear reactor environments and the nuclear weapons environment. Unfortunately semiconductor devices in these high radiation environments have shown an increasing susceptibility to failure. Currently a great deal of money, time and manpower is being utilized to find ways to harden these devices. Hardening is the process of making a device less susceptible to radiation damage and signal upset, thereby increasing system reliability. The penalty inherent in manufacturing high density microcircuits is a decrease in the radiation hardness of the integrated circuit. A new device is needed that can be used in a high radiation environment in conjunction with semiconductors. This new device will require medium to low power requirements, minaturization and speed equivalent to a semiconductor. A

device that has demonstrated great potential to meet the above requirements is the thermionic integrated circuit (TIC). The TIC is a new technology being developed by D. Lynn and J. McCormick et al. at Los Alamos National Laboratory [Ref. 1]. Initial tests show TIC devices are orders of magnitude more resistant to total radiation dose than other integrated circuits. Experimentation on the response of these devices to single event upset is required.

The TIC device is a combination of vacuum tube and integrated circuit technology. A typical single TIC device, a triode, is shown in Fig. 1.1 [Ref. 1]. The device is similar to a standard triode in which the cathode emits electrons, the anode collects electrons and the grid provides gain by modulating electron flow. The cathode, anode and heater are photolithographically delineated onto either alumina (Al_2O_3) or sapphire (Al_2O_3) substrates.

In any high energy radiation environment, the Al_2O_3 will be exposed to ionizing radiation. Ionizing radiation generates electron-hole pairs inside the Al_2O_3 , creating radiation induced conductivity (RIC). RIC is transient conductivity with pulse times in the nanosecond to microsecond range. Only the high energy thermalized electrons contribute to the RIC since low energy electrons are trapped in approximately 10^{-9} to 10^{-10} sec. High energy electrons that pass through TICs deposit their energy by ionization and displacement damage. Displacement damage

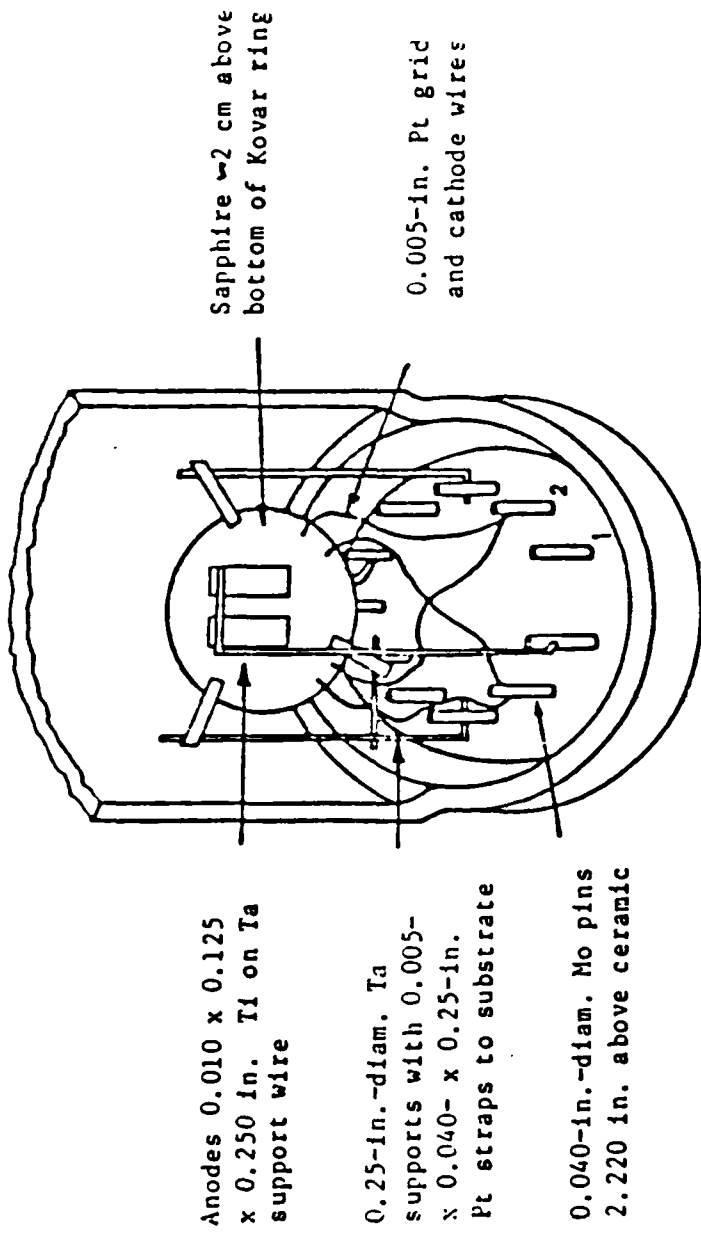


Fig. 1.1. Radiation test triode package configuration. Pin connections during test: 1--not used; 2--cathode through $1\text{ k}\Omega$; 3--shield through $1\text{ k}\Omega$; 4--not used; 5--heater Ground; 6--heater +33 V; 7--not used; 8--not used; 9--shield pin floating; 10--grid through $1\text{ k}\Omega$; 11--anode to +60 V.

usually degrades the device by significantly decreasing carrier concentration, carrier lifetime and carrier mobility.

To simulate high intensity ionizing radiation, the Naval Postgraduate School's S-band 100 MeV electron linear accelerator (LINAC) was used. This thesis will discuss the electron induced conductivity (EIC) of high intensity ionizing radiation utilizing 30 and 100 MeV thermalized electrons on single crystal sapphire and poly-crystalline alumina (Al_2O_3).

II. THEORY

A. GENERAL MECHANISMS

1. Energy Levels in Crystalline Insulators

A crystalline insulator is a solid that is built up from its constituent atoms, ions and molecules. These elementary building blocks are packed together in a three-dimensional array called a crystal. Cohesive forces bind the atoms, ions and molecules of the crystal causing the electron energy levels associated with the isolated components to be modified and bunched into bands. The behavior of the energy bands in the crystalline structure determine the fundamental electronic properties of the material. The energy bands may form gaps as shown in Fig. 2.1. The valence band is filled with electrons, the conduction band is unoccupied and they are separated by the energy gap E_g . The size of the energy gap determines the electronic properties of the material. In insulating materials, E_g generally ranges from 5eV to 10eV. The single crystalline sapphire Al_2O_3 and polycrystalline alumina Al_2O_3 , used in this thesis have energy gaps of 9eV.

Energy bands in a crystalline insulator are modified by the existence of lattice irregularities. The irregularities give rise to localized energy levels lying between the conduction band and valance band. The

CONDUCTION

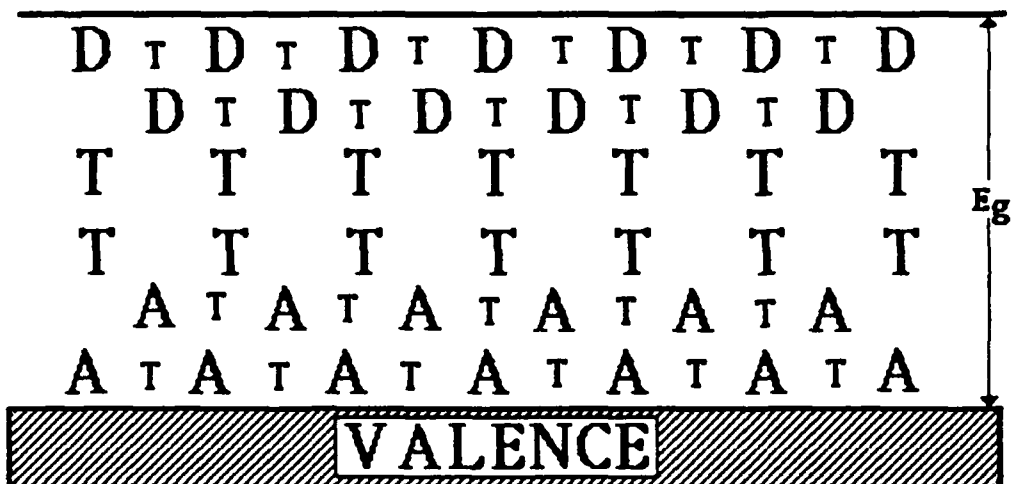


Figure 2.1. Band structure in a crystalline insulator. There is a well defined energy gap E_g between the filled valence band and the empty conduction band. Lattice imperfections and impurities that are localized states act as traps, shown as T in the energy gap. Impurities such as dislocations and point defects give rise to donor levels shown as D and acceptors shown as A.

irregularities include impurity atoms, stoichiometric excesses, of one or more of the species of atoms, and deformation of the lattice.

In Fig. 2.1, T depicts localized energy states, called traps, that capture pseudo-free carriers. Impurities such as dislocations and point defects give rise to donor levels, D, and acceptor levels, A.

. Traps

Traps are localized energy states which are capable of capturing charge carriers temporarily. These charge carriers are then thermally emitted into the appropriate band thereby generating recombination. Levy has shown that undoped samples of Al_2O_3 have 3 distinct absorption bands (trapping sites) at energy levels of 6.2eV, 5.45eV, and 4.82eV. After irradiation, the samples show 8 more distinct trapping sites [Ref. 2]. The presence of traps reduces conductivity and response time.

The rate of trapping is given by Eq. (2.1) [Ref. 3]:

$$D = N[1-f(E)]V\sigma n \quad (2.1)$$

where,

n free electron density in the conduction band

v thermal velocity

σ ≡ trapping cross section

N ≡ trap density

f(E) ≡ Fermi probability function

The product, $V\sigma$ is the volume swept out per unit time by a particle of cross section σ [Ref. 3]. The electron is trapped if the localized state lies within the volume swept out by $V\sigma$. The value of σ may change if a large electric field (on the order of 10^4 - 10^5 V/cm) is applied. This is called the Poole-Frenkel effect.

The process, in which the initial bombarding electron strikes a lattice atom, is known as the primary collision. The target atom of the lattice is known as the primary knock-on atom. The energy required to displace an atom from its lattice site is called the "threshold energy", E_d . If an atom receives an energy less than E_d , the probability the atom will be displaced is zero. If an atom receives energy greater than E_d , the atom will be displaced. Seitz and Koehler have determined that an E_d of 25eV is required to displace an atom in a solid [Ref. 4]. Arnold and Compton have determined that the minimum threshold energy is 50eV for Al and 90eV for O [Ref. 5].

3. Recombination Centers

Recombination centers are localized impurities or radiation induced lattice deformations located in an otherwise perfect crystalline insulator. These impurities give rise to trapping sites which trap and hold one type of

charge carrier. The carrier remains in the trapping site until the opposite carrier enters the trapping site, causing annihilation. Shallow traps are localized states close to the edges of the valence and conduction bands. Recombination centers are deep energy states in the middle of the energy band gap.

B. ELECTRON INTERACTION WITH MATTER

Electrons interact with matter by elastic scattering with a nucleus, inelastic scattering with atomic electrons and production of secondary knock-on atoms.

As a result of the collision between the high energy electron and the nucleus of the lattice atom, the incident electron imparts some of its energy to the lattice atom. The recoiling atom interacts with surrounding atoms, transferring energy to the rest of the lattice. If the energy of the primary recoiling atom is low, the result is a heating of the crystal lattice. As the energy transferred to the recoil atom increases, a threshold energy E_d is reached. Above E_d the recoil atom is removed from the lattice site to an interstitial site. The movement of the atom from the lattice creates a vacancy. This is referred to as a displacement.

During inelastic Coulomb scattering, high energy electrons interact with the nucleus or atomic electrons of the target atoms. Interaction with the atomic electrons

changes the direction of the bombarding electron causing radiation. Radiation caused by an energy loss of the incident electron is called bremsstrahlung radiation. Bremsstrahlung radiation is given off when an electron slows down as it passes through material.

Secondary knock-on atoms are generated by recoiling atoms with energies greater than 50eV. These atoms interact with the surrounding atoms causing a cascading effect.

Stopping power, as defined by Enge, "is the amount of energy lost by a particle per unit length of path through the stopping material" [Ref. 6]. For electrons, Berger and Seltzer have separated total stopping power into two categories: 1)Collision stopping power and 2)Radiative stopping power. Radiative and collision stopping power both slow electrons.

Collision stopping power is the mechanism which creates ionization energy. Ionization energy is absorbed in the material close to the path of the electron beam. The radiative energy lost due to bremsstrahlung is deposited far from the track of the electron beam. In thin samples, such as the substrates of Al_2O_3 , radiative energy loss is not deposited into the material. Collision stopping power causes the energy deposition which is the damage mechanism of importance to this thesis. Therefore, only the collision stopping power will be considered.

The computer simulations of 30 and 100 MeV electron beams incident on a thin cylindrical target of Al₂O₃, were performed using a Cray computer at the Los Alamos National Laboratory. The Cyltran code used is one of the Integrated Tiger Series codes for Coupled Electron /Photon Monte Carlo Transport. Figures 2.2-2.5 illustrate the results of the modeling in graphic form. The angular distribution graphs, Figures 2.2-2.3, show that the overwhelming majority of electrons emerging from the material are at angles between 0 and 18 degrees. The incident electrons shows little deflection as they pass through the material.

The transmitted energy spectrum graphs, Figures 2.4-2.5, show that the majority of electrons leaving the material are at energies between 27-30 or 90-100 MeV. Only a small percentage of the total energy is lost from the beam. Therefore, the Cyltran code confirms that the Al₂O₃ substrate is a thin sample.

1. Collision Stopping Power

The formulas used for collision stopping power in this section are a refinement of Bethe and Heitlers stopping and scattering power theory. The electron mass collision stopping power is given by the formula developed by Rohrlich, Carlson, and Uehling:

$$\frac{1}{\rho} \frac{dE}{dx} \text{ col} = \frac{2\pi N r_e^2 m c^2 Z}{\beta^2 A} \left[\ln\left(\frac{T}{I}\right)^2 + \ln\left(1+\frac{\tau}{2}\right) + F(\tau) - \delta \right] \quad (2.2)$$

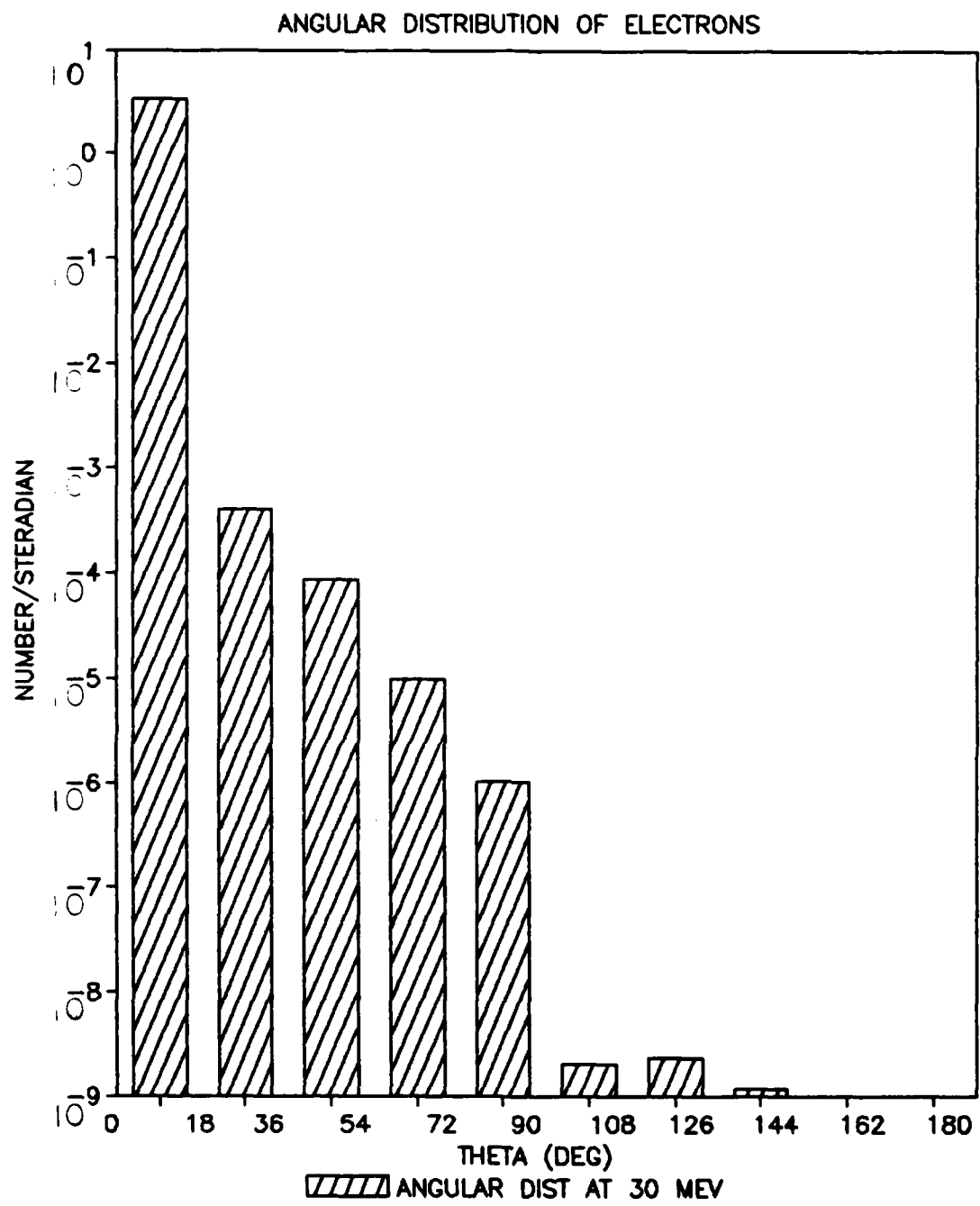


Figure 2.2. Computer simulation of angular distributions of transmitted and reflected electrons normalized to one incident 30 MeV electron.

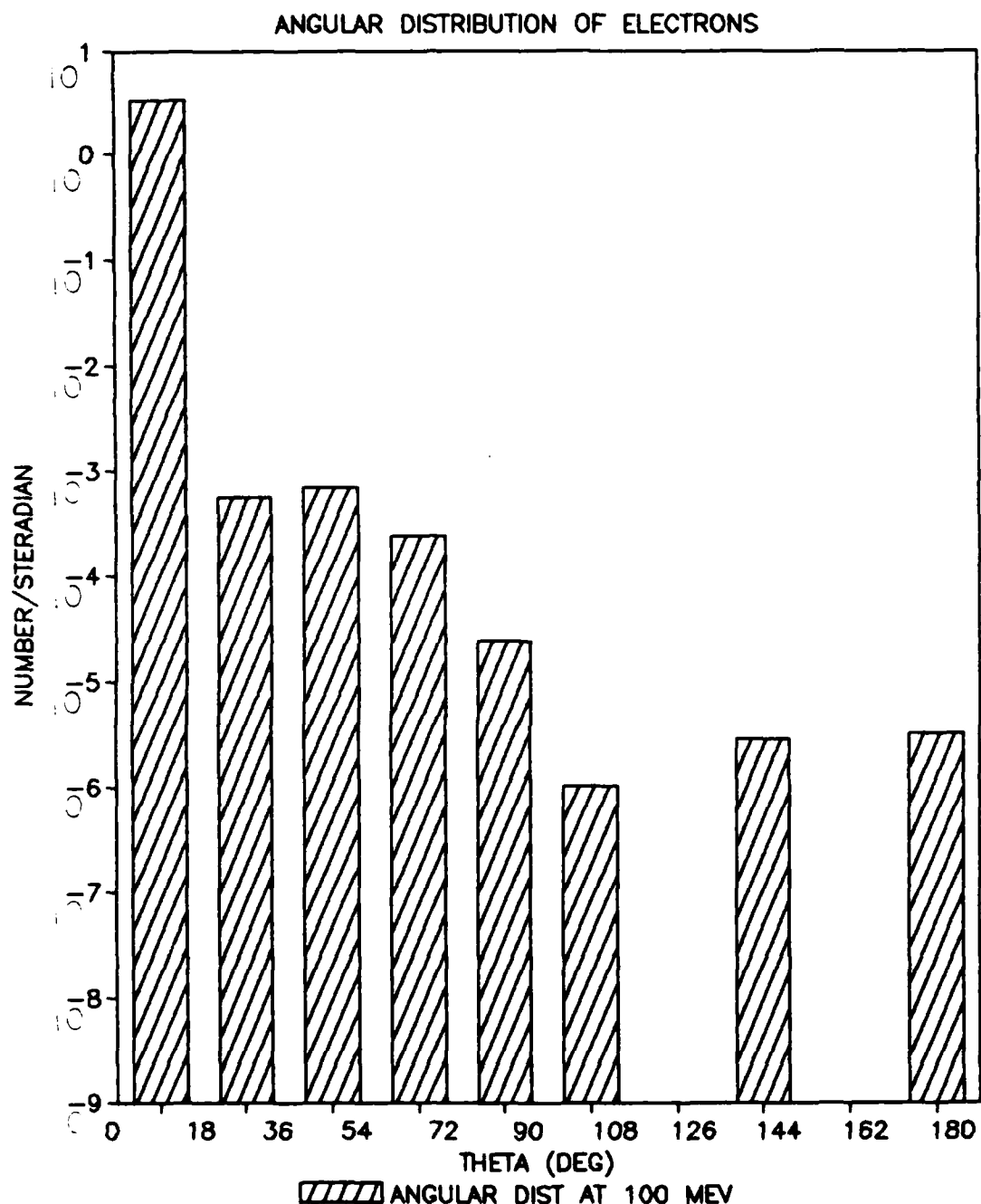


Figure 2.3. Computer simulation of angular distributions of transmitted and reflected electrons normalized to one incident 100 MeV electron.

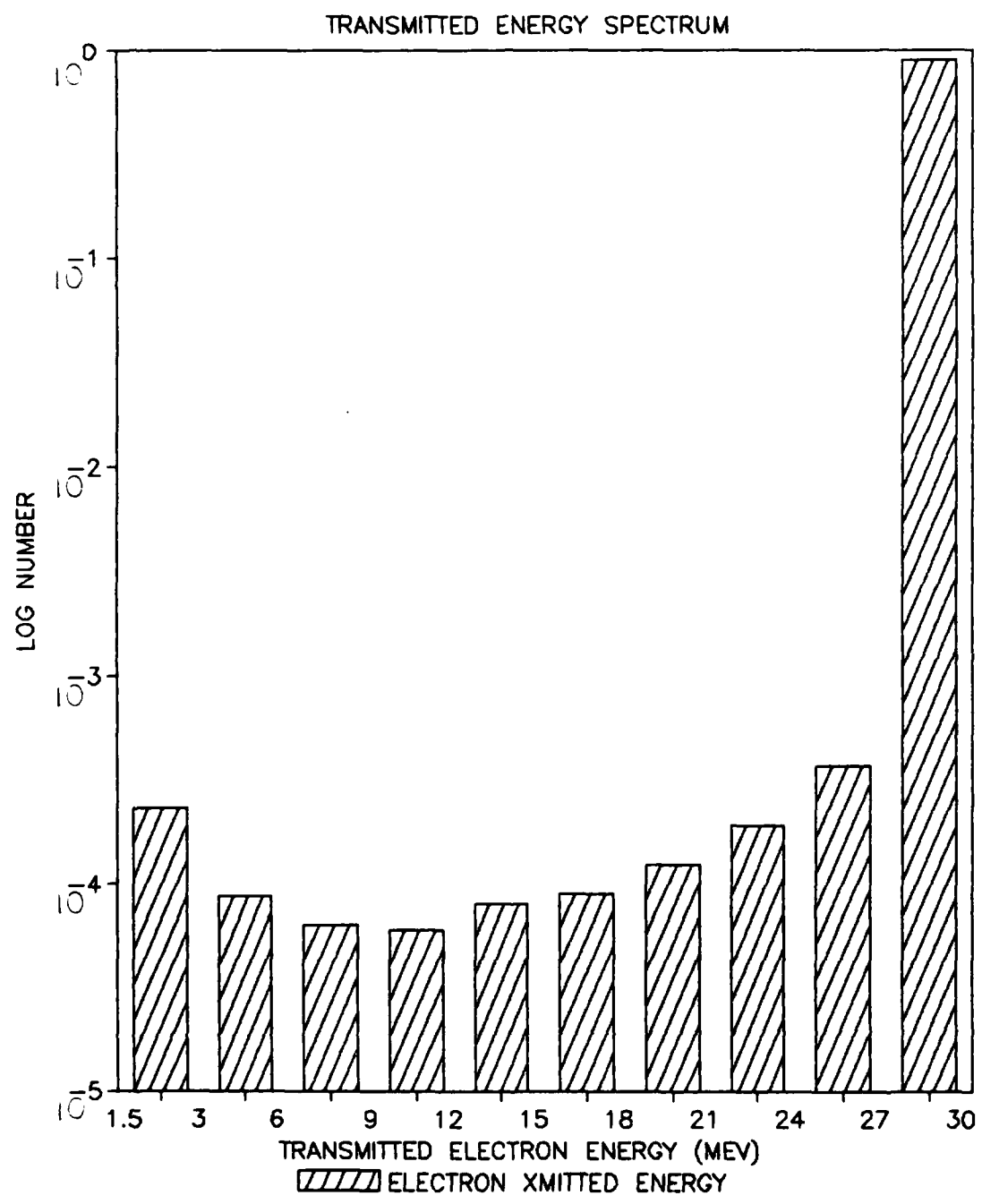


Figure 2.4. Computer simulation of the energy spectra for transmitted electrons normalized to one incident 30 MeV electron.

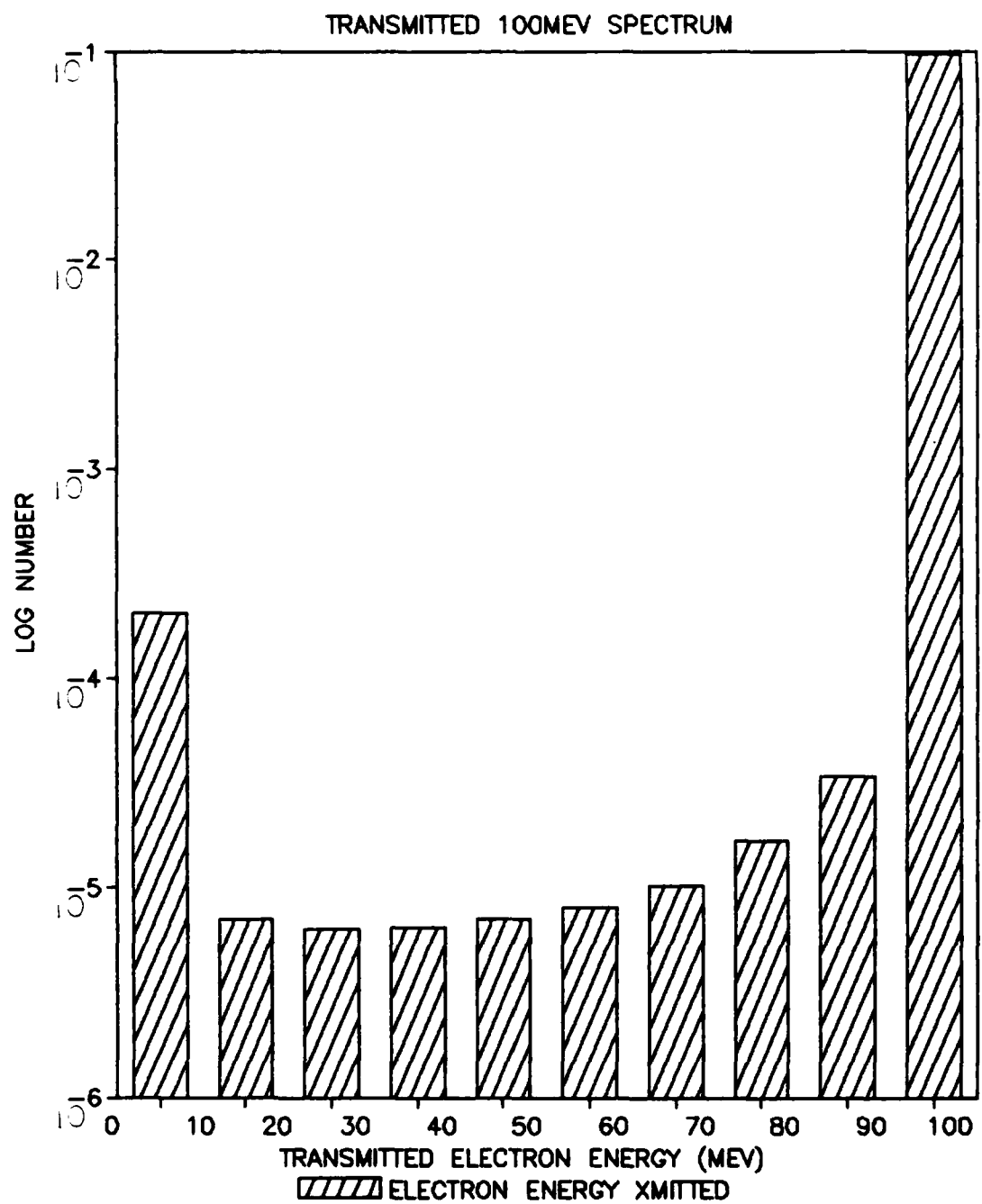


Figure 2.5. Computer simulation of the energy spectra for transmitted electrons normalized to one incident 100 MeV electron.

where,

$$F(\tau) = (1-\beta^2) \left[\frac{1+\tau^2-(2\tau+1)\ln 2}{8} \right] \quad (2.3)$$

the quantity;

$$.5 \left[\ln \left(\frac{T}{I} \right)^2 + \ln \left(1 + \frac{\tau}{2} \right) + F(\tau) - \delta \right] \quad (2.4)$$

is the stopping power per atomic electron [Ref. 7].

$N \equiv$ Avagadro's number 6.023×10^{23}

$Z \equiv$ atomic No. of target atoms

$I \equiv$ mean excitation energy $mc^2 \equiv$ electron rest energy

$\beta \equiv$ velocity of high speed electron/velocity of light

$\tau \equiv T/mc^2$ kinetic energy of incident electron per rest mass

$r_0 \equiv$ classical rest energy

$A \equiv$ atomic Wt. of target atoms

The collision stopping power for electrons in Al_2O_3 is 1.75 MeV cm^2/gram for 30 MeV electrons and 1.851 MeV cm^2/gram for 100 MeV electrons [Ref. 7].

2. Radiative Stopping Power

Mass radiative stopping power corresponds to the energy lost by bremsstrahlung. Bremsstrahlung creates a photon as the high energy electron decelerates in the field of an atomic nucleus or atomic electron.

Refinements of Bethe and Heitler's stopping power and scattering theory have led to the following formulation:

$$\frac{1}{\rho} \frac{dE}{dx} \text{ rad A} = N \alpha r_0^2 Z^2 \phi_{in} \left[1 + \left(\frac{1}{Z} \right) \phi_E / \phi_{in} \right] \quad (2.5)$$

where the ratio ϕ_E / ϕ_{in} is assumed to be unity [Ref. 7].

$N \equiv$ Avagodros's number 6.023×10^{23}

$Z \equiv$ atomic No. of target atoms

$r_0 \equiv$ classical electron radius

$\alpha \equiv$ fine structure constant, $Z/137$

$E \equiv T + mc^2$ total energy of electron

$\phi_{in} \equiv$ scaled radiative energy-loss cross sections for electron-nucleus interaction.

$\phi_E \equiv$ scaled radiative energy-loss cross sections for electron-electron interaction.

$A \equiv$ atomic Wt. of target atoms

3. Dose Measurement

High energy electrons traveling through material are slowed by numerous collisions. The incident electron continuously loses energy and travels a certain range until it comes to rest. Range is defined as the average length of path an electron travels until it is stopped by the medium due to energy loss [Ref. 6].

Dose is a measure of the total amount of energy deposited in the target material. Dose is given in rads (100 ergs/gram) material. The target material must be specified. In this thesis, Al_2O_3 will always be the target material.

Front surface dose for a thin sample will be used. The relativistic electrons of the beam accelerated at 30 MeV and 100 MeV are virtually unaffected by the sample material. The computer model using the Cyltran code shows that 99% of the 30 and 100 MeV electrons bombarding the sample of Al_2O_3 , emerge with their initial energy (see Figures 2.4-2.5). Since the energy loss is so small for the electrons, the collision stopping power can be considered a constant.

The energy going into excitation and ionization of the lattice atoms is absorbed in the material close to the track of the bombarding electron. The energy lost by bombarding electrons caused by bremsstrahlung travels far from the electron track before it is absorbed. Front surface dose for a thin sample is expressed by the following formula Eq. (2.6) [Ref. 10].

$$R = 1.6 \times 10^{-9} \Phi \frac{1}{\rho} \frac{dE}{dx} \text{ col} \quad \text{rad(material)} \quad (2.6)$$

$\frac{1}{\rho} \frac{dE}{dx}$ ≡ Collision stopping power for Al_2O_3 [Ref. 7]

Φ ≡ Fluence = electrons/cm²

C. RADIATION EFFECTS OF ELECTRONS IN INSULATORS

High energy electron irradiation of crystalline insulators introduces changes in the mechanical and physical properties of the insulator. The changes are caused by displacement damage, ionization effects, and excitation of the lattice atoms.

1. Displacement Damage

When an atom is displaced from the lattice, it leaves behind a vacancy in the lattice. If the displaced atom comes to rest in a non-equilibrium position between lattice sites, it is called an interstitial. The energy required to permanently displace an atom is called the displacement threshold energy, E_d . E_d is 50eV for Al and 90eV for O [Ref. 5].

Displacements are caused when high energy electrons bombard the target material. When a high energy electron enters the material, it collides with the nucleus of a lattice atom. If the collision imparts sufficient energy to displace the atom from its lattice site, it creates a vacancy-interstitial pair known as a Frenkel pair.

As a result of the collision, the primary knock-on atom is ionized. The knock-on atom is now a charged particle that continues to move through the insulator losing energy in Coulomb interactions. The coulomb interactions ionize more atoms, creating a cascade of charged particles.

Eventually, all the knock-on atoms come to rest. Some of the atoms will be in interstitial positions, while others recombine with vacancies. The Frenkel pairs form defect clusters due to the small mean free path of the knock-on atoms. The defect clusters may recombine or migrate to a free surface. The defect clusters that migrate

to the free surface are annihilated through annealing. The defect clusters may move throughout the lattice until they form stable displacements. These stable displacements cause the permanent radiation damage observed in insulators.

The number of Frenkel pairs created per incident electron in Al_2O_3 is calculated using the following Equations (2.7-14) [Refs. 8-9]:

$$N_o = \frac{(\rho N)(\text{Number of atoms})}{A \text{ molecule}} \quad (2.7)$$

$N_o \equiv$ Number of lattice atoms per cm^3

$\rho \equiv$ density of Al_2O_3 , 3.97 g/cm^3

$A \equiv$ atomic Wt., 82 g/mole

5 atoms/molecule

$N \equiv$ Avagadro's number 6.023×10^{23}

$$T_m = \frac{2[E+2mc^2]E}{Mc^2} \quad (2.8)$$

$T_m \equiv$ maximum energy transferred

$E \equiv$ incident electron energy (30 MeV or 100 MeV)

$mc^2 \equiv$ rest mass energy (.511 MeV)

$M \equiv$ atomic Wt. of target atom (Al or O)

$c^2 \equiv$ 931.5 MeV/amu

$$T = E_d \left[\frac{\ln T - 1 + \pi\alpha}{E_d} \right] \quad (2.9)$$

$T \equiv$ average energy transferred

$E_d \equiv$ displacement threshold energy (50eV Al Or 90ev O)

$\alpha \equiv$ fine structure constant, $Z/137$

$Z \equiv$ atomic No.

$$\text{Lamda} = \frac{4M_1 M_2}{(M_1 + M_2)^2} \quad (2.10)$$

where,

Lamda \equiv a scaling factor for the molecule (Al_2O_3)

$M_1 \equiv 26.98$ (amu) for Al

$M_2 \equiv 15.99$ (amu) for O

$$\mu(T) = \frac{BT}{E_d} \quad (2.11)$$

$B \equiv .5$ Kinchin and Pease constant

$$\sigma_D = \frac{2.495 \times 10^{-29} \text{ cm}^2 Z^2}{\beta^4 \Gamma^2} \left\{ \frac{(T_m - 1) - \beta^2 \ln T_m}{E_d} + \pi \alpha \beta \left\{ \left[\frac{2\sqrt{T_m} - 1}{E_d} \right] - \ln \frac{T_m}{E_d} \right\} \right\} \quad (2.12)$$

$\beta \equiv v/c$

$v \equiv$ speed of electron

$c \equiv$ speed of light

$\Gamma \equiv \sqrt{1-\beta^2}$

$\Gamma \equiv E/mc^2$

$E \equiv$ energy of incident electron

$$\sigma_{\text{tot}} = \sigma_D \mu(T) \quad (2.13)$$

σ_{tot} \equiv total cross section due to primaries and secondaries

$$N_F = \phi_E \sigma_a N_0$$

(2.14)

where,

$N_F \equiv$ No. of Frenkel defects/cm³

$\sigma_a N_0 \equiv$ No. of Frenkel pairs created/incident electron

The calculated value for $\sigma_a N_0$ was 1.017 Frenkel pairs created per electron.

The following assumptions were made when using the previous Frenkel pair equations:

1. If the energy is greater than E_d , displacements will occur.
2. The crystal arrangement of the atoms in the lattice structure is not considered.
3. Annealing is not considered.
4. Atom-atom collisions are treated as hard sphere collisions.
5. Crystal lattice atoms are considered to be stationary.
6. The long range effects of other atoms in the lattice are not considered.
7. Glancing collisions are not considered, even though an energy loss does occur.
8. There is no accounting for ionization loss.
9. The number of replacements per primary atom are not considered.
10. Damage is considered homogenous.

2. Ionization

Ionization is the formation of an ion by the addition or removal of an electron from a neutral atom or

molecule. An electron beam deposits energy in a material by ionizing the lattice atoms of the target material. The ionized atom produces a positive ion and a free electron. The free electrons may ionize other lattice atoms creating secondary free electrons. In addition, the photon processes (photoelectric, Compton effects and pair production) can ionize atoms and produce free secondary electrons.

As the target material is bombarded and ionized, an internal space charge is generated from the trapping of carriers. The space charge sets up a polarized field in the material and an electric field is produced in the insulator. The free electrons, both primaries and secondaries, tend to drift through the insulator under the influence of the electric field. Therefore, an increase in conductivity results.

Some of the secondary electrons will escape from the insulator. The ionized atoms and electrons will slow down and recombine, or be trapped in the impurity sites. Charge carriers trapped at impurity sites alter the electrical properties of the insulator, permanently increasing the conductivity.

The photoelectric effect occurs when an incident photon becomes completely absorbed by the lattice atom, and an atomic electron is removed from the atom. Photoelectric collisions are not important at energies greater than 1 MeV.

The Compton effect results from collisions between photons and atomic electrons. If a photon collides with an atomic electron, it imparts energy to the electron. When the atomic electron absorbs sufficient energy, it leaves the atom and becomes a free electron (called a Compton electron). The incident photon is scattered at a reduced energy. The Compton electron moves through the insulator's crystal structure as a negative charge carrier.

If the Compton electron has an energy greater than 200eV, it can produce displacements and secondary electrons. Ionization of a lattice atom requires 80eV. The Compton electrons constitute what is called a Compton current. In an insulator the Compton current may exceed the dielectric strength of the insulator, resulting in breakdown of the insulator.

3. Pair Production

Incident photons of energies greater than 1.02 MeV can be completely absorbed. In the place of the photon a positron-electron pair is produced, whose total energy is equal to that of the incident photon. This process is called pair production.

4. Electron Excitation

High energy electrons produce electron excitation of the lattice atoms via the coulomb electrostatic field. If the excited electron absorbs enough energy it is ionized. The ionization produces charge carriers. Charge carriers in

insulators recombine or become trapped in defect sites, within approximately 10^{-10} to 10^{-12} secs. Once trapped, the carriers may manifest as permanent changes in the electrical and physical properties of the insulator.

D. CONDUCTIVITY

1. Electrical Conductivity of Al₂O₃

Electrical conductivity of an insulator is much lower than that of a metal at room temperature. The electrical conductivity of sapphire is 10^{-12} ($\Omega\text{-cm}$)⁻¹ and 10^{-9} ($\Omega\text{-cm}$)⁻¹ for alumina. These values are from 14 to 17 orders of magnitude lower than the nominal value of 10^7 ($\Omega\text{-cm}$)⁻¹ for metals. As the temperature is increased, electrical conductivity decreases in metals. Electrical conductivity increases in sapphire and alumina with increasing temperature. It is obvious that charge carriers in metals are far different than the charge carriers in sapphire and alumina.

Some conduction by electron flow occurs, but the electrons are so tightly bound in Al₂O₃ that they will not move appreciably in an applied field. The charge that is transported is due to the charged ions Al and O. This carrier transport implies a diffusion flow of ions during conduction. Diffusion in sapphire and alumina occurs as the ions move via lattice vacancies. In the absence of an electric field, no net motion of ions takes place because

the probability of motion in any direction is random. The addition of an electric field directs the ions to flow in one direction. The end result is a net transport of both matter and charge.

Since diffusive transport is very small at room temperature, Al_2O_3 exhibits little conductivity. As the temperature increases, diffusion increases causing conductivity to increase. The conductivity and diffusion coefficient, D, are related by Eq. (2.15) [Ref. 11].

$$\sigma = \frac{nZ^2q^2D}{kT} \quad (2.15)$$

where,

n = number of ions per cubic meter

Z = valence ion

D = diffusion coefficient = $D_0 \exp [-Q/RT]$

Q = activation energy

R = gas constant

T = absolute temperature

q = charge

k = Boltzmann's constant

2. Electron Induced Conductivity (EIC) of Al_2O_3

During electron irradiation the sapphire and alumina substrates become conductive. The behavior of the samples is equivalent to a constant capacitor, C, shunted with a resistor, R(t), that varies with time.

The high energy electrons of the beam enter the substrate and lose energy in ionizing collisions with lattice atoms. The ionization creates electrons and holes which generate an avalanche of secondary electrons. While the electrons have sufficient energy, they will continue to cascade, creating more electron hole pairs. The cascading of free electrons is directed when a field is applied, and is called electron induced conductivity (EIC) or radiation induced conductivity (RIC).

The EIC process occurs in the first nanosecond to microsecond of the electron irradiated pulse. High energy particles passing through target materials incur quantum energy losses ranging from 10-30eV [Ref.12]. The quantum energy losses have not been considered in this model. The equations that express RIC are the following:

$$\sigma = N_e q \mu_e + N_h q \mu_h \quad (2.16)$$

where,

N_e ≡ concentration of free electrons

q ≡ charge

μ_e ≡ mobility of the electron

N_h ≡ concentration of holes

μ_h ≡ mobility of the holes

Holes in insulators are usually trapped within a time period of 10^{-4} to 10^{-5} secs. For the purpose of this thesis, holes

will be assumed to be immobile, [Ref. 13] and will be ignored. Eq. (2.16) reduces to:

$$\sigma = Nq\mu \quad (2.17)$$

where,

N ≡ concentration of free electrons

q ≡ charge

μ ≡ mobility of the electron.

RIC is next split into two components σ_p (prompt conductivity) and σ_d (delayed conductivity) expressed in Equations (2.18-2.19) [Ref. 13].

$$\sigma = \sigma_p + \Sigma \sigma_d \quad (2.18)$$

$$\sigma_p = K\Gamma^\delta \quad (2.19)$$

where,

Γ ≡ Dose rate

K ≡ coefficient for determining the slope of conductivity vs dose rate (obtained from experimental curves [Ref. 1]).

δ ≡ a scaling factor (obtained from experimental curves [Ref. 1])

Delayed conductivity is extremely small and assumed negligible. Delayed conductivity will not be considered in this thesis [Ref. 13].

III. EXPERIMENT

A. SAMPLE FABRICATION

Four devices were fabricated to test the response of EIC. Two of the devices were 30 mil-sapphire substrates and two were 25 mil-alumina substrates. The sapphire used was manufactured by Union Carbide. The alumina was manufactured by Coors. These materials are of high purity developed to meet the needs of the integrated circuit industry. The sapphire and alumina substrates are circular disks measuring 2 cm in diameter.

Photolithographically delineated heaters are incorporated on each side of the sapphire substrate. One side of the sapphire substrate has two electrodes with 3 mil- separation. The electrodes are placed on the heater using an evaporation process. The electrodes of the sapphire substrate are fabricated by evaporating tungsten, molybdenum and titanium onto the substrate.

The alumina samples have one heater photolithographically delineated on one side of the substrate. On the opposite side of the substrate, are two metal electrodes with 3 mil- separation. Tungsten is the first metal put onto the substrate using a sputtering process. The molybdenum and titanium are evaporated onto the alumina substrate.

The substrates are then enclosed by glass envelopes with an eleven pin configuration typical of a vacuum tube. Fig. 3.1 is a photograph of the EIC test device. The samples are processed using the normal vacuum bakeout and activation cycle [Ref 1].

B. PRE-IRRADIATION AND POST-IRRADIATION MEASUREMENTS

The optimum EIC test device temperature, determined by Los Alamos National Laboratory, is 1073 K [Ref. 1]. The test device heater voltage was determined by measuring the temperature heater substrate with an optical pyrometer. The temperature readings were accurate to ± 5 K.

Steady state resistance and conductivity of the Al_2O_3 samples were determined by plotting current vs voltage curves. The initial and post-irradiation resistance data was measured using a Keithley 617 electrometer, as shown in Fig. 3.2.

C. NPS LINAC

The Naval Postgraduate School (NPS) linear accelerator (LINAC) is a traveling wave type machine. It is patterned after those built at Stanford University in the early 1950's. The LINAC is a disk loaded circular wave-guide thirty feet long, constructed in three ten foot sections. It consists of a series of three klystrons used to accelerate electrons to relativistic energies from 15 MeV to 100 MeV.

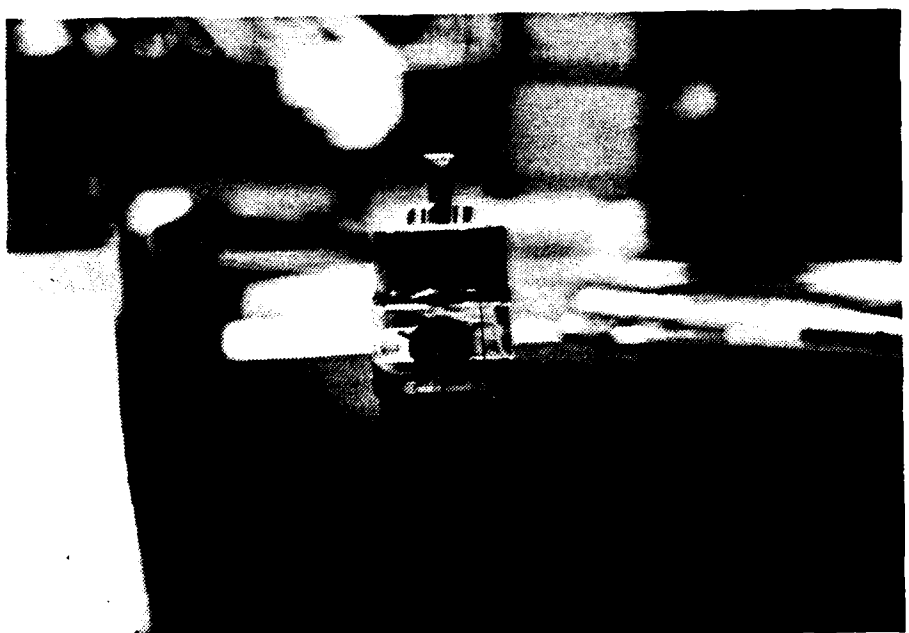


Figure 3.1. Sapphire substrate enclosed by glass vacuum tube.

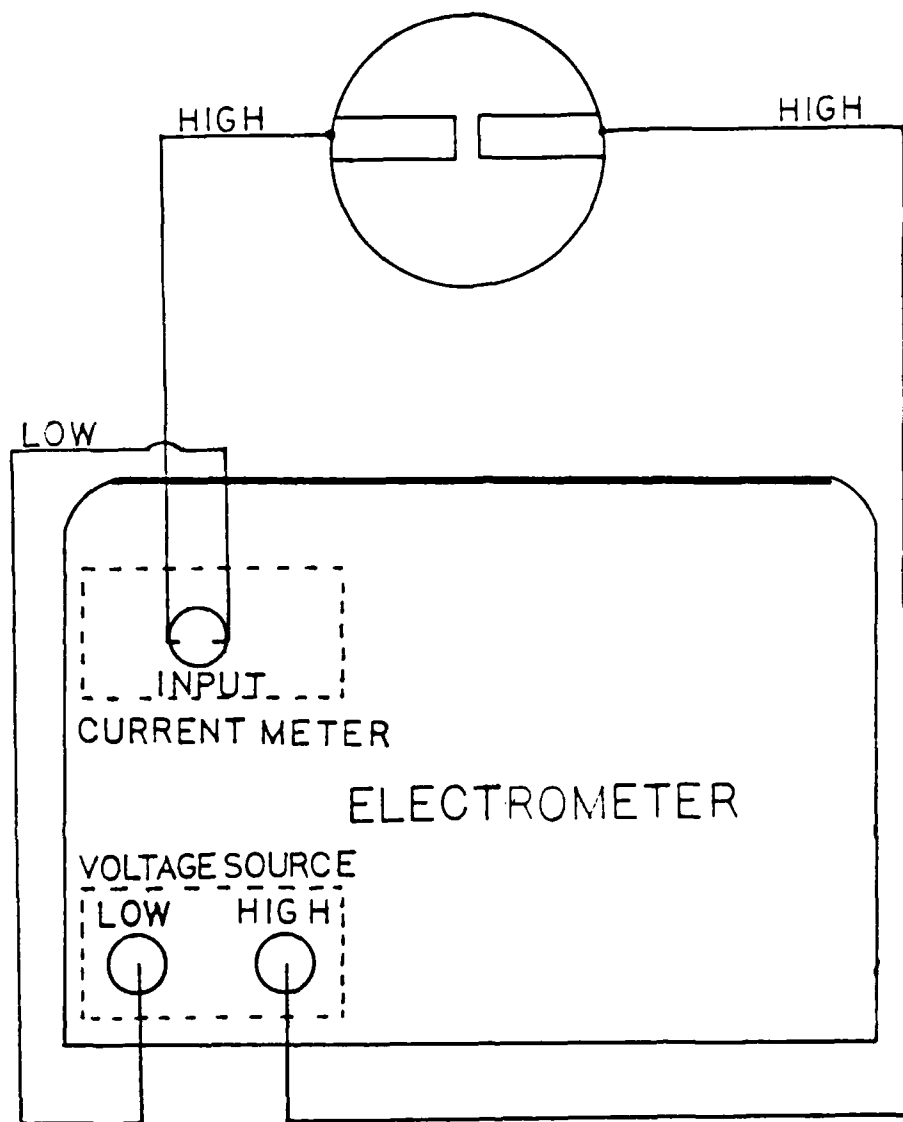


Figure 3.2. Test equipment set up for current vs voltage measurement across the substrate.

EIC experiments conducted using 30 MeV electrons utilized only one klystron. The experiments conducted using 100 MeV electrons required all three klystrons. The LINAC pulses sixty times per second with a 1-μsec pulse.

Relativistic electrons are focused on a target which is placed inside the target chamber, (held at a vacuum of 1-μtorr) or just outside the target chamber. Targets placed outside the target chamber are placed as close as possible to the target chamber window (a thin aluminum plate). The electron beam is focused and shaped using deflection and focusing magnets.

Electron fluence is measured utilizing a secondary emission monitor (SEM) located inside the target chamber. As electrons strike the SEM, a capacitor is charged and voltage is measured across the capacitor using a voltage integrator circuit. This charge relationship is given by the following equation:

$$Q_S = CV \quad (3.1)$$

where Q_S is the total SEM charge, C is the capacitance and V is the accumulated voltage. The total beam charge that has passed through the SEM is determined using:

$$Q_B = Q_S / 0.026 \quad (3.2)$$

where Q_B is the total beam charge.

Previous research on scattering experiments used a Faraday cup to calibrate the large SEM. Efficiency for the

large SEM was found to be 6% [Ref. 14]. The Faraday cup has since been removed and the large SEM has become the standard.

The small SEM used in this thesis was calibrated against the large SEM. Efficiency for the small SEM is 2.6%. Thus 0.026 is the efficiency factor used in Eq. (3.2). Using Eq.'s (3.1) and (3.2) the total number of beam electrons, (N), is given by

$$N = CV/0.026q \quad (3.3)$$

where q is the charge of an electron.

Fluence is determined by dividing both sides of Eq. (3.3) by the area A . Fluence is the number of electrons per unit area of the beam expressed as

$$\Phi \equiv \text{Fluence} = CV/0.026qA \quad (3.4)$$

D. TEST PROCEDURE

The EIC test device was installed in its test fixture as shown in Fig. 3.3. The device was heated to its correct temperature by monitoring the heater voltage. The sample was heated very slowly, approximately 1 Volt/min, to prevent thermal shock to the substrate. Once the correct heater voltage was obtained, the device was allowed to bake for at least fifteen minutes prior to irradiation. During the baking period a fluorescent target equal in height with the substrate was placed on the test fixture. For these EIC



Figure 3.3. EIC test device plugged into its test fixture.

experiments the test device and test fixture were placed just outside the vacuum test chamber window.

The electron beam was focused on the fluorescent target. Video cameras monitored the fluorescent target and relayed the picture to the control room. The electron beam appears as a very bright area on the fluorescent target. In the control room the electron beam is adjusted and focused into a circular disk of 1 cm². A circle is drawn on the video monitor around the electron beam.

The electron beam was shut off and the test device was positioned as close to the target chamber window as possible, (there was approximately a 5mm gap between chamber and tube) directly in front of the electron beam.

The EIC experiment consisted of the following steps:

1. A bias voltage was applied (0-250 volts positive, 0-(-100) volts negative) across the EIC metal electrodes.
2. The device was irradiated using 30 MeV or 100 MeV electrons. The irradiation time was from 20 to 30 secs.
3. The response was viewed with an oscilloscope. The device response was recorded by photographing the oscilloscope CRT.
4. The beam was shut off for 1-3 minutes to allow the internal space charge to dissipate.
5. A new bias voltage was applied and steps 1-4 repeated.

Attempts to dissipate internal space charge by removing the applied field and irradiating the device for several seconds were unsuccessful. This process annihilated about

70% of the internal space charge. The only way to annihilate all the internal space charge was to shut off the electron beam and allow the space charge to dissipate.

IV. DATA AND RESULTS

A. STEADY STATE RESISTIVITY AND CONDUCTIVITY

Pre-irradiation and post irradiation measurements of steady state current and voltage were made for the sapphire and alumina substrate samples. The plots of these current vs voltage measurements are illustrated in Figs. 4.1-4.2. Resistivity was determined by computing the inverse slope of the curves. Conductivity (σ) was calculated using the following equations:

$$\sigma = \frac{I}{RA} \quad (4.1)$$

$$\sigma = \frac{I}{RLt} \quad (4.2)$$

$$\sigma = \frac{1}{RL(t/\lambda)} \quad (4.3)$$

where,

λ ≡ distance of separation between the electrodes
(3mils)

L ≡ width across the electrode (29.7mils)

R ≡ resistivity

t ≡ carrier penetration depth into the substrate

$\frac{1}{t/\lambda}$ ≡ .624, a scale factor calculated using a Laplace equation computer program. R. Dooley of Los Alamos National Laboratory determined the scale factor.
Fig. 4.3 illustrates the conductivity calculation geometry.

Steady state pre-irradiation and post-irradiation data is presented in Table 4.1.

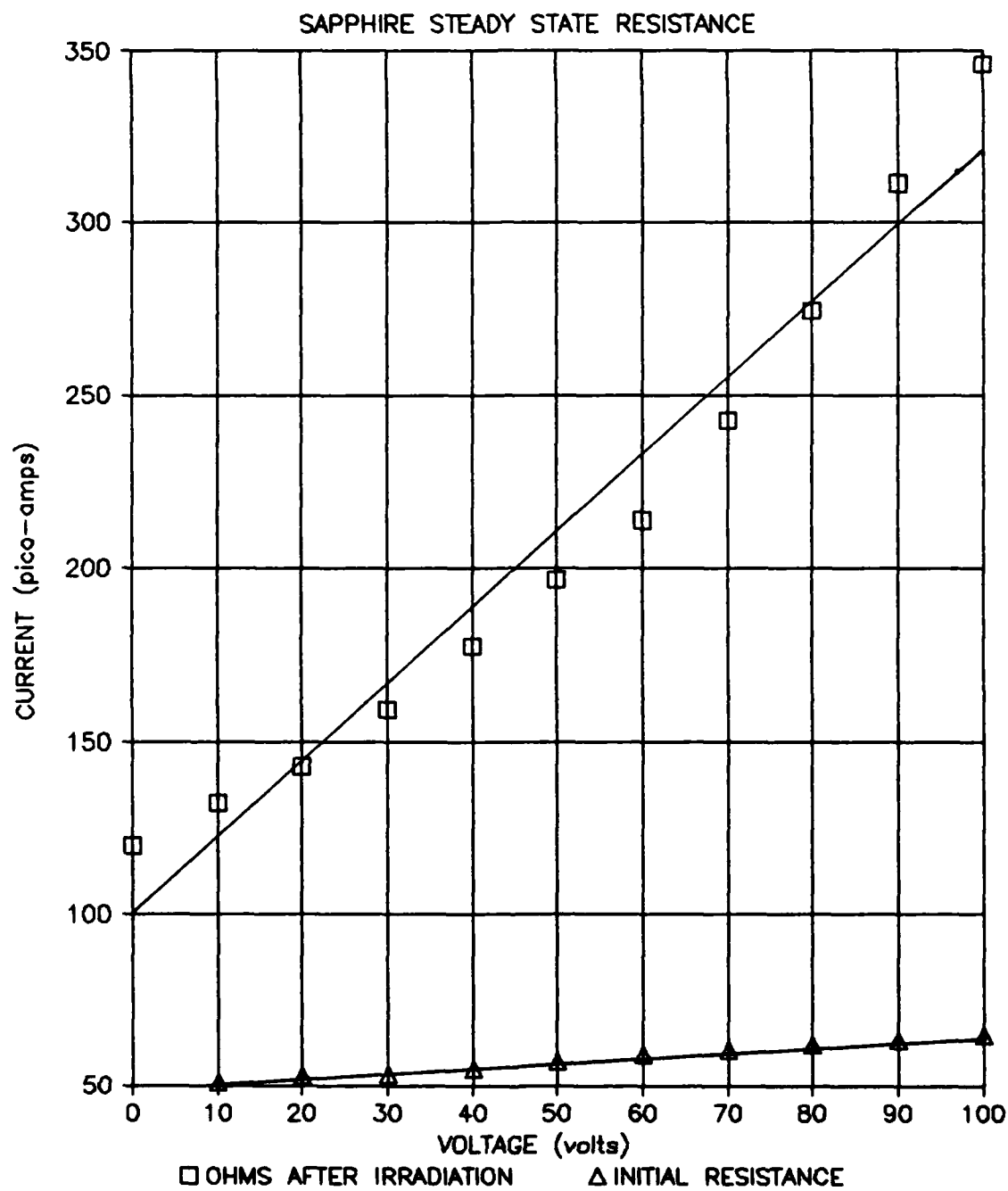


Figure 4.1. Current vs voltage plots before and after electron irradiation of sapphire. Resistivity is the slope. Initial resistivity was 6.36×10^{12} ($\Omega\text{-cm}$) and resistivity after irradiation was 4.5×10^{11} ($\Omega\text{-cm}$).

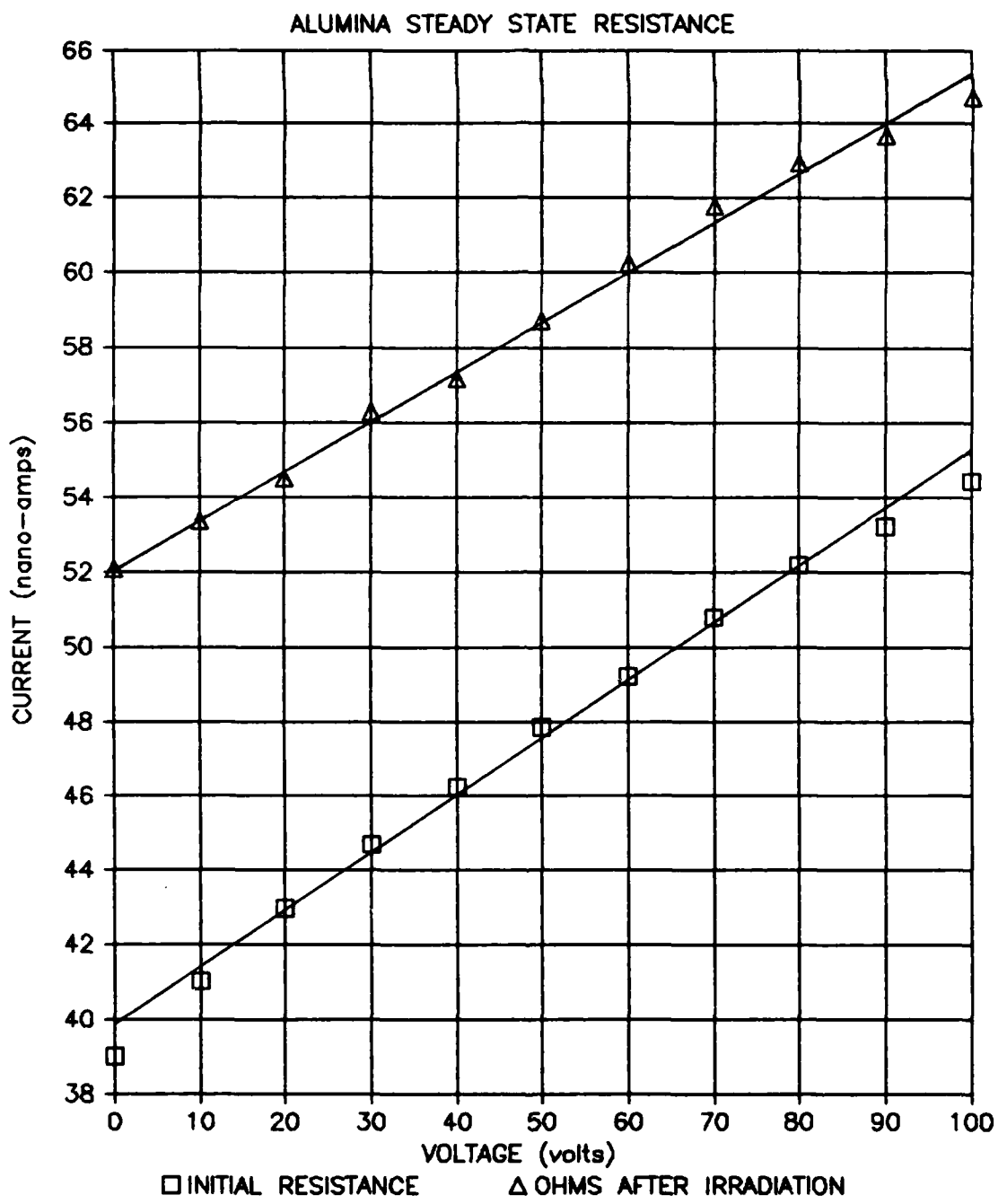


Figure 4.2. Current vs voltage plots before and after electron irradiation of alumina. Resistivity is the inverse slope. Initial resistivity was $6.29 \times 10^{+9}$ ($\Omega\text{-cm}$) and resistivity after irradiation was $7.60 \times 10^{+9}$ ($\Omega\text{-cm}$).

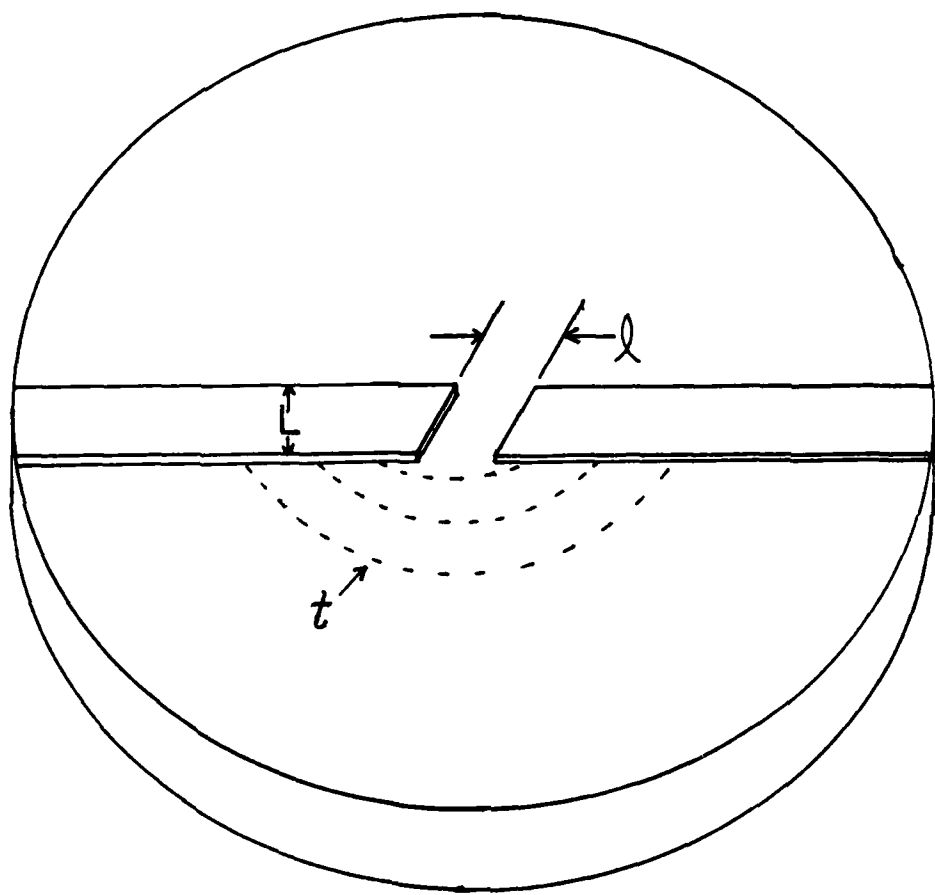


Figure 4.3. Conductivity calculation geometry of a sample substrate with two electrodes a distance ℓ apart.

TABLE 4.1. CHARACTERISTIC VALUES FOR SAMPLES SAPPHIRE AND ALUMINA

	Pre-Irradiation			30 MeV Irradiation		
	Sapphire	Alumina	Sapphire	Alumina	Sapphire	Alumina
Resistivity ($\Omega\text{-cm}$)	6.36×10^{12}	6.29×10^9	4.50×10^{11}	7.60×10^{17}		
Conductivity ($\Omega\text{-cm}$) ⁻¹	1.30×10^{-12}	1.31×10^{-9}	1.84×10^{-11}	1.78×10^{-17}		
EIC ($\Omega\text{-cm}$) ⁻¹					1.85×10^{-13}	2.81×10^{-14}
Fluence (elec/cm^2)			1.77×10^{15}	2.67×10^{15}	1.77×10^{15}	2.67×10^{15}
Flux ($\text{elec/cm}^2\text{-s}$)			2.08×10^{15}	5.20×10^{14}	2.08×10^{15}	5.20×10^{14}
Dose . rads(Si)			5.14×10^7	7.72×10^7	5.14×10^7	7.72×10^7
Dose rate . rads(Si)/s			6.02×10^7	1.51×10^7	6.02×10^7	1.51×10^7

B. TRANSIENT EIC

The sapphire and alumina substrates were irradiated using 30 MeV electrons. The fluence varied from 10^{14} to 10^{15} electrons/cm². The dose rate was 10^7 rad(Si)/sec. Transient EIC is shown by the photograph in Fig. 4.4. The transient EIC at various bias voltages is presented in Appendix A.

In Fig. 4.4 the measured voltage (V_x) is along the y-coordinate and time is along the x-coordinate. The straight heavy white line at the lower left corner is the zero reference line for the electron beam response. The fuzzy line immediately following the zero reference line is assumed to be carried by noise from the electron gun, and is ignored. V_x is measured from the zero point to the peak of the white line trace. In this picture V_x is $18\text{mV} \pm 0.5\text{mV}$. V_x changes as bias voltage is changed.

In both sapphire and alumina, an increase in positive bias voltage increased V_x . A bias voltage of 150 volts gave the maximum V_x for sapphire. As the bias voltage was increased from 150-250 volts a large decrease in V_x was observed. A limiting peak of V_x was not observed in alumina, as the voltage was increased to a maximum of 250 volts bias.

Then a negative bias was applied, sapphire and alumina showed a decrease in V_x . For alumina, V_x was zero when a bias voltage of -110 volts was applied. V_x was zero in

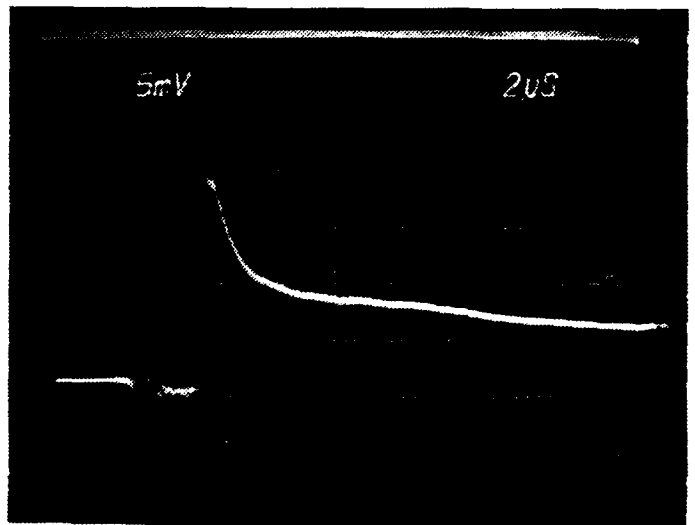


Figure 4.4. Sample photograph of alumina irradiated with 100 MeV electrons.

sapphire when a bias voltage of -22 volts was applied.

Photographs in Appendix A illustrate these findings.

EIC was determined in the following way. A plot was made of V_x vs bias voltage, see Figs. 4.5-4.6. The slope of this curve was computed. The slope was used in the following equation:

$$\frac{\Delta I_x}{V_{bias}} = \frac{\text{slope}}{\text{sensing resistor}} \quad (4.4)$$

where the sensing resistance was 50Ω .

$\Delta I_x \equiv$ change in current

$V_{bias} \equiv$ applied bias voltage

Resistivity was found by taking the inverse of Eq. (4.4). EIC was calculated using the resistivity from Equations (4.1-4.3). The EIC data is presented in Table 4.1.

C. DOSE RATE CALCULATIONS

Dose rate was determined using the following equations.

$$Q = \frac{\langle I \rangle \text{ beam current}}{\text{Number of pulses/sec}} \quad (4.5)$$

$$\dot{\Phi} \equiv \text{Flux} = \frac{Q \text{ (coulombs/sec)}}{\text{Area } (1.602 \times 10^{-19}) \text{ coul/electron}} \quad (4.6)$$

$$\dot{\Phi} = \frac{\text{electrons}}{\text{cm}^2 \cdot \text{sec}} \quad (4.7)$$

$$\dot{r} = 1.6 \times 10^{-9} \dot{\Phi} \frac{1}{\rho} \frac{dE}{dx} \frac{\text{rads(material)}}{\text{col sec}} \quad (4.8)$$

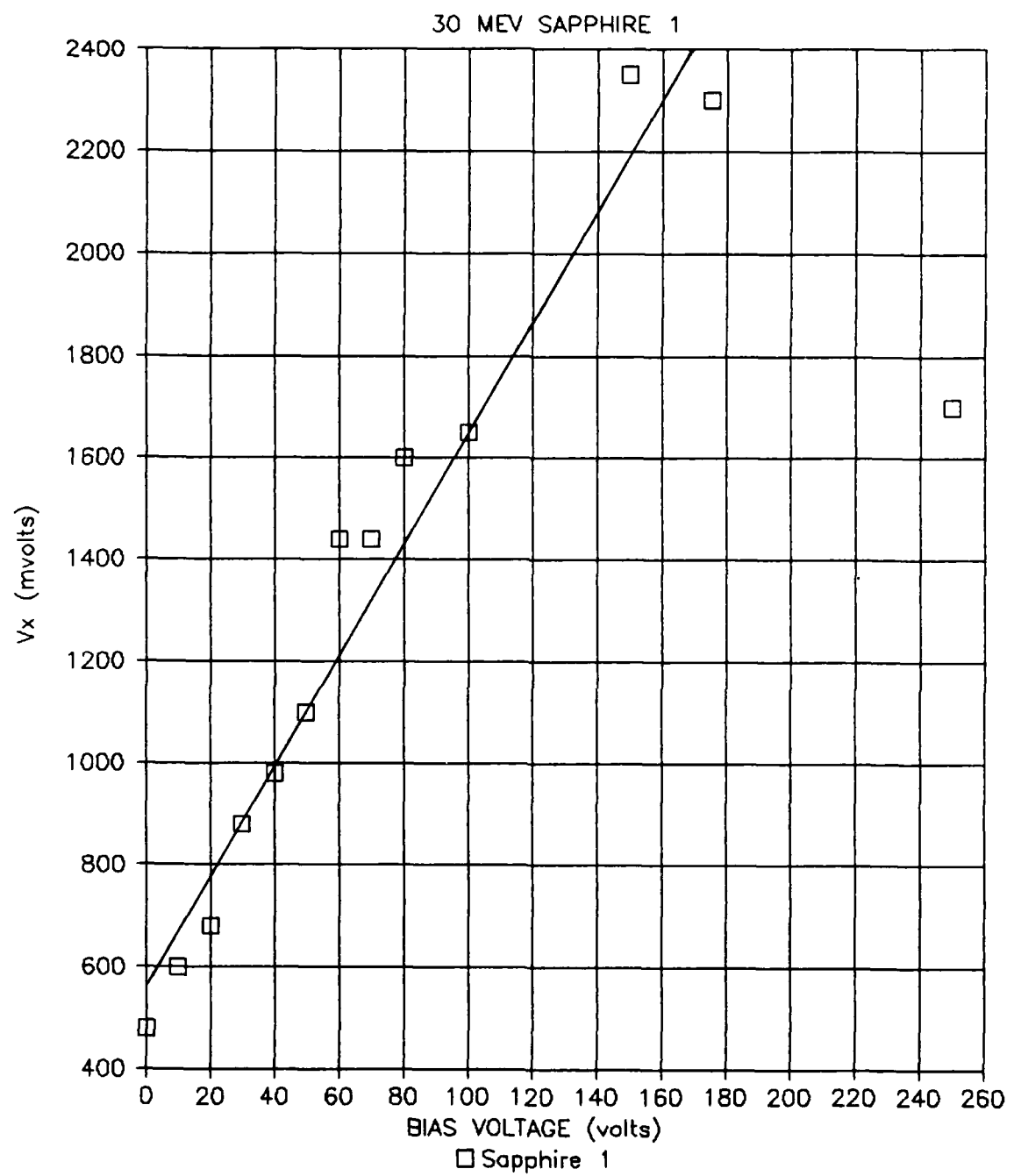


Figure 4.5. Changes in measured voltage (V_x) vs bias voltage for a sapphire sample.

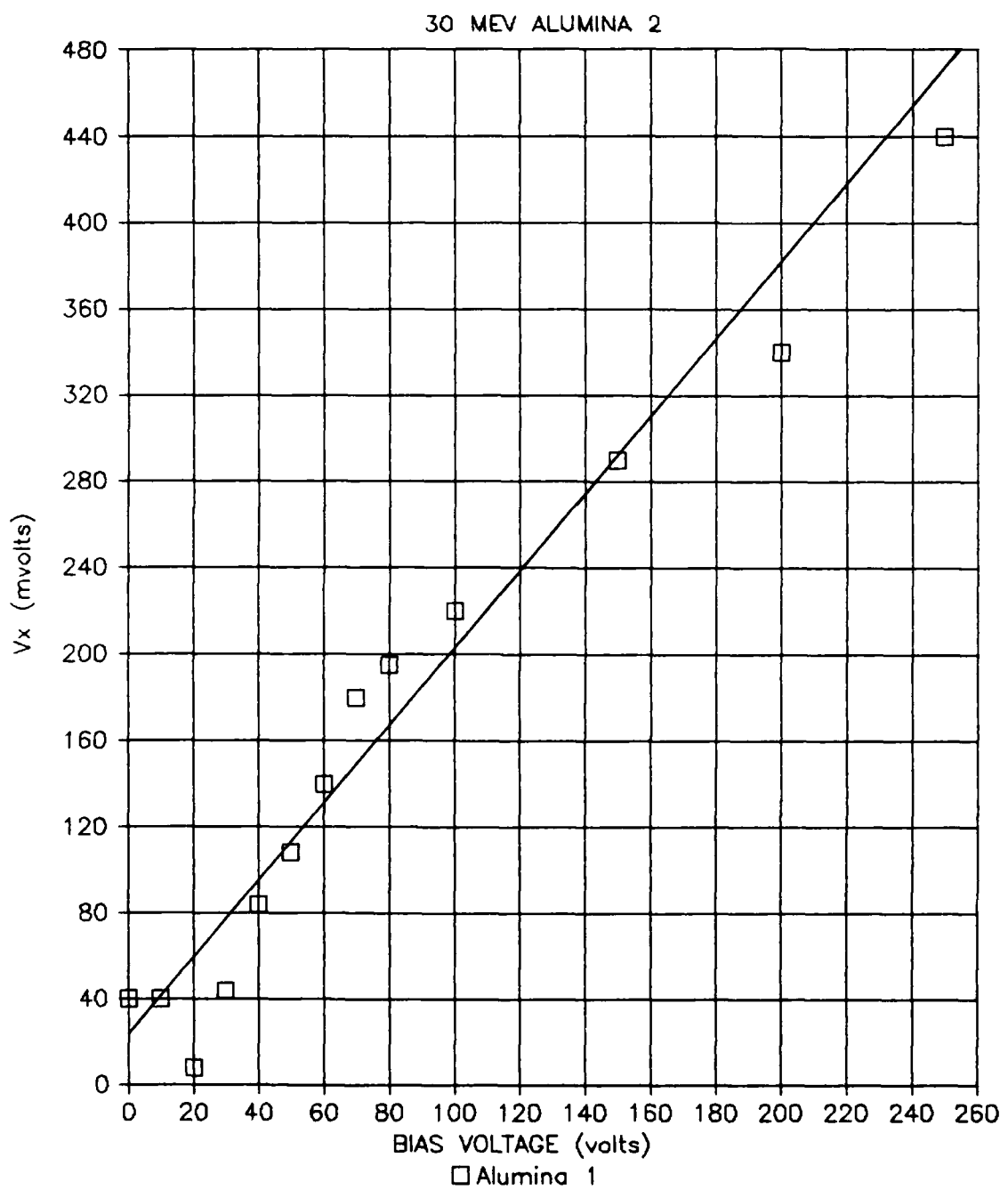


Figure 4.6. Changes in measured voltage (V_x) vs bias voltage for an alumina sample.

where, Eq. (4.8) is a variation of Rudi's dose Eq. (2.6) [Ref. 10] and $dE/\rho dx$ is the stopping power [Ref.7].

In radiation effects, damage is normally scaled to silicon. A scaling factor is determined by dividing the silicon stopping power by the stopping power of the sample material, using the same electron beam energy. The scaling factor for aluminum oxide (Al_2O_3) at 30 MeV is 1.034. A typical calculation of dose rate, using $\langle I \rangle = 2 \times 10^{-3}$ amps, yields a flux of 2.08×10^{15} electrons/cm²-sec. The calculated dose rate is 6.02×10^7 rads(Si)/sec.

V. DISCUSSION OF RESULTS

The sapphire sample #2, was irradiated using 100 MeV electrons. The heater substrate had more than 25 very small holes distributed throughout the substrate. The holes did not interfere with actual heater operation. The sample was activated to a heater temperature of 1073 K, three times prior to irradiation.

Upon initial irradiation sapphire #2 displayed the characteristic EIC trace on the oscilloscope (see Appendix A for photographs). After about 20 minutes of continuous electron bombardment, the EIC trace no longer showed a characteristic Vx. The trace displayed fuzzy negative peaks.

The response of the device shows a breakdown of the substrate. The sapphire substrate broke down at a positive bias of about 30 volts. The dose rate at the time of breakdown was 1.28×10^6 rads(Si)/sec. The substrate appears to have broken down due to surface flashover.

Surface flashover is generated when a high voltage is applied across an insulator [Ref. 15-16]. The 100 MeV electron irradiation of sapphire #2 produced a large voltage applied through electrodes across the substrate. As the substrate absorbs the electron beam energy, a surface charge begins to form. A cascade of secondary electrons generates

a secondary emmission of thermalized electrons. These thermalized electrons in turn increase both surface charge and internal space charge. A low resistance breakdown path formed across the substrate because the substrate heater had holes, and substrate breakdown occurred.

Surface flashover did not occur in the other sapphire and alumina samples. There was no low resistance breakdown path available in the other samples. The other substrate samples stabilized and a large space charge was observed.

Relativistic electrons produce a uniform distribution of electrons and holes in radiated material. In EIC experiments, two metal electrodes A and B on the substrate material ensure a path for electron flow, see Fig 3.2. As the electron beam strikes the substate, free electrons are generated inside the bulk material.

The free electrons are swept out almost immediately, in about 1 picosecond, by the self-induced electric field. The oscilloscope shows a large negative trace with a fast rise time of 0.5 μ sec. The trace exponentially decays and returns to the zero reference line. This behavior demonstrates the large polarization due to internal space charge.

Holes are left in the substrate and they migrate while annealing takes place. The time period of annealing is from miliseconds to as long as days.

As the positive bias voltage is increased, more electrons are swept from electrode A across the substrate

and out of electrode B. The trace on the oscilloscope shows a large positive increase in V_x . The EIC follows the rise time of the radiation pulse then decays exponentially, similar to a capacitor.

When a negative bias voltage is applied, a large positive trace on the oscilloscope is observed. The positive trace becomes more negative as the negative bias is increased. The EIC current was smaller in magnitude when a negative bias was applied. Positive bias causes a greater EIC current magnitude because EIC thermalized electrons add to the positive bias voltage electrons. When negative bias is applied EIC current acts as a barrier to the applied negative bias voltage. The result is a smaller magnitude for the measured voltage V_x .

The response exhibited by a capacitor shunted by a resistance $R(t)$ which varies with time, is very similar to the behavior of the substrates. Oscillogram photographs in Appendix A illustrate the different EIC measured values for the different applied bias voltages.

Plots of V_x vs bias voltage, (Figs. 4.5-4.6) clearly show a linear relationship. Van Lint et al. Face, et al. and Pomerantz et al. [Refs. 13,17,18] observed this same linear relationship.

At 1073 K, annealing of radiation damage in TIC can be virtually ignored. Any annihilation through annealing of displacement clusters is an on going process at TIC

operating temperatures. The annealing of radiation damage is incorporated during the irradiation and is not observed.

As electrons bombard a sample more traps form and recombinations take place. As dose accumulates, the dose rate response should exhibit some change. Neither sapphire or alumina exhibited change as the dose accumulated for a given dose rate. Arguello observed instead, that TIC triode circuit characteristics stabilized as dose increased to 1.86×10^7 rads(Si) [Ref.19].

There was no significant difference recorded when bombarding alumina with 100 MeV electrons or 30 MeV electrons (see Appendix A). This is not surprising since collision stopping powers between 100 MeV electrons and 30 MeV electrons vary by only 0.1 MeV cm²/gram.

EIC for sapphire was experimentally determined to be 1.85×10^{-3} ($\Omega\text{-cm}$)⁻¹ at a dose rate of 6.02×10^7 rads(Si)/sec. Alumina EIC was 2.81×10^{-4} ($\Omega\text{-cm}$)⁻¹ at 1.51×10^7 rads(Si)/sec. Using Eqn. 2.19 with $K=7.7 \times 10^{-13}$ and $\delta=1$, the prompt conductivity for an undoped Linde crystal is $\approx 10^{-4}$ ($\Omega\text{-cm}$)⁻¹ [Ref. 1]. This value is ≈ 2 orders of magnitude different than the experimental values calculated for sapphire and alumina. Since K is a function of ionization and varies according to electron-hole pair recombination, K can change by orders of magnitude. The crystalline structure, traps and impurities generated during manufacture all contribute to the values of K.

VI. CONCLUSION

Electron induced conductivity (EIC) is an important damage mechanism in integrated circuits. EIC can cause single-event upset in critical electronic components of weapon systems, communication systems and navigational systems. Thermionic integrated circuits (TIC) are orders of magnitude more resistant to total dose radiation than any other integrated circuits available. To ensure TIC devices are more resistant to single event upset, materials used in the substrates must have the lowest EIC possible.

Experiments were conducted to observe the EIC in undoped single crystal sapphire (Al_2O_3) and undoped poly-crystalline alumina (Al_2O_3). The Naval Postgraduate School's linear accelerator provided 30 and 100 MeV electrons. The high energy electrons provided a maximum dose rate of 1.28×10^9 rads(Si)/sec. The experimentally determined EIC for sapphire was 1.85×10^{-9} ($\Omega\text{-cm}$) $^{-1}$ when bombarded at a dose rate of 6.02×10^7 rad(Si)/sec. Using a dose rate of 1.51×10^7 rad(Si)/sec the experimentally determined EIC for alumina was 2.81×10^{-4} ($\Omega\text{-cm}$) $^{-1}$.

Alumina was an order of magnitude more resistant to EIC than sapphire. The EIC characteristics of sapphire and alumina remained unchanged as the total dose increased. Alumina was irradiated using 30 and 100 MeV electrons. The

EIC results using 100 MeV electrons did not differ from the results when 30 MeV electrons were used.

Alumina, being a naturally disordered and opaque material, exhibited greater radiation hardness than sapphire. The processing of devices, of thickness less than 20-mils, is easier for sapphire than alumina.

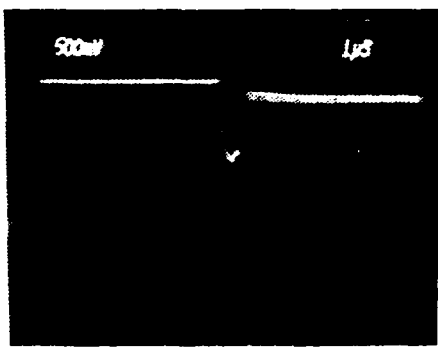
Further radiation studies should be conducted using TIC devices. If the processing problems presented by alumina cannot be overcome, other materials must be tested. Radiation studies should be conducted using doped sapphire. Doping sapphire should enhance radiation hardness and decrease radiation induced conductivity.

TIC devices show great promise for use in hostile radiation environments. The use of alumina for the substrate of these devices ensures they will be as resistant to single event upset as possible.

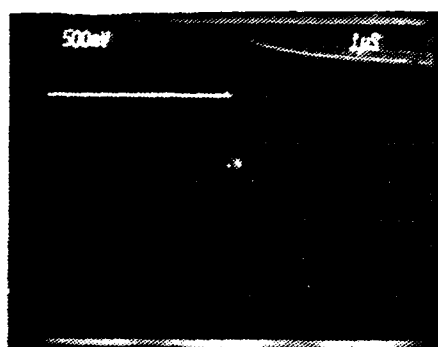
APPENDIX A

ELECTRON INDUCED CONDUCTIVITY PHOTOGRAPHS:

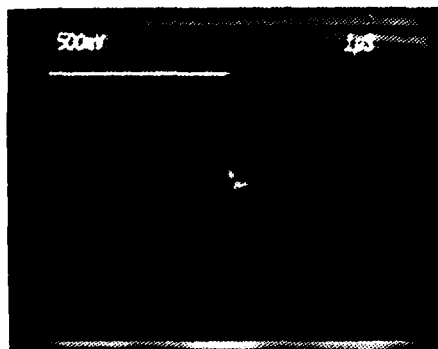
Enclosed are photographs of electron induced conductivity (EIC), for sapphire and alumina irradiated with 30 MeV and 100 MeV electrons. The photographs are presented from left to right. Time is along the x-coordinate and the measured value (V_x) is along the y-coordinate. The straight heavy white line, located at the lower or upper left hand corner of the photographs, is the zero reference point. After the zero reference point, a fuzzy line normally appears, this is assumed to be caused by the electron gun, and should be ignored. V_x is measured from the baseline to the peak of the white line trace. Under each photograph the measured value, V_x , is designated along with the corresponding bias voltage.



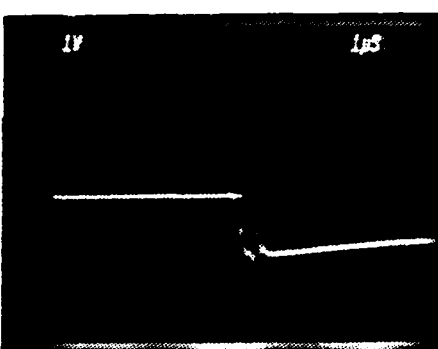
Vx = 650mV at 0V bias



Vx = 1650mV at 10V bias

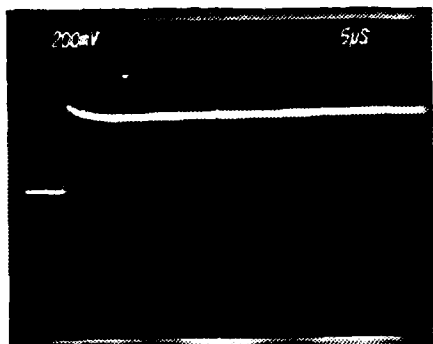


Vx = 2000mV at 20V bias

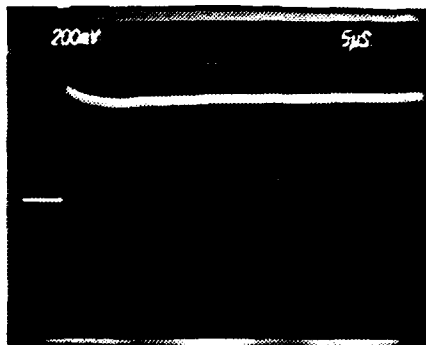


Breakdown at 30V bias

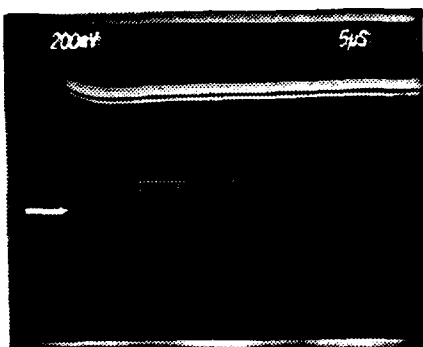
Figure A1.1. Photographs of sapphire #2 irradiated with 100 MeV electrons.



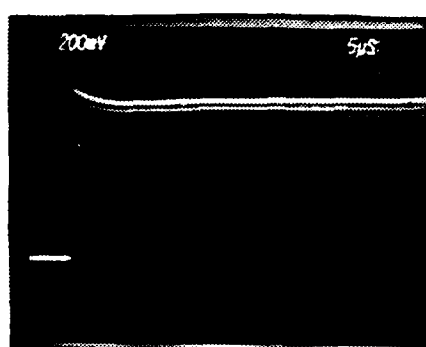
V_x = 480mV at 0V bias



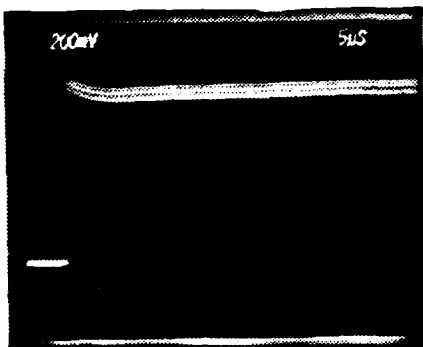
V_x = 600mV at 10V bias



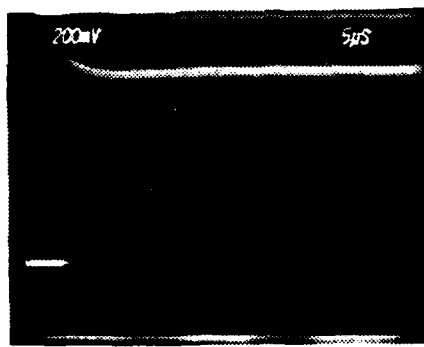
V_x = 680mV at 20V bias



V_x = 880mV at 30V bias

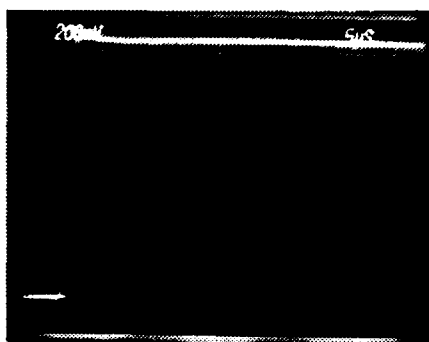


V_x = 980mV at 40V bias

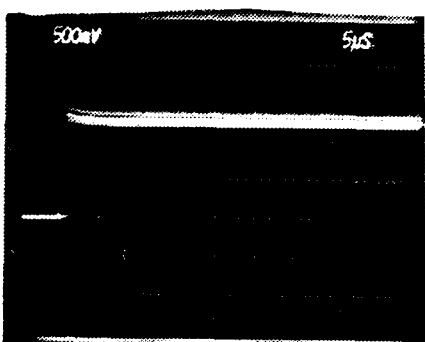


V_x = 1100mV at 50V bias

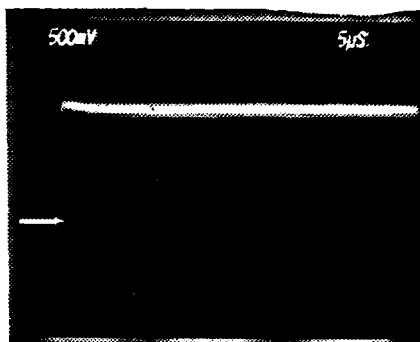
Figure A1.2. Photographs of sapphire irradiated with 30 MeV electrons



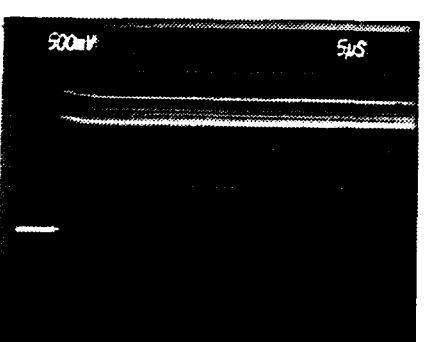
V_x = 1440mV at 60V bias



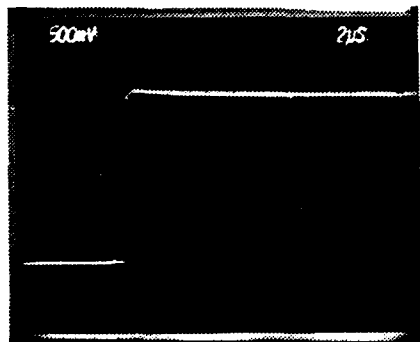
V_x = 1440mV at 70V bias



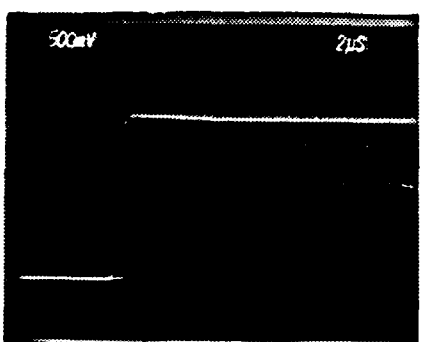
V_x = 1600mV at 80V bias



V_x = 1650mV at 100V bias

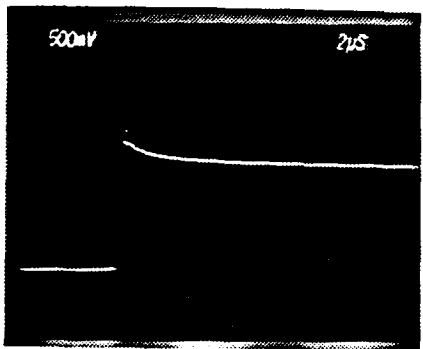


V_x = 2350mV at 150V bias

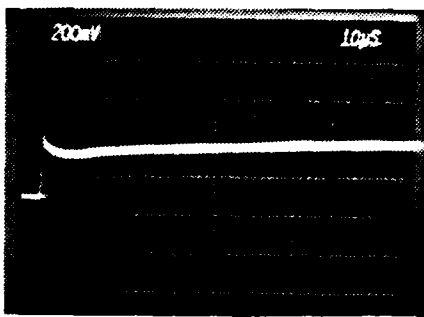


V_x = 2300mV at 175V bias

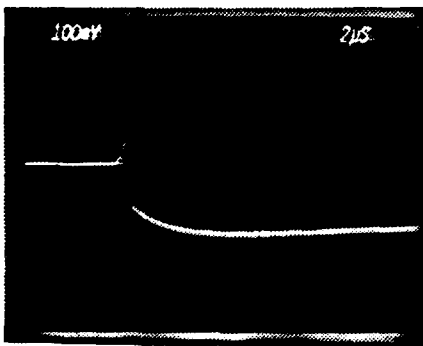
Figure A1.3. Photographs of sapphire irradiated with 30 MeV electrons. Positive bias voltages range from 60V to 175V.



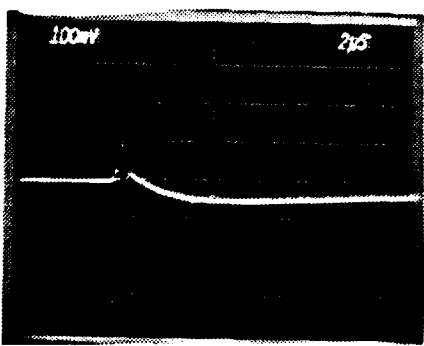
$V_x = 1700 \text{ mV}$ at 250V bias



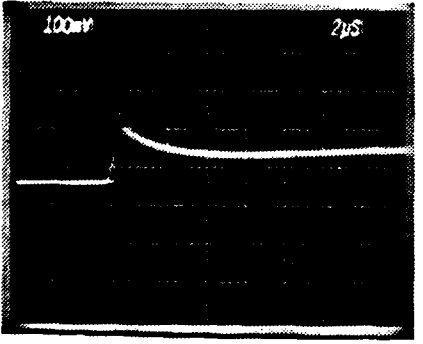
$V_x = 320\text{mV}$ at 0V bias



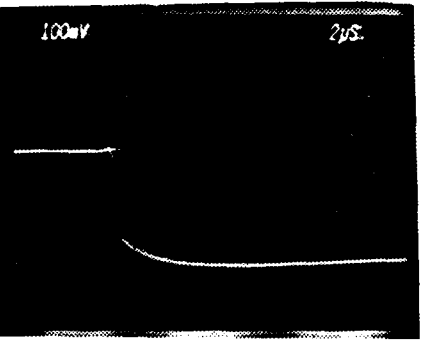
$V_x = 140\text{mV}$ at -10V bias



$V_x = 30\text{mV}$ at -20V bias

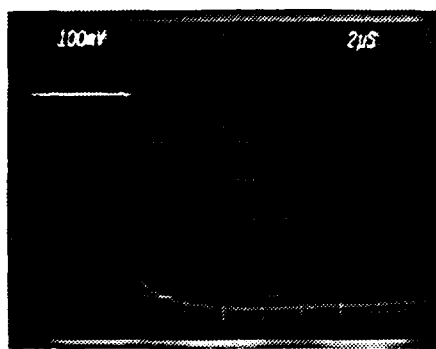


$V_x = -100\text{mV}$ at -30V bias

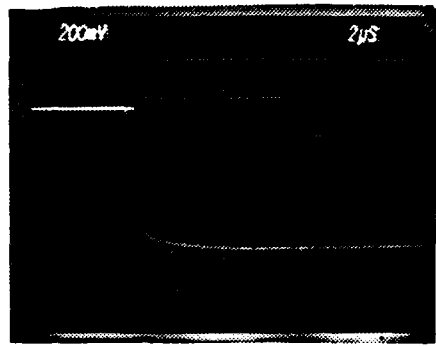


$V_x = -115\text{mV}$ at -40V bias

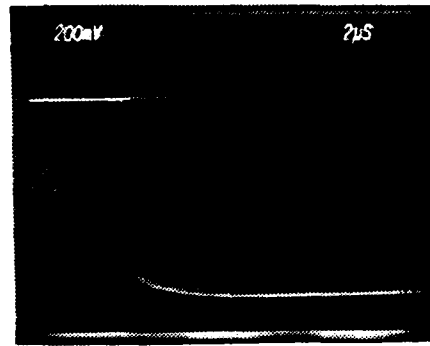
Figure A1.4. Photographs of sapphire irradiated with 30 MeV electrons. Bias voltages range from 250V to -40V.



$V_x = -450\text{mV}$ at -60V Bias

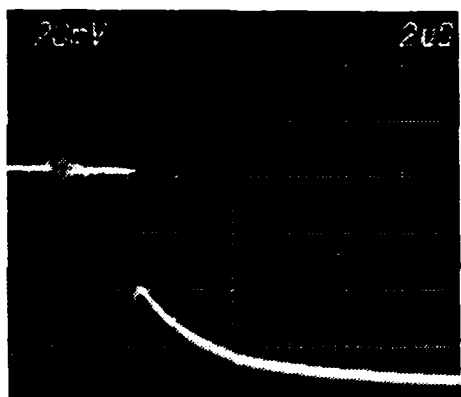


$V_x = -680\text{mV}$ at -80V bias

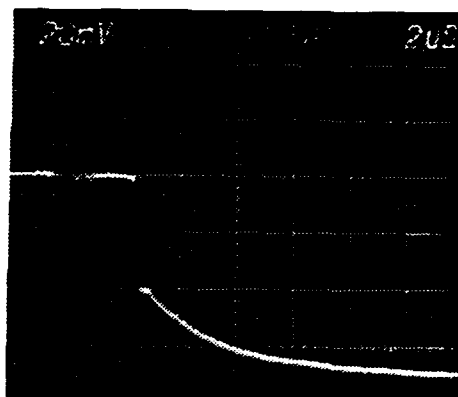


$V_x = -920\text{mV}$ at -100V bias

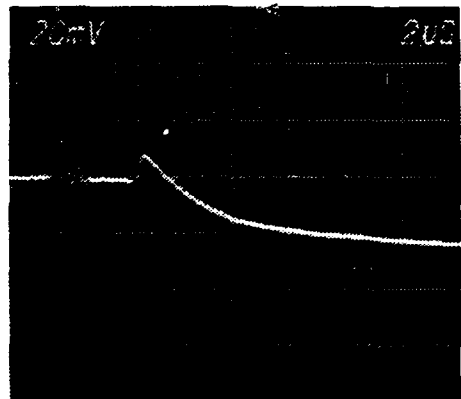
Figure A1.5. Photographs of sapphire irradiated with 30 MeV electrons. Negative bias voltages range from -60V to -100V .



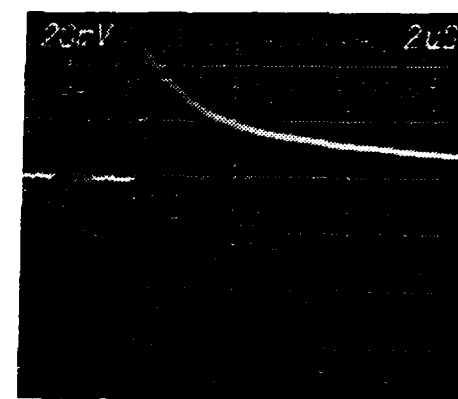
$V_x = -40\text{mV}$ at OV bias



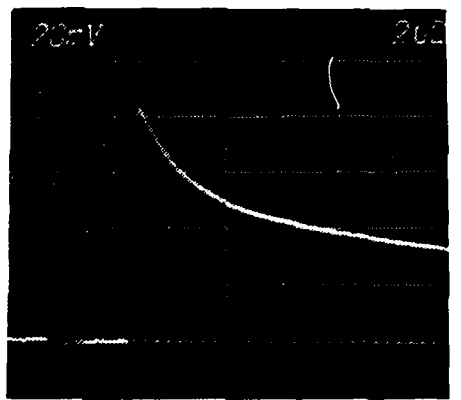
$V_x = -40\text{mV}$ at 10V bias



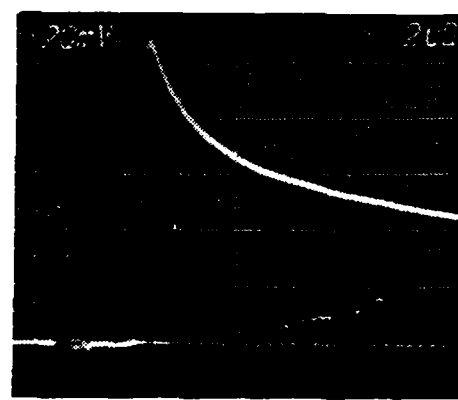
$V_x = 8\text{mV}$ at 20V bias



$V_x = 44\text{mV}$ at 30V bias

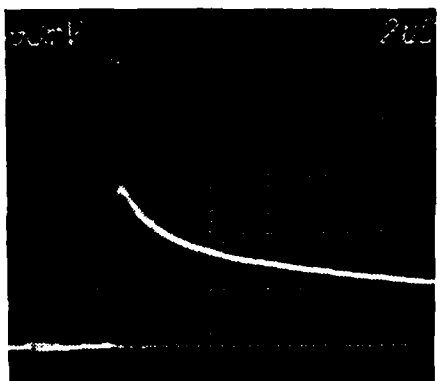


$V_x = 84\text{mV}$ at 40V bias

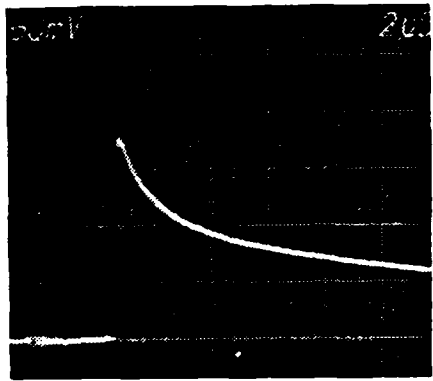


$V_x = 108\text{mV}$ at 50V bias

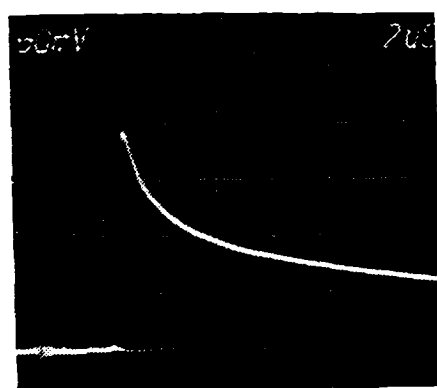
Figure A1.6. Alumina irradiated with 30 MeV electrons.
Positive bias voltages range from OV to 50V.



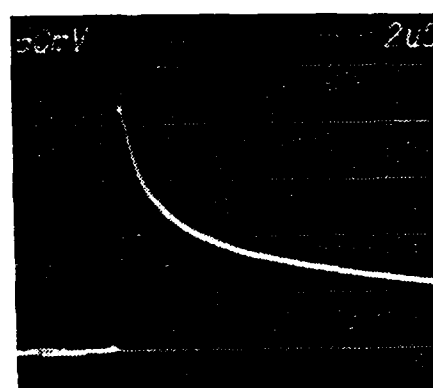
V_x = 140mV at 60V bias



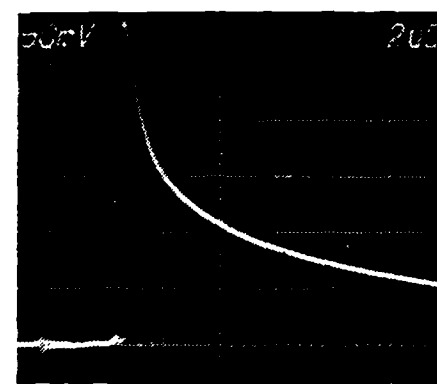
V_x = 180mV at 70V bias



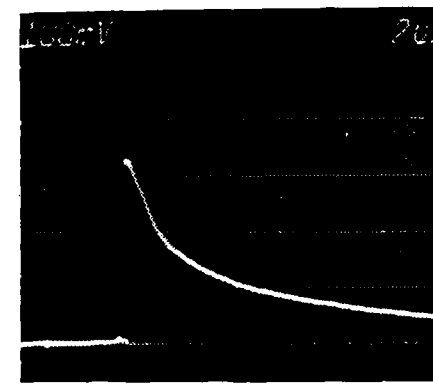
V_x = 195mV at 80V bias



V_x = 220mV at 100V bias

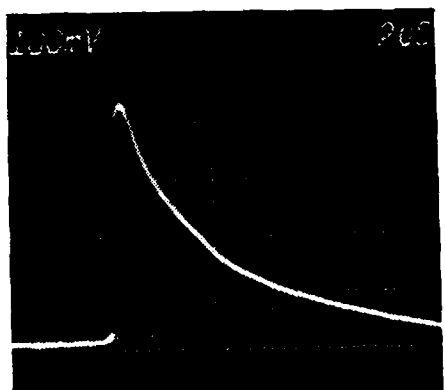


V_x = 290mV at 150V bias

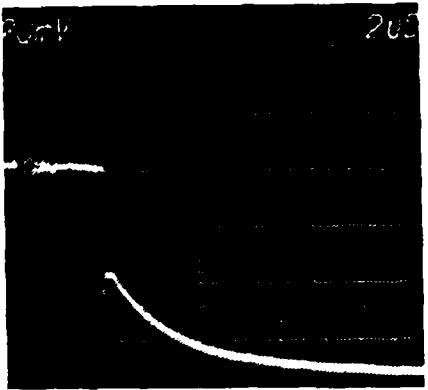


V_x = 340mV at 200V bias

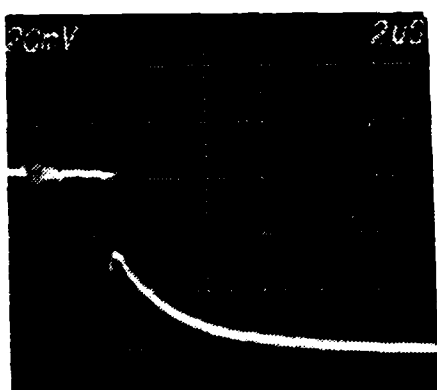
Figure A1.7. Alumina irradiated with 30MeV. Positive bias voltages ranging from 60V to 200V.



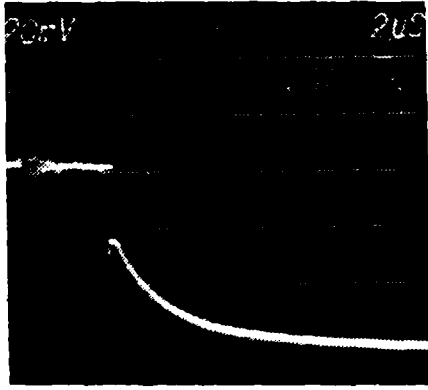
V_x = 440mV at 250V bias



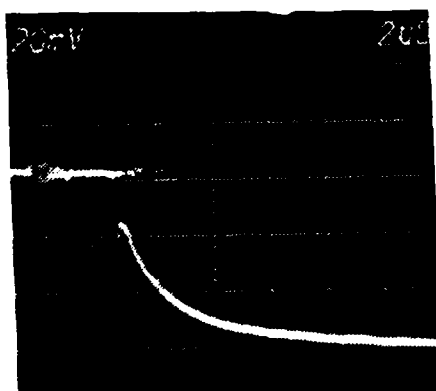
V_x = -40mV at 0V bias



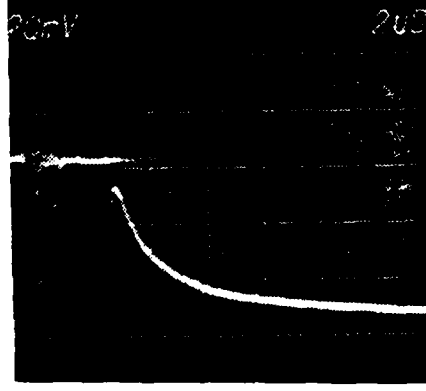
V_x = -24mV at -10V bias



V_x = -22mV at -20V bias

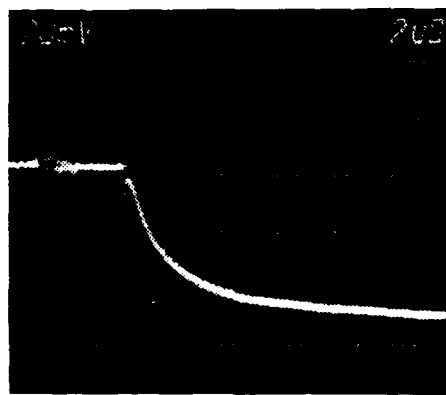


V_x = -15mV at -40V bias

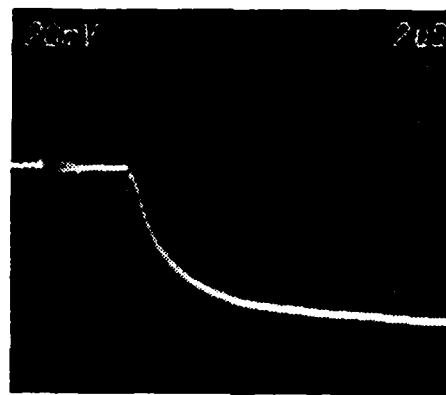


V_x = -6mV at -60V

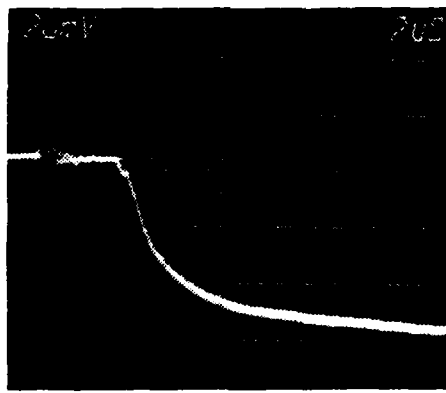
Figure A1.8. Alumina irradiated with 30 MeV electrons.
Bias voltages range from 250V to -60V.



V_x = -4mV at -80V bias



V_x = -2mV at -100V bias

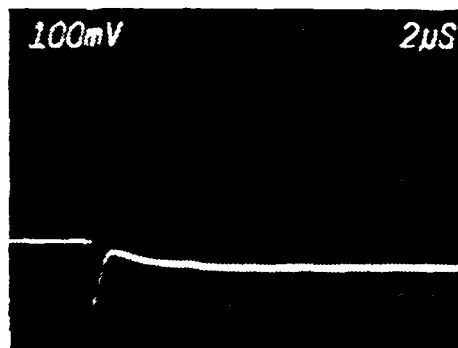


V_x = 0mV at -110V bias

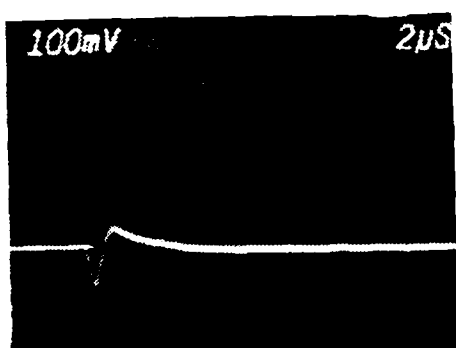
Figure A1.9. Alumina irradiated with 30 MeV electrons.
Negative bias voltages range from -80V to -110V.



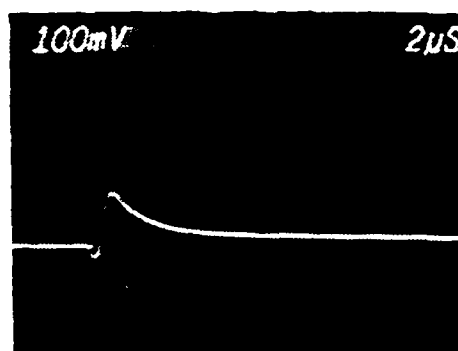
V_x = -52mV at 0V bias



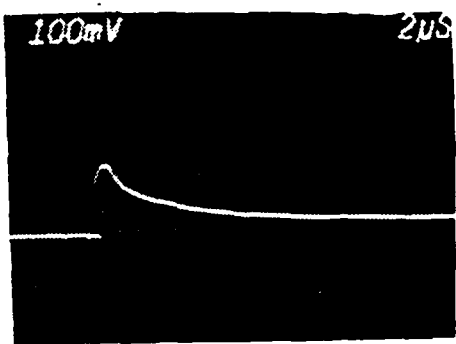
V_x = -20mV at 30V bias



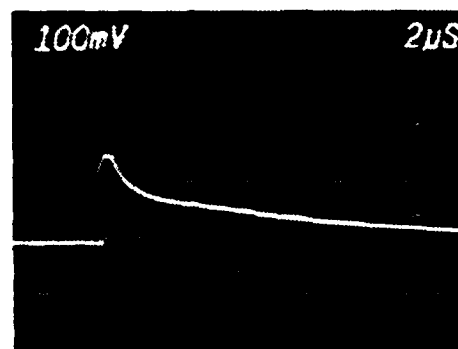
V_x = 40mV at 40V bias



V_x = 100mV at 60V bias

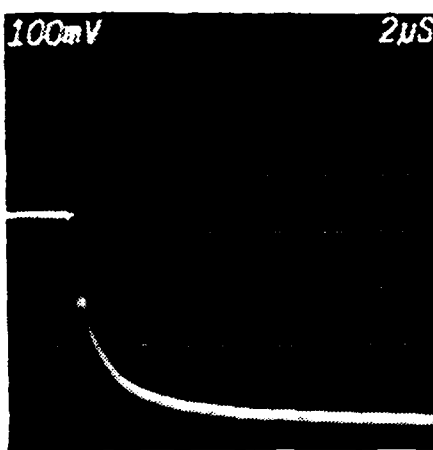


V_x = 130mV at 100V bias

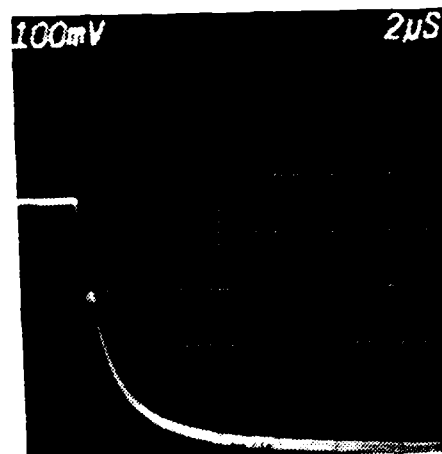


V_x = 160mV at 150V bias

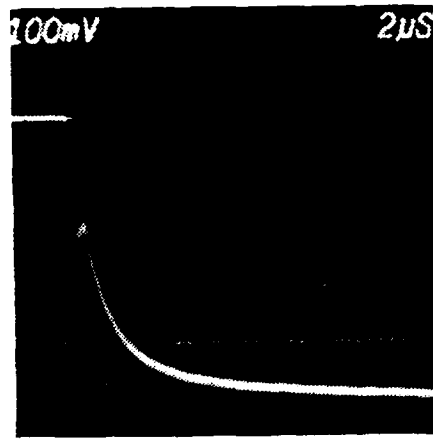
Figure A1.10. Alumina irradiated with 100 MeV electrons.
Positive bias voltages range from 0V to 150V.



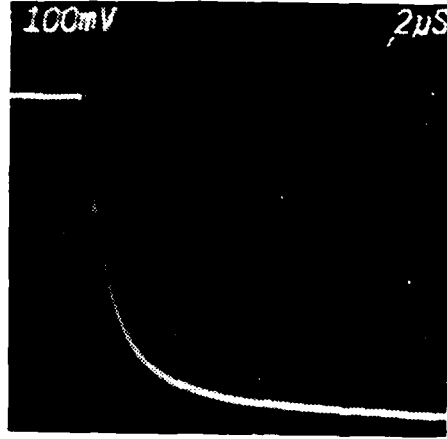
V_x = 210mV at 200V bias



V_x = 310mV at 250V bias

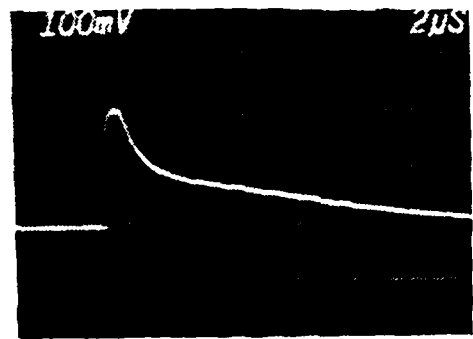


V_x = -220mV at 0V bias

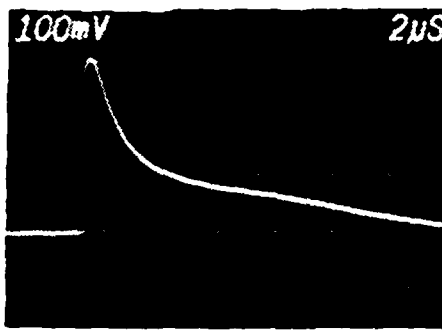


V_x = -160V at -30V bias

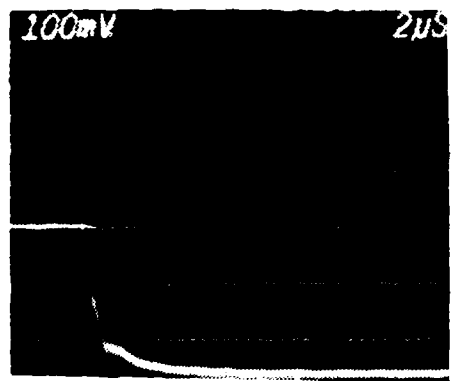
Figure A.1.11. Alumina irradiated with 100 MeV electrons.
Bias voltage range from 250V to -30V.



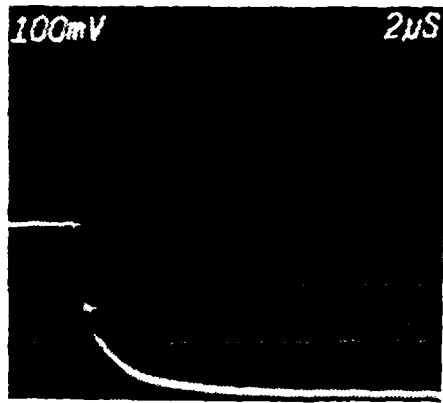
$V_x = -150\text{mV}$ at -40V bias



$V_x = -130\text{mV}$ at -60V bias



$V_x = -180\text{mV}$ at -80V bias



$V_x = -180\text{mV}$ at -100V bias

Figure A.1.12. Alumina irradiated with 100 MeV electrons.
Negative bias voltages range from -40V to -100V .

APPENDIX B

TEST EQUIPMENT LIST:

1. Hewlett Packard 6209B DC Power Supply:
0-320V, 0-.1A
2. Hewlett Packard 6205B Dual DC Power Supply:
0-40V, .3A/0-20V, .6A
3. Hewlett Packard Harrison 6200B DC Power Supply:
0-40V, .75A/0-20V, 1.5A
4. Keithley 617 Programmable Electrometer
5. Tektronix 7603 Oscilloscope
7B85 delayed timing base, 7A26 dual trace
6. Tektronix 7904 Oscilloscope
7B85 delayed timing base, 7A26 dual trace
7. Ohmite Ohm-Ranger
resistance range 1 ohm thru 11,111,110 ohms
8. Weller Electronic Soldering Station
9. Tektronix C-5C Oscilloscope Camera
10. Tektronix C-51 Oscilloscope Camera

APPENDIX C

INPUT PROGRAM FOR ELECTRON PHOTON TRANSPORT ACCEPT CODE - CYLTRAN

To determine coupled electron/photon transport through a multimaterial target, CYLTRAN, a computer simulation code was used. CYLTRAN is part of the Integrated Tiger Series (ITS) of Coupled Electron/Photon Monte Carlo Transport codes. CYLTRAN was used on Cray computers, (at Los Alamos National Laboratory) to simulate 30 MeV and 100 MeV electrons incident on an Al_2O_3 circular disk target. Enclosed is the Accept input program, the 30 MeV and 100 MeV cross sections, and Monte Carlo executions of 30 MeV and 100 Mev incident electrons.

```

PROGRAM XGEN - DECEMBER 1, 1984
VERSION 1.0

END OF FILE ON UNIT 5 - XGEN

SUMMARY OF INPUT DATA

MAXIMUM CROSS SECTION ENERGY = 3.0000e+01
MATERIAL 1 SOLID/LIQUID
DENSITY-RATIO 3.9650e+00
DENSITY 1.0000e+00
SYMBOL ATOMIC NUMBER WEIGHT FRACTION

1 0 8 4.7100e-01
2 AL 13 6.2800e-01
0

* BEGIN EXECUTING PHOTON CROSS SECTION SUBROUTINE - PGEN
* END OF PGEN SUBROUTINE
* BEGIN EXECUTING ELECTRON CROSS SECTION SUBROUTINE - DATPAC
* END OF DATPAC SUBROUTINE

```

30.0 MEV CROSS SECTIONS SAPPHIRE

```

* ELECTRON CROSS SECTIONS FOR MATERIAL NUMBER 1
* -----
* ITRN 121P ISGN 15UB INEL ICYC NCYC NMAX EMAX
* 5 0 1 40 1 1 0 64 3.0000e+01
* INPUT DATA TAPE IDENTIFICATION
* DATATAPE-2 (RESTER AINGER PH-RAD CORR). B4 STERNHEIMER SETS. 30 JAN 6
* OUTOUR DENSITY
* 1.2000e-01 3.9650e+00

```

ORANGE TABLE

```

0 EMAX NCYC NCAL T(NMAX+1) NCAL T(NCAL)
3.0000e+01 8 9.1700e-01 64 1.17100e-01 120 9.98390e-04
0 JMAX LMAX
0 2 1
0 2 A V
0 8.00000 15.99339 0.47100
0 13.00000 26.98140 0.532900
0 PI PD
0 121.89239 121.89239
0

```

C - PARAMETERS FOR DENSITY EFFECT

```

PI C B DM X1 X0
121.89239 -3.22088 0.10476 3.00000 3.00000 0.20000
121.89239 -3.22088 0.10476 3.00000 3.00000 0.20000

```

```

EFFECTIVE Z/A = 0.48039 EFFECTIVE MEAN IONIZATION RADIATION
ENERGY STOPPING POWER TOTAL RADIATION
N COLLISION RADIATION CORR
MEV CM2/G MEV CM2/G MEV CM2/G MEV CM2/G

```

20	0.3638e-04	0.2182e+01	0.7452e-03	0.719e+01	0.7226e-06	0.000e+00	0.5539e-05	0.726e-06	0.000e+00	0.8976e-03	0.000e+00	0.981e-05	0.724e-09
119	0.6868e-03	0.3035e+01	0.7457e-03	0.304e-03	0.728e-06	0.128e-05	0.4248e-05	0.728e-06	0.000e+00	0.9151e-03	0.000e+00	0.9465e-05	0.217e-08
118	0.1873e-03	0.8986e+01	0.483e-03	0.888e+01	0.483e-06	0.005e-05	0.631e-05	0.631e-05	0.000e+00	0.9156e-03	0.000e+00	0.365e-05	0.194e-08
117	1.2946e-03	0.9036e+01	0.7447e-03	0.703e+01	0.7226e-06	0.166e-05	0.8304e-05	0.8304e-05	0.000e+00	0.9155e-03	0.000e+00	1.604e-05	0.194e-08
116	1.4119e-03	0.1155e+01	0.7441e-03	0.7120e+01	0.101e-05	0.101e-05	0.101e-05	0.101e-05	0.000e+00	0.102e-04	0.000e+00	0.844e-05	0.372e-08
115	1.8372e-03	0.7488e+01	0.7434e-03	0.7488e+01	0.285e-05	0.3466e-05	0.8995e-05	0.8995e-05	0.000e+00	0.102e-04	0.000e+00	1.162e-04	0.132e-08
114	1.8791e-03	0.3096e+01	0.7427e-03	0.3276e+01	0.470e-05	0.100e-05	0.470e-05	0.470e-05	0.000e+00	0.102e-04	0.000e+00	1.5178e-04	0.132e-08
113	0.3211e-03	0.6146e+01	0.7419e-03	0.6145e+01	0.7429e-05	0.472e-05	0.751e-05	0.751e-05	0.000e+00	0.102e-04	0.000e+00	2.4468e-04	0.132e-08
112	1.9566e-03	0.7123e+01	0.4018e-03	0.7123e+01	0.204e-05	0.634e-05	0.634e-05	0.634e-05	0.000e+00	0.102e-04	0.000e+00	2.821e-04	0.2042e-08
111	2.1775e-03	0.3355e+01	0.609e-03	0.3356e+01	0.250e-05	0.609e-05	0.609e-05	0.609e-05	0.000e+00	0.102e-04	0.000e+00	3.286e-04	0.2412e-08
110	2.3748e-03	0.8016e+01	0.7306e-03	0.8026e+01	0.220e-05	0.626e-05	0.729e-05	0.729e-05	0.000e+00	0.102e-04	0.000e+00	3.762e-04	0.2782e-08
109	2.5895e-03	0.4018e+01	0.7318e-03	0.4016e+01	0.181e-05	0.286e-05	0.181e-05	0.181e-05	0.000e+00	0.102e-04	0.000e+00	4.395e-04	0.3122e-08
108	2.6232e-03	0.4224e+01	0.7367e-03	0.4225e+01	0.285e-05	0.884e-05	0.112e-05	0.112e-05	0.000e+00	0.102e-04	0.000e+00	5.628e-04	0.3799e-08
107	3.0795e-03	0.2600e+01	0.7367e-03	0.261e+01	0.426e-05	0.830e-05	0.193e-05	0.193e-05	0.000e+00	0.102e-04	0.000e+00	1.788e-04	0.2466e-08
106	3.3593e-03	0.4106e+01	0.7339e-03	0.4106e+01	0.421e-05	0.921e-05	0.773e-05	0.773e-05	0.000e+00	0.102e-04	0.000e+00	1.228e-04	0.2466e-08
105	3.6621e-03	0.2772e+01	0.7223e-03	0.2772e+01	0.242e-05	0.703e-05	0.304e-05	0.304e-05	0.000e+00	0.102e-04	0.000e+00	2.821e-04	0.2042e-08
104	3.8938e-03	0.2546e+01	0.7205e-03	0.3474e+01	0.250e-05	0.609e-05	0.115e-04	0.115e-04	0.000e+00	0.102e-04	0.000e+00	1.312e-04	0.1668e-08
103	4.3559e-03	0.3722e+01	0.2486e+01	0.3230e+01	0.882e-05	0.615e-05	0.881e-05	0.881e-05	0.000e+00	0.102e-04	0.000e+00	2.187e-04	0.1675e-08
102	4.7493e-03	0.1305e+01	0.7368e-03	0.1305e+01	0.300e-05	0.938e-05	0.938e-05	0.938e-05	0.000e+00	0.102e-04	0.000e+00	3.212e-04	0.2122e-08
101	5.7790e-03	0.2935e+01	0.7286e-03	0.2935e+01	0.300e-05	0.938e-05	0.938e-05	0.938e-05	0.000e+00	0.102e-04	0.000e+00	1.221e-04	0.1668e-08
100	5.8477e-03	0.7586e+01	0.7286e-03	0.7586e+01	0.300e-05	0.938e-05	0.938e-05	0.938e-05	0.000e+00	0.102e-04	0.000e+00	2.610e-04	0.1879e-07
99	6.1589e-03	0.2988e+01	0.7033e+01	0.2988e+01	0.300e-05	0.938e-05	0.938e-05	0.938e-05	0.000e+00	0.102e-04	0.000e+00	2.744e-04	0.1914e-07
98	6.7181e-03	0.2477e+01	0.7179e-03	0.2478e+01	0.300e-05	0.938e-05	0.938e-05	0.938e-05	0.000e+00	0.102e-04	0.000e+00	2.225e-04	0.1668e-07
97	7.3222e-03	0.2775e+01	0.1544e-03	0.2776e+01	0.300e-05	0.938e-05	0.938e-05	0.938e-05	0.000e+00	0.102e-04	0.000e+00	1.44e-04	0.1668e-07
96	7.9871e-03	0.1339e+01	0.1286e-03	0.1339e+01	0.188e-04	0.188e-04	0.917e-04	0.917e-04	0.000e+00	0.102e-04	0.000e+00	2.054e-04	0.1668e-07
95	8.7100e-03	0.1998e+01	0.1026e-03	0.1998e+01	0.102e-04	0.219e-04	0.102e-04	0.219e-04	0.000e+00	0.102e-04	0.000e+00	3.242e-04	0.1668e-07
94	9.4826e-03	0.1045e+01	0.1045e-03	0.1045e+01	0.104e-04	0.219e-04	0.104e-04	0.219e-04	0.000e+00	0.102e-04	0.000e+00	3.554e-04	0.1668e-07
93	1.0358e-03	0.1035e+02	0.1035e-03	0.1035e+02	0.1035e-04	0.1035e-04	0.1035e-04	0.1035e-04	0.000e+00	0.102e-04	0.000e+00	4.076e-04	0.1668e-07
92	1.1295e-03	0.1037e+02	0.1037e-03	0.1037e+02	0.1037e-04	0.1037e-04	0.1037e-04	0.1037e-04	0.000e+00	0.102e-04	0.000e+00	4.742e-04	0.1668e-07
91	1.2316e-03	0.1037e+02	0.1037e-03	0.1037e+02	0.1037e-04	0.1037e-04	0.1037e-04	0.1037e-04	0.000e+00	0.102e-04	0.000e+00	5.533e-04	0.1668e-07
90	1.3433e-03	0.1037e+02	0.4416e-03	0.1037e+02	0.1037e-04	0.1037e-04	0.1037e-04	0.1037e-04	0.000e+00	0.102e-04	0.000e+00	6.421e-04	0.1668e-07
89	1.4848e-03	0.1037e+02	0.3593e-03	0.1037e+02	0.1037e-04	0.1037e-04	0.1037e-04	0.1037e-04	0.000e+00	0.102e-04	0.000e+00	7.421e-04	0.1668e-07
88	1.5979e-03	0.1037e+02	0.1323e-03	0.1037e+02	0.1037e-04	0.1037e-04	0.1037e-04	0.1037e-04	0.000e+00	0.102e-04	0.000e+00	8.421e-04	0.1668e-07
87	1.7420e-03	0.1037e+02	0.1833e-03	0.1037e+02	0.1037e-04	0.1037e-04	0.1037e-04	0.1037e-04	0.000e+00	0.102e-04	0.000e+00	9.718e-04	0.1668e-07
86	1.8997e-03	0.1037e+02	0.1037e-03	0.1037e+02	0.1037e-04	0.1037e-04	0.1037e-04	0.1037e-04	0.000e+00	0.102e-04	0.000e+00	1.076e-03	0.1668e-07
85	2.0716e-03	0.1037e+02	0.1037e-03	0.1037e+02	0.1037e-04	0.1037e-04	0.1037e-04	0.1037e-04	0.000e+00	0.102e-04	0.000e+00	1.217e-03	0.1668e-07
84	2.2591e-03	0.1037e+02	0.1037e-03	0.1037e+02	0.1037e-04	0.1037e-04	0.1037e-04	0.1037e-04	0.000e+00	0.102e-04	0.000e+00	1.4173e-03	0.1668e-07
83	2.4632e-03	0.1037e+02	0.1037e-03	0.1037e+02	0.1037e-04	0.1037e-04	0.1037e-04	0.1037e-04	0.000e+00	0.102e-04	0.000e+00	1.771e-03	0.1668e-07
82	2.6855e-03	0.1037e+02	0.1037e-03	0.1037e+02	0.1037e-04	0.1037e-04	0.1037e-04	0.1037e-04	0.000e+00	0.102e-04	0.000e+00	2.171e-03	0.1668e-07
81	3.2471e-03	0.1037e+02	0.1037e-03	0.1037e+02	0.1037e-04	0.1037e-04	0.1037e-04	0.1037e-04	0.000e+00	0.102e-04	0.000e+00	2.717e-03	0.1668e-07
80	3.9484e-03	0.1037e+02	0.1037e-03	0.1037e+02	0.1037e-04	0.1037e-04	0.1037e-04	0.1037e-04	0.000e+00	0.102e-04	0.000e+00	3.494e-03	0.1668e-07
79	3.4810e-03	0.7074e+02	0.1037e-03	0.7074e+02	0.1037e-04	0.1037e-04	0.1037e-04	0.1037e-04	0.000e+00	0.102e-04	0.000e+00	4.040e-03	0.1668e-07
78	3.7932e-03	0.5933e+02	0.1037e-03	0.5933e+02	0.1037e-04	0.1037e-04	0.1037e-04	0.1037e-04	0.000e+00	0.102e-04	0.000e+00	4.744e-03	0.1668e-07
77	4.1432e-03	0.1037e+02	0.1037e-03	0.1037e+02	0.1037e-04	0.1037e-04	0.1037e-04	0.1037e-04	0.000e+00	0.102e-04	0.000e+00	5.533e-03	0.1668e-07
76	4.5162e-03	0.1037e+02	0.1037e-03	0.1037e+02	0.1037e-04	0.1037e-04	0.1037e-04	0.1037e-04	0.000e+00	0.102e-04	0.000e+00	6.426e-03	0.1668e-07
75	4.9271e-03	0.1037e+02	0.1037e-03	0.1037e+02	0.1037e-04	0.1037e-04	0.1037e-04	0.1037e-04	0.000e+00	0.102e-04	0.000e+00	7.421e-03	0.1668e-07
74	5.3713e-03	0.1037e+02	0.1037e-03	0.1037e+02	0.1037e-04	0.1037e-04	0.1037e-04	0.1037e-04	0.000e+00	0.102e-04	0.000e+00	8.421e-03	0.1668e-07
73	5.8593e-03	0.1037e+02	0.1037e-03	0.1037e+02	0.1037e-04	0.1037e-04	0.1037e-04	0.1037e-04	0.000e+00	0.102e-04	0.000e+00	9.421e-03	0.1668e-07
72	6.3857e-03	0.1037e+02	0.1037e-03	0.1037e+02	0.1037e-04	0.1037e-04	0.1037e-04	0.1037e-04	0.000e+00	0.102e-04	0.000e+00	1.042e-02	0.1668e-07
71	6.9160e-03	0.1037e+02	0.1037e-03	0.1037e+02	0.1037e-04	0.1037e-04	0.1037e-04	0.1037e-04	0.000e+00	0.102e-04	0.000e+00	1.142e-02	0.1668e-07
70	7.5397e-03	0.1037e+02	0.1037e-03	0.1037e+02	0.1037e-04	0.1037e-04	0.1037e-04	0.1037e-04	0.000e+00	0.102e-04	0.000e+00	1.242e-02	0.1668e-07
69	8.2884e-03	0.1037e+02	0.1037e-03	0.1037e+02	0.1037e-04	0.1037e-04	0.1037e-04	0.1037e-04	0.000e+00	0.102e-04	0.000e+00	1.342e-02	0.1668e-07
68	9.0364e-03	0.1037e+02	0.1037e-03	0.1037e+02	0.1037e-04	0.1037e-04	0.1037e-04	0.1037e-04	0.000e+00	0.102e-04	0.000e+00	1.442e-02	0.1668e-07
67	9.8532e-03	0.1037e+02	0.1037e-03	0.1037e+02	0.1037e-04	0.1037e-04	0.1037e-04	0.1037e-04	0.000e+00	0.102e-04	0.000e+00	1.542e-02	0.1668e-07
66	1												

```

57 2.3138e-01 2.158e+00 7.731e-03 2.168e+00 6.959e-02 2.106e-03 5.300e-01 0.000e+00 5.582e-03 3.818e-03 3.738e-05
58 2.8859e-01 2.083e+00 7.922e-03 2.050e+00 7.957e-02 2.237e-03 5.551e-01 0.000e+00 3.808e-03 3.975e-03 7.807e-05
59 2.7072e-01 2.036e+00 8.154e-03 2.021e+00 8.093e-02 2.316e-03 5.513e-01 0.000e+00 3.805e-03 3.975e-03 7.807e-05
60 1.951e-01 1.951e-00 8.418e-03 1.958e+00 8.065e-01 2.316e-03 6.068e-01 0.000e+00 4.314e-03 1.26e-02 9.051e-05
61 3.0195e-01 3.0195e-00 8.891e-03 3.021e+00 8.065e-01 2.315e-03 6.212e-01 0.000e+00 4.314e-03 1.26e-02 9.051e-05
62 3.2145e-01 3.2145e-00 8.708e-03 3.203e+00 8.065e-01 2.315e-03 6.212e-01 0.000e+00 4.314e-03 1.26e-02 9.051e-05
63 3.8446e-01 3.8446e-00 8.404e-03 3.853e+00 8.055e-01 2.308e-03 6.570e-01 0.000e+00 4.903e-03 1.425e-02 1.220e-04
64 5.9476e-01 5.9476e-00 8.417e-03 5.939e+00 8.055e-01 2.308e-03 6.570e-01 0.000e+00 4.903e-03 1.425e-02 1.220e-04
65 6.2991e-01 6.2991e-00 8.424e-03 6.230e+00 8.042e-01 2.302e-03 6.812e-01 0.000e+00 5.258e-03 1.788e-02 1.650e-04
66 4.2985e-01 4.2985e-00 8.424e-03 4.230e+00 8.042e-01 2.302e-03 6.812e-01 0.000e+00 5.258e-03 1.788e-02 1.650e-04
67 4.8875e-01 4.8875e-00 8.424e-03 4.730e+00 8.042e-01 2.187e-03 7.177e-01 0.000e+00 5.955e-03 2.228e-02 2.428e-04
68 5.1118e-01 5.1118e-00 8.424e-03 5.634e+00 8.042e-01 2.187e-03 7.177e-01 0.000e+00 5.955e-03 2.419e-02 2.626e-04
69 6.0749e-01 6.0749e-00 8.424e-03 6.843e+00 8.042e-01 2.483e-03 7.177e-01 0.000e+00 5.955e-03 2.419e-02 2.626e-04
70 7.2291e-01 7.2291e-00 8.424e-03 7.977e-01 8.042e-01 2.795e-03 7.177e-01 0.000e+00 5.955e-03 2.419e-02 2.626e-04
71 7.8834e-01 7.8834e-00 8.424e-03 8.988e-01 8.042e-01 3.108e-03 7.177e-01 0.000e+00 5.955e-03 2.419e-02 2.626e-04
72 8.5869e-01 8.5869e-00 8.424e-03 9.591e-01 8.042e-01 3.423e-03 7.177e-01 0.000e+00 5.955e-03 2.419e-02 2.626e-04
73 9.3750e-01 9.3750e-00 8.424e-03 1.048e-01 8.042e-01 3.736e-03 7.177e-01 0.000e+00 5.955e-03 2.419e-02 2.626e-04
74 1.0224e+00 1.0224e+00 8.424e-03 1.217e-01 8.042e-01 4.042e-03 7.177e-01 0.000e+00 5.955e-03 2.419e-02 2.626e-04
75 1.1459e+00 1.1459e+00 8.424e-03 1.298e-01 8.042e-01 4.352e-03 7.177e-01 0.000e+00 5.955e-03 2.419e-02 2.626e-04
76 1.2958e+00 1.2958e+00 8.424e-03 1.511e-01 8.042e-01 4.664e-03 7.177e-01 0.000e+00 5.955e-03 2.419e-02 2.626e-04
77 1.5031e+00 1.5031e+00 8.424e-03 1.722e-01 8.042e-01 5.074e-03 7.177e-01 0.000e+00 5.955e-03 2.419e-02 2.626e-04
78 1.7816e+00 1.7816e+00 8.424e-03 1.933e-01 8.042e-01 5.484e-03 7.177e-01 0.000e+00 5.955e-03 2.419e-02 2.626e-04
79 1.9169e+00 1.9169e+00 8.424e-03 2.145e-01 8.042e-01 5.894e-03 7.177e-01 0.000e+00 5.955e-03 2.419e-02 2.626e-04
80 2.2294e+00 2.2294e+00 8.424e-03 2.356e-01 8.042e-01 6.304e-03 7.177e-01 0.000e+00 5.955e-03 2.419e-02 2.626e-04
81 2.4316e+00 2.4316e+00 8.424e-03 2.567e-01 8.042e-01 6.715e-03 7.177e-01 0.000e+00 5.955e-03 2.419e-02 2.626e-04
82 2.6717e+00 2.6717e+00 8.424e-03 2.778e-01 8.042e-01 7.126e-03 7.177e-01 0.000e+00 5.955e-03 2.419e-02 2.626e-04
83 2.9116e+00 2.9116e+00 8.424e-03 2.989e-01 8.042e-01 7.537e-03 7.177e-01 0.000e+00 5.955e-03 2.419e-02 2.626e-04
84 3.1934e+00 3.1934e+00 8.424e-03 3.200e-01 8.042e-01 7.948e-03 7.177e-01 0.000e+00 5.955e-03 2.419e-02 2.626e-04
85 3.4886e+00 3.4886e+00 8.424e-03 3.433e-01 8.042e-01 8.359e-03 7.177e-01 0.000e+00 5.955e-03 2.419e-02 2.626e-04
86 3.7800e+00 3.7800e+00 8.424e-03 3.754e-01 8.042e-01 8.770e-03 7.177e-01 0.000e+00 5.955e-03 2.419e-02 2.626e-04
87 4.0946e+00 4.0946e+00 8.424e-03 4.075e-01 8.042e-01 9.181e-03 7.177e-01 0.000e+00 5.955e-03 2.419e-02 2.626e-04
88 4.4955e+00 4.4955e+00 8.424e-03 4.386e-01 8.042e-01 9.592e-03 7.177e-01 0.000e+00 5.955e-03 2.419e-02 2.626e-04
89 4.8831e+00 4.8831e+00 8.424e-03 4.717e-01 8.042e-01 9.993e-03 7.177e-01 0.000e+00 5.955e-03 2.419e-02 2.626e-04
90 5.2777e+00 5.2777e+00 8.424e-03 5.028e-01 8.042e-01 1.039e-02 7.177e-01 0.000e+00 5.955e-03 2.419e-02 2.626e-04
91 5.6674e+00 5.6674e+00 8.424e-03 5.339e-01 8.042e-01 1.079e-02 7.177e-01 0.000e+00 5.955e-03 2.419e-02 2.626e-04
92 6.0571e+00 6.0571e+00 8.424e-03 5.650e-01 8.042e-01 1.119e-02 7.177e-01 0.000e+00 5.955e-03 2.419e-02 2.626e-04
93 6.4378e+00 6.4378e+00 8.424e-03 5.961e-01 8.042e-01 1.159e-02 7.177e-01 0.000e+00 5.955e-03 2.419e-02 2.626e-04
94 6.8285e+00 6.8285e+00 8.424e-03 6.272e-01 8.042e-01 1.199e-02 7.177e-01 0.000e+00 5.955e-03 2.419e-02 2.626e-04
95 7.2192e+00 7.2192e+00 8.424e-03 6.583e-01 8.042e-01 1.239e-02 7.177e-01 0.000e+00 5.955e-03 2.419e-02 2.626e-04
96 7.6100e+00 7.6100e+00 8.424e-03 6.894e-01 8.042e-01 1.279e-02 7.177e-01 0.000e+00 5.955e-03 2.419e-02 2.626e-04
97 8.0108e+00 8.0108e+00 8.424e-03 7.210e-01 8.042e-01 1.319e-02 7.177e-01 0.000e+00 5.955e-03 2.419e-02 2.626e-04
98 8.3916e+00 8.3916e+00 8.424e-03 7.521e-01 8.042e-01 1.359e-02 7.177e-01 0.000e+00 5.955e-03 2.419e-02 2.626e-04
99 8.7824e+00 8.7824e+00 8.424e-03 7.832e-01 8.042e-01 1.399e-02 7.177e-01 0.000e+00 5.955e-03 2.419e-02 2.626e-04
100 9.1632e+00 9.1632e+00 8.424e-03 8.143e-01 8.042e-01 1.439e-02 7.177e-01 0.000e+00 5.955e-03 2.419e-02 2.626e-04
101 9.5440e+00 9.5440e+00 8.424e-03 8.454e-01 8.042e-01 1.479e-02 7.177e-01 0.000e+00 5.955e-03 2.419e-02 2.626e-04
102 9.9248e+00 9.9248e+00 8.424e-03 8.765e-01 8.042e-01 1.519e-02 7.177e-01 0.000e+00 5.955e-03 2.419e-02 2.626e-04
103 1.0302e+01 1.0302e+00 8.424e-03 9.076e-01 8.042e-01 1.559e-02 7.177e-01 0.000e+00 5.955e-03 2.419e-02 2.626e-04
104 1.0679e+01 1.0679e+00 8.424e-03 9.387e-01 8.042e-01 1.599e-02 7.177e-01 0.000e+00 5.955e-03 2.419e-02 2.626e-04
105 1.1213e+01 1.1213e+00 8.424e-03 9.718e-01 8.042e-01 1.639e-02 7.177e-01 0.000e+00 5.955e-03 2.419e-02 2.626e-04
106 1.1731e+01 1.1731e+00 8.424e-03 1.003e+00 8.042e-01 1.679e-02 7.177e-01 0.000e+00 5.955e-03 2.419e-02 2.626e-04
107 1.2239e+01 1.2239e+00 8.424e-03 1.034e+00 8.042e-01 1.719e-02 7.177e-01 0.000e+00 5.955e-03 2.419e-02 2.626e-04
108 1.2737e+01 1.2737e+00 8.424e-03 1.065e+00 8.042e-01 1.759e-02 7.177e-01 0.000e+00 5.955e-03 2.419e-02 2.626e-04
109 1.3225e+01 1.3225e+00 8.424e-03 1.106e+00 8.042e-01 1.799e-02 7.177e-01 0.000e+00 5.955e-03 2.419e-02 2.626e-04
110 1.3713e+01 1.3713e+00 8.424e-03 1.147e+00 8.042e-01 1.839e-02 7.177e-01 0.000e+00 5.955e-03 2.419e-02 2.626e-04
111 1.4191e+01 1.4191e+00 8.424e-03 1.188e+00 8.042e-01 1.879e-02 7.177e-01 0.000e+00 5.955e-03 2.419e-02 2.626e-04
112 1.4679e+01 1.4679e+00 8.424e-03 2.168e+00 8.042e-01 1.919e-02 7.177e-01 0.000e+00 5.955e-03 2.419e-02 2.626e-04
113 1.5167e+01 1.5167e+00 8.424e-03 2.379e+00 8.042e-01 1.959e-02 7.177e-01 0.000e+00 5.955e-03 2.419e-02 2.626e-04
114 1.5655e+01 1.5655e+00 8.424e-03 2.590e+00 8.042e-01 1.999e-02 7.177e-01 0.000e+00 5.955e-03 2.419e-02 2.626e-04
115 1.6143e+01 1.6143e+00 8.424e-03 2.801e+00 8.042e-01 2.039e-02 7.177e-01 0.000e+00 5.955e-03 2.419e-02 2.626e-04
116 1.6631e+01 1.6631e+00 8.424e-03 3.012e+00 8.042e-01 2.079e-02 7.177e-01 0.000e+00 5.955e-03 2.419e-02 2.626e-04
117 1.7119e+01 1.7119e+00 8.424e-03 3.223e+00 8.042e-01 2.119e-02 7.177e-01 0.000e+00 5.955e-03 2.419e-02 2.626e-04
118 1.7607e+01 1.7607e+00 8.424e-03 3.434e+00 8.042e-01 2.159e-02 7.177e-01 0.000e+00 5.955e-03 2.419e-02 2.626e-04
119 1.8095e+01 1.8095e+00 8.424e-03 3.645e+00 8.042e-01 2.199e-02 7.177e-01 0.000e+00 5.955e-03 2.419e-02 2.626e-04
120 1.8583e+01 1.8583e+00 8.424e-03 3.856e+00 8.042e-01 2.239e-02 7.177e-01 0.000e+00 5.955e-03 2.419e-02 2.626e-04
121 1.9071e+01 1.9071e+00 8.424e-03 4.067e+00 8.042e-01 2.279e-02 7.177e-01 0.000e+00 5.955e-03 2.419e-02 2.626e-04
122 1.9559e+01 1.9559e+00 8.424e-03 4.278e+00 8.042e-01 2.319e-02 7.177e-01 0.000e+00 5.955e-03 2.419e-02 2.626e-04
123 2.0047e+01 2.0047e+00 8.424e-03 4.489e+00 8.042e-01 2.359e-02 7.177e-01 0.000e+00 5.955e-03 2.419e-02 2.626e-04
124 2.0535e+01 2.0535e+00 8.424e-03 4.699e+00 8.042e-01 2.399e-02 7.177e-01 0.000e+00 5.955e-03 2.419e-02 2.626e-04
125 2.1023e+01 2.1023e+00 8.424e-03 4.910e+00 8.042e-01 2.439e-02 7.177e-01 0.000e+00 5.955e-03 2.419e-02 2.626e-04
126 2.1511e+01 2.1511e+00 8.424e-03 5.121e+00 8.042e-01 2.479e-02 7.177e-01 0.000e+00 5.955e-03 2.419e-02 2.626e-04
127 2.1999e+01 2.1999e+00 8.424e-03 5.332e+00 8.042e-01 2.519e-02 7.177e-01 0.000e+00 5.955e-03 2.419e-02 2.626e-04
128 2.2487e+01 2.2487e+00 8.424e-03 5.543e+00 8.042e-01 2.559e-02 7.177e-01 0.000e+00 5.955e-03 2.419e-02 2.626e-04
129 2.2975e+01 2.2975e+00 8.424e-03 5.754e+00 8.042e-01 2.599e-02 7.177e-01 0.000e+00 5.955e-03 2.419e-02 2.626e-04
130 2.3463e+01 2.3463e+00 8.424e-03 5.965e+00 8.042e-01 2.639e-02 7.177e-01 0.000e+00 5.955e-03 2.419e-02 2.626e-04
131 2.3951e+01 2.3951e+00 8.424e-03 6.176e+00 8.042e-01 2.679e-02 7.177e-01 0.000e+00 5.955e-03 2.419e-02 2.626e-04
132 2.4439e+01 2.4439e+00 8.424e-03 6.387e+00 8.042e-01 2.719e-02 7.177e-01 0.000e+00 5.955e-03 2.419e-02 2.626e-04
133 2.4927e+01 2.4927e+00 8.424e-03 6.598e+00 8.042e-01 2.759e-02 7.177e-01 0.000e+00 5.955e-03 2.419e-02 2.626e-04
134 2.5415e+01 2.5415e+00 8.424e-03 6.809e+00 8.042e-01 2.799e-02 7.177e-01 0.000e+00 5.955e-03 2.419e-02 2.626e-04
135 2.5893e+01 2.5893e+00 8.424e-03 7.020e+00 8.042e-01 2.839e-02 7.177e-01 0.000e+00 5.955e-03 2.419e-02 2.626e-04
136 2.6381e+01 2.6381e+00 8.424e-03 7.231e+00 8.042e-01 2.879e-02 7.177e-01 0.000e+00 5.955e-03 2.419e-02 2.626e-04
137 2.6869e+01 2.6869e+00 8.424e-03 7.442e+00 8.042e-01 2.919e-02 7.177e-01 0.000e+00 5.955e-03 2.419e-02 2.626e-04
138 2.7357e+01 2.7357e+00 8.424e-03 7.653e+00 8.042e-01 2.959e-02 7.177e-01 0.000e+00 5.955e-03 2.419e-02 2.626e-04
139 2.7845e+01 2.7845e+00 8.424e-03 7.864e+00 8.042e-01 2.999e-02 7.177e-01 0.000e+00 5.955e-03 2.419e-02 2.626e-04
140 2.8333e+01 2.8333e+00 8.424e-03 8.075e+00 8.042e-01 3.039e-02 7.177e-01 0.000e+00 5.955e-03 2.419e-02 2.626e-04
141 2.8821e+01 2.8821e+00 8.424e-03 8.286e+00 8.042e-01 3.079e-02 7.177e-01 0.000e+00 5.955e-03 2.419e-02 2.626e-04
142 2.9309e+01 2.9309e+00 8.424e-03 8.497e+00 8.042e-01 3.119e-02 7.177e-01 0.000e+00 5.955e-03 2.419e-02 2.626e-04
143 2.9797e+01 2.9797e+00 8.424e-03 8.708e+00 8.042e-01 3.159e-02 7.177e-01 0.000e+00 5.955e-03 2.419e-02 2.626e-04
144 3.0285e+01 3.0285e+00 8.424e-03 8.919e+00 8.042e-01 3.199e-02 7.177e-01 0.000e+00 5.955e-03 2.419e-02 2.626e-04
145 3.0773e+01 3.0773e+00 8.424e-03 9.130e+00 8.042e-01 3.239e-02 7.177e-01 0.000e+00 5.955e-03 2.419e-02 2.626e-04
146 3.1261e+01 3.1261e+00 8.424e-03 9.341e+00 8.042e-01 3.279e-02 7.177e-01 0.000e+00 5.955e-03 2.419e-02 2.626e-04
147 3.1749e+01 3.1749e+00 8.424e-03 9.552e+00 8.042e-01 3.319e-02 7.177e-01 0.000e+00 5.955e-03 2.419e-02 2.626e-04
148 3.2237e+01 3.2237e+00 8.424e-03 9.763e+00 8.042e-01 3.359e-02 7.177e-01 0.000e+00 5.955e-03 2.419e-02 2.626e-04
149 3.2725e+01 3.2725e+00 8.424e-03 9.974e+00 8.042e-01 3.399e-02 7.177e-01 0.000e+00 5.955e-03 2.419e-02 2.626e-04
150 3.3213e+01 3.3213e+00 8.424e-03 1.018e+01 8.042e-01 3.439e-02 7.177e-01 0.000e+00 5.955e-03 2.419e-02 2.626e-04
151 3.3691e+01 3.3691e+00 8.424e-03 1.039e+01 8.042e-01 3.479e-02 7.177e-01 0.000e+00 5.955e-03 2.419e-02 2.626e-04
152 3.4179e+01 3.4179e+00 8.424e-03 1.060e+01 8.042e-01 3.519e-02 7.177e-01 0.000e+00 5.955e-03 2.419e-02 2.626e-04
153 3.4667e+01 3.4667e+00 8.424e-03 1.081e+01 8.042e-01 3.559e-02 7.177e-01 0.000e+00 5.955e-03 2.419e-02 2.626e-04
154 3.5155e+01 3.5155e+00 8.424e-03 1.102e+01 8.042e-01 3.599e-02 7.177e-01 0.000e+00 5.
```

ZONE MATERIAL PLANE (CM) PLANE (CM) RADIUS (CM) RADIUS (CM) CUTOFF (MEV) FORCING FRACTION
 1 0.0000e+00 2.917000e-03 0.00000e+00 9.52500e-01 1.500e+00 5.000e-01

* SOURCE INFORMATION *

* SOURCE ELECTRONS
 THE MAXIMUM SOURCE ENERGY IS 30.00000 MEV
 THE GLOBAL ELECTRON CUTOFF ENERGY IS 0.0000 MEV
 THE PHOTON CUTOFF ENERGY IS 0.0000 MEV
 COORDINATES OF THE POINT SOURCE OR THE CENTER OF THE BEAM (DISK) SOURCE ARE
 X = 0.0000e+00 CM Y = 0.0000e+00 CM Z = 0.0000e+00 CM
 THE RADIUS OF THE BEAM (DISK) SOURCE IS 0.0000e+00 CM
 REFERENCE DIRECTION FOR ANGULAR DISTRIBUTION IS DEFINED BY
 THETA = 0.000 DEGREES PHI = 0.000 DEGREES

OMNIDIRECTIONAL SOURCE IN REFERENCE DIRECTION
 THE STANDARD ERROR ESTIMATES ARE BASED ON 10 BATCHES OF 100000 HISTORIES EACH

* OUTPUT OPTIONS *

* ELECTRON-ESCAPE ENERGY CLASSIFICATIONS (MEV)
 27.00000 24.00000 21.00000 18.00000 15.00000 12.00000
 9.00000 6.00000 3.00000 1.50000

* ELECTRON-ESCAPE POLAR ANGLE CLASSIFICATIONS (DEGREES)
 18.00000 36.00000 54.00000 72.00000 90.00000 108.00000
 128.00000 144.00000 162.00000 180.00000

* ELECTRON-ESCAPE AZIMUTH ANGLE CLASSIFICATIONS (DEGREES)
 180.00000 180.00000 182.00000 180.00000

* PHOTON-ESCAPE ENERGY CLASSIFICATIONS (MEV)
 27.00000 24.00000 21.00000 18.00000 15.00000 12.00000
 9.00000 6.00000 3.00000 0.01000

* PHOTON-ESCAPE POLAR ANGLE CLASSIFICATIONS (DEGREES)
 18.00000 36.00000 54.00000 72.00000 90.00000 108.00000
 128.00000 144.00000 162.00000 180.00000

* PHOTON-ESCAPE AZIMUTH ANGLE CLASSIFICATIONS (DEGREES)
 180.00000 180.00000 182.00000 180.00000

* ELECTRON-FLUX ENERGY CLASSIFICATIONS (MEV)
 27.00000 24.00000 21.00000 18.00000 15.00000 12.00000
 9.00000 6.00000 3.00000 1.50000

* PHOTON-FLUX ENERGY CLASSIFICATIONS (MEV)
 27.00000 24.00000 21.00000 18.00000 15.00000 12.00000
 9.00000 6.00000 3.00000 0.01000

* PHYSICAL OPTIONS *

* ELECTRON COLLISION AND RADIATION ENERGY LOSS STRAGGLING
 ONE-STEP-ELECTRON PRODUCTION
 ONE-COUPLED-INELASTIC SCATTERING DEFLECTIONS
 OBERRSTRÄHLUNG INTRINSIC ANGLE OF EMISSION FROM TABULATED DISTRIBUTION
 OPHTON-PRODUCED ELECTRONS FOLLOWED

MATERIAL NO. 1
 ELECTRON RANGE AT MAXIMUM SOURCE ENERGY IS 0.12774e+02 (G/CM**2)
 K-X-RAY QUANTA FOLLOWED
 ELECTRON IMPACT IONIZATION SAMPLED

MATERIAL NO. 2
 ELECTRON RANGE AT MAXIMUM SOURCE ENERGY IS 0.13516e+02 (G/CM**2)
 K-X-RAY QUANTA FOLLOWED
 ELECTRON IMPACT IONIZATION SAMPLED

* ANNIHILATION QUANTA FOLLOWED
 THE VOLUME RATIO IS 0.100000000000e+01

* 30.0 MEV TEST PROGRAM

AZIMUTHAL INTERVAL IS 0.00000 TO 180.00000 DEGREES
 (NUMBER/(MEV*SR)). NORMALIZED TO ONE PARTICLE

A graph with the y-axis labeled "E (MeV)" and the x-axis labeled "THE TA = 162.000". The curve starts at approximately (0, 180) and decreases monotonically, approaching a horizontal asymptote at low values of E.

30.0000	-27.0000	0.00e+00	99
27.0000	-24.0000	0.00e+00	99
24.0000	-21.0000	0.00e+00	99
21.0000	-18.0000	0.00e+00	99
18.0000	-15.0000	0.00e+00	99
15.0000	-12.0000	0.00e+00	99
12.0000	-9.0000	0.00e+00	99
9.0000	-6.0000	0.00e+00	99
6.0000	-3.0000	0.00e+00	99
3.0000	-1.5000	0.00e+00	99

ENERGY SPECTRA AND ANGULAR DISTRIBUTIONS OF ELECTRONS LATERALLY ESCAPING

AZIMUTHAL INTERVAL IS 0.00000 TO 180.00000 DEGREES
 (NUMBER/(MEV*SR)). NORMALIZED TO ONE PARTICLE

1,000
1,000
36,000
18,000
1,000
36,000
54,000
36,000
54,000
36,000
54,000
72,000
72,000
90,000
90,000

66 00+600.0 66 00+600.0 66 00+600.0 66 00+600.0

0.00e+00 99 0.00e+00 99 0.00e+00 99 0.00e+00 99 0.00e+00 99

ENERGY SPECTRA AND ANGULAR DISTRIBUTIONS OF ELECTRONS

AZIMUTHAL INTERVAL IS .0.00000 TO 180.00000 DEG
(NUMBER/(MEV.SR). NORMALIZED TO ONE PARTICLE)

— 3 —

卷之三

ପ୍ରକାଶକ ମେଳିତିକା

卷之三

1996-0006

ENERGY SPECTRA OF TRANSMITTED PHOTONS

(NUMBER/MEV. NORMALIZED TO ONE INCIDENT PARTICLE)

30.0000	-	27.0000	1.53e-05	15
27.0000	-	24.0000	3.10e-05	7
24.0000	-	21.0000	4.43e-05	10
21.0000	-	18.0000	5.03e-05	9
18.0000	-	15.0000	7.23e-05	7
15.0000	-	12.0000	9.00e-05	5
12.0000	-	9.0000	1.24e-04	10
9.0000	-	6.0000	1.92e-04	3
6.0000	-	3.0000	3.67e-04	1
3.0000	-	0.0100	3.31e-03	

卷之三

卷之三

0 E (MEV) ENERGY SPECTRA OF REFLECTED PHOTONS
(NUMBER/MEV. NORMALIZED TO ONE INCIDENT PARTICLE)

30.0000	-	27.0000	0.00e+00	99
27.0000	-	24.0000	0.00e+00	99
24.0000	-	21.0000	0.00e+00	99
21.0000	-	18.0000	0.00e+00	99
18.0000	-	15.0000	0.00e+00	99
15.0000	-	12.0000	0.00e+00	99
12.0000	-	9.0000	0.00e+00	99
9.0000	-	6.0000	0.00e+00	99
6.0000	-	3.0000	0.00e+00	99
3.0000	-	0.0100	4.87e-04	2

0 E (MEV) ENERGY SPECTRA OF LATERALLY ESCAPING PHOTONS
(NUMBER/MEV. NORMALIZED TO ONE INCIDENT PARTICLE)

30.0000	-	27.0000	0.00e+00	99
27.0000	-	24.0000	0.00e+00	99
24.0000	-	21.0000	0.00e+00	99
21.0000	-	18.0000	0.00e+00	99
18.0000	-	15.0000	0.00e+00	99
15.0000	-	12.0000	0.00e+00	99
12.0000	-	9.0000	0.00e+00	99
9.0000	-	6.0000	0.00e+00	99
6.0000	-	3.0000	0.00e+00	99
3.0000	-	0.0100	6.03e-10	48

0 PHI (DEG)= 0.000 ANGULAR DISTRIBUTIONS OF TRANSMITTED AND REFLECTED PHOTON INTENSITY
(MEV/SR. NORMALIZED TO ONE INCIDENT PARTICLE)

0.0000	-	18.0000	1.14e-01	2
18.0000	-	36.0000	1.56e-04	2
36.0000	-	54.0000	2.74e-05	59
54.0000	-	72.0000	6.21e-06	59
72.0000	-	90.0000	5.31e-06	24
90.0000	-	108.0000	4.39e-06	5
108.0000	-	126.0000	6.83e-06	5
126.0000	-	144.0000	6.14e-06	5
144.0000	-	162.0000	7.29e-06	8
162.0000	-	180.0000	6.88e-06	6

0 PHI (DEG)= 0.000 ANGULAR DISTRIBUTIONS OF LATERALLY ESCAPING PHOTON INTENSITY
(MEV/SR. NORMALIZED TO ONE INCIDENT PARTICLE)

0.0000	-	18.0000	0.00e+00	99
18.0000	-	36.0000	0.00e+00	99
36.0000	-	54.0000	0.00e+00	99
54.0000	-	72.0000	0.00e+00	99
72.0000	-	90.0000	1.19e-10	715
90.0000	-	108.0000	3.14e-10	68
108.0000	-	126.0000	0.00e+00	99
126.0000	-	144.0000	0.00e+00	99
144.0000	-	162.0000	0.00e+00	99
162.0000	-	180.0000	0.00e+00	99

0.000050 0.000036
 0.000049 0.000044
 0.000127 0.000099
 O RATIO OF SCATTERING TO SCATTERING PLUS PAIR PRODUCTION ATTENUATION COEFFICIENTS
 0.003562 0.004484 0.006042 0.007307 0.009323 0.012006
 0.019266 0.026255 0.040730 0.052435 0.071847 0.087451
 0.11168 0.151439 0.230586 0.302629 0.428773 0.511521
 0.627310 0.701006 0.785222 0.875673 0.958669 0.990310
 1.000000
 OK SHELL IONIZATION DATA
 OK BINDING ENERGY (MEV), PHOTOEFFECT EFFICIENCY AND FLUORESCENT EFFICIENCY
 OK X-RAY ENERGIES (MEV) 0.50756
 OK X-RAY ACCUMULATED RELATIVE INTENSITIES 0.010690
 OK GAUGER ELECTRON ENERGIES (MEV) 0.010690
 OK GAUGER ELECTRON ACCUMULATED RELATIVE INTENSITIES 0.010690
 1.000000 1.000000 1.000000
 1.000000 1.000000 1.000000
 1.000000 1.000000 1.000000
 1.000000 1.000000 1.000000
 * ELECTRON CROSS SECTION DATA FROM PROGRAM DATPAC
 *
 * NUMBER OF SETS ON DATAPAC TAPE = 2
 *
 * 100.0 MEV CROSS SECTIONS FOR PHOTOCONDUCTORS
 *
 *
 MATERIAL DENSITY DETOUR
 1 0.47000e+01 0.73100e+00 A
 2 0.39720e+02 0.21200e+00 M
 0.15000e+02 0.309720e+02 0.48200e+00
 0.45000e+02 0.114820e+03 0.78400e+00
 NSET ITRM ITZP ISZN ISUB INAL ICYC NCYC NMAX
 1 5 0 1 40 1 1 64 64 64 1.0000000e+02 3.9062500e-01 2.3175160e+01
 1
 DATAPREP DATA FOR DATAPAC SET 1 33 40 121 2.3175160e+01
 2
 MATERIAL DENSITY DETOUR
 2 0.53100e+01 0.39500e+00 M
 0.31000e+02 0.59720e+02 0.48200e+00
 0.33000e+02 0.74922e+02 0.51800e+00
 NSET ITRM ITZP ISZN ISUB INAL ICYC NCYC NMAX
 2 5 0 1 40 1 1 64 64 64 1.0000000e+02 3.9062500e-01 2.54000300e+01
 LMAX LMAX
 2 2
 DATAPREP DATA FOR DATAPAC SET 2 33 40 121 2.3400030e+01
 2
 COLLISION / TOTAL DE/DX RATIOS FOR DATAPAC SET 2
 2
 CUMULATIVE BREMSTRAHLUNG CROSS SECTIONS FOR DATAPAC SET 2
 2
 CUMULATIVE BREMSTRAHLUNG ANGULAR DISTRIBUTIONS FOR DATAPAC SET 2
 2
 LANGAUS - EQUIPROBABLE ENDPOINTS FOR INTERPOLATION
 2
 K X-RAY PRODUCTION FOR DATAPAC SET 2
 2
 O PHOTOLELECTRON ANGULAR DISTRIBUTIONS
 2
 O PAIR ELECTRON ENERGY DIVISION DISTRIBUTION (LEAD)
 2
 * BEGIN READING INPUT
 *
 * BEGIN READING INPUT
 *
 * TITLE
 * 30.0 MEV TEST PROGRAM
 *
 * SOURCE
 * ELECTRONS ENERGY 30.0
 * DEFAULT SOURCE PHASE SPACE PARAMETERS
 * POSITION 0.0 0.0 0.0
 * SOURCE-RADIUS 0.98250
 * WARNING. ILLEGAL COMMAND LINE - INFORMATION IGNORED

```

--> SOURCE - RADIUS 0.95250
--> BIDODIRECTORIAL Z-AXIS
--> HISTORIES 1000000 OTHER OPTIONS
BATCHES 10
CUTOFF 0.05 .001
WARNING, ILLEGAL COMMAND LINE - INFORMATION IGNORED
-->CUTOFF 0.05 .001
***** OUTPUT OPTIONS *****
ELECTRON-ESCAPE
NBINE 10
NBINT 10
NBINE 10
NBINT 10
NBINE 10
NBINT 10
ELECTRON-FLUX 1 1
NBINE 10
NBINT 10
PHOTON-FLUX 1
NBINE 10
NBINT 10
***** GEOMETRY *****
GEOMETRY 1 RI R0 MAT IZR NZ NR ECUT PTC2
0.0 0.0 0.00297 0.0 0.95250 1 1 1 0.0 0.5
0 EOF ON UNIT 5 BEGIN PROCESSING INPUT
***** COMPARISON OF STORAGE REQUIREMENTS VS ALLOCATIONS *****
NUMBER OF MATERIALS ON CROSS SECTION FILE
LENGTH OF ELECTRON CROSS SECTION GRID
ELECTRON ENERGY GRID LENGTH FOR SAMPLING BREWS, PHOTON ENERGY
PHOTON ENERGY GRID LENGTH FOR SAMPLING BREWS, PHOTON ENERGY
ELECTRON ANGLE GRID LENGTH FOR SAMPLING BREWS, PHOTON SCATTERING ANGLE
PHOTON ANGLE GRID LENGTH FOR SAMPLING BREWS, PHOTON ANGLE
PHOTON ENERGY GRID LENGTH FOR SAMPLING BREWS, PHOTON ANGLE
ELECTRON ENERGY GRID LENGTH FOR SAMPLING BREWS, PHOTON ANGLE
PHOTON ENERGY GRID LENGTH FOR SAMPLING BREWS, PHOTON ANGLE
ELECTRON ANGLE GRID LENGTH FOR SAMPLING PHOTO-ELECTRON DIRECTION
PHOTON ENERGY GRID LENGTH FOR SAMPLING PAIR ELECTRON ENERGY
ELECTRON ENERGY GRID LENGTH FOR SAMPLING PAIR ELECTRON ENERGY
GAUSSIAN FUNCTION GRID FOR SAMPLING ELECTRON ENERGY LOSS STRAGGLING
GAUSSIAN FUNCTION GRID FOR SAMPLING ELECTRON ENERGY LOSS STRAGGLING
MAXIMUM NUMBER OF TABLES OF PHOTON CROSS SECTIONS
MAXIMUM LENGTH OF PHOTON CROSS SECTION TABLE
NUMBER OF ELECTRON ESCAPE ENERGY BINS
NUMBER OF PHOTON ESCAPE ENERGY BINS
NUMBER OF ELECTRON ESCAPE POLAR ANGLE BINS
NUMBER OF PHOTON ESCAPE POLAR ANGLE BINS
LENGTH OF SOURCE SPECTRUM ENERGY GRID
NUMBER OF PULSE HEIGHT ENERGY BINS
NUMBER OF ELECTRON FLUX ENERGY BINS
NUMBER OF PHOTON FLUX ENERGY BINS
NUMBER OF ELECTRON ESCAPE AZIMUTHAL ANGLE BINS
NUMBER OF PHOTON ESCAPE AZIMUTHAL ANGLE BINS
NUMBER OF PHOTON FLUX ZONES
NUMBER OF PROBLEM ZONES
SIZE OF DOUBLY DIFFERENTIAL BREWS DISTRIBUTION
SIZE OF SINGLE DIFFERENTIAL BREWS DISTRIBUTION
SIZE OF GOLDSMITH-SAUNDERS ANGULAR DISTRIBUTION
NO. OF ELECTRON ESCAPE AZIMUTHAL ANGLE BINS
NO. OF PHOTON ESCAPE AZIMUTHAL ANGLE BINS
***** GEOMETRY DEPENDENT INPUT *****
NUMBER OF INPUT ZONES = 1
NUMBER OF INPUT ZONES = 1
RIGHT INNER OUTER ELECTRON PHOTON

```

PROGRAM ITS - DECEMBER 16, 1984

VERSION 1.0

C Y L I N D E R

NUMBER OF MATERIALS

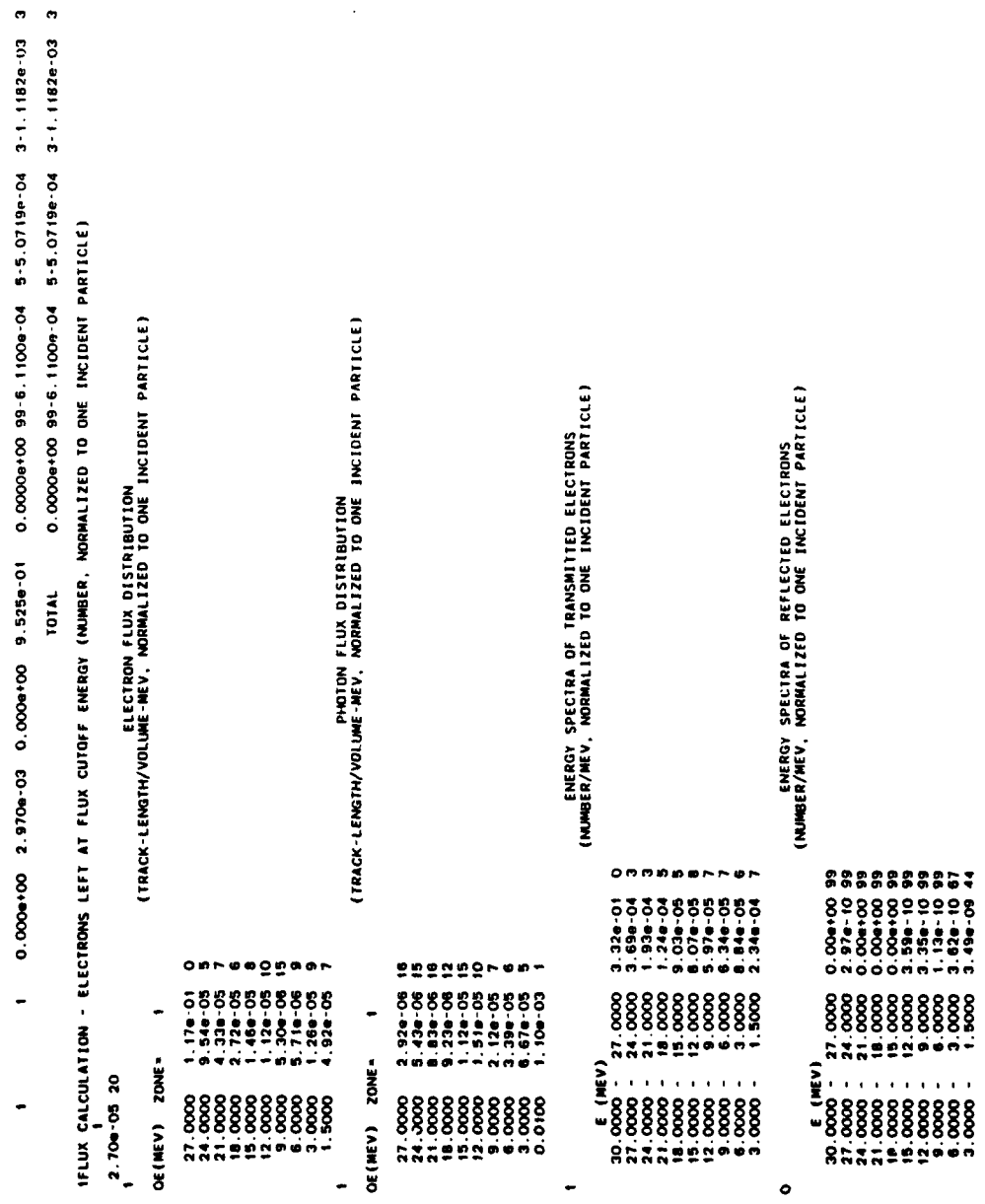
2

GAMMA RAY CROSS SECTION DATA FOR MATERIAL NUMBER 1

	PAIR	NTAB	NTAX	6	39	7	3	2	3	4	
ENERGIES (MEV)				000	00000	800	00000	500	00000	400	00000
100.00000	000	00000	100	00000	80	00000	60	00000	300	00000	
200.00000	150	00000	150	00000	100	00000	80	00000	50	00000	
400.00000	30	00000	30	00000	20	00000	15	00000	10	00000	
6.00000	5.	00000	5.	00000	4.	00000	3.	00000	2.	00000	
1.00000	0.	80000	0.	80000	0.	60000	0.	50000	0.	40000	
0.20000	0.	15000	0.	15000	0.	10000	0.	80000	0.	60000	
0.04000	0.	03000	0.	03000	0.	027540	0.	026000	0.	025000	
0.027940	0.	026000	0.	026000	0.	015000	0.	010000	0.	008000	
0.004238	0.	004000	0.	004000	0.	003938	0.	003938	0.	003938	
0.003938	0.	003730	0.	003730	0.	002144	0.	002144	0.	002144	
0.002144	0.	002000	0.	002000	0.	001500	0.	001500	0.	001500	
0.00144	0.	001300	0.	001300	0.	00114	0.	00114	0.	00114	
0.00114	0.	001050	0.	001050	0.	00104	0.	00104	0.	00104	
0.00104	0.	001000	0.	001000	0.	00100	0.	00100	0.	00100	
0.00100	0.	000950	0.	000950	0.	00095	0.	00095	0.	00095	
0.00095	0.	000900	0.	000900	0.	00089	0.	00089	0.	00089	
0.00089	0.	000850	0.	000850	0.	00084	0.	00084	0.	00084	
0.00084	0.	000800	0.	000800	0.	00079	0.	00079	0.	00079	
0.00079	0.	000750	0.	000750	0.	00074	0.	00074	0.	00074	
0.00074	0.	000700	0.	000700	0.	00069	0.	00069	0.	00069	
0.00069	0.	000650	0.	000650	0.	00064	0.	00064	0.	00064	
0.00064	0.	000600	0.	000600	0.	00059	0.	00059	0.	00059	
0.00059	0.	000550	0.	000550	0.	00054	0.	00054	0.	00054	
0.00054	0.	000500	0.	000500	0.	00049	0.	00049	0.	00049	
0.00049	0.	000450	0.	000450	0.	00044	0.	00044	0.	00044	
0.00044	0.	000400	0.	000400	0.	00039	0.	00039	0.	00039	
0.00039	0.	000350	0.	000350	0.	00034	0.	00034	0.	00034	
0.00034	0.	000300	0.	000300	0.	00029	0.	00029	0.	00029	
0.00029	0.	000250	0.	000250	0.	00024	0.	00024	0.	00024	
0.00024	0.	000200	0.	000200	0.	00019	0.	00019	0.	00019	
0.00019	0.	000150	0.	000150	0.	00014	0.	00014	0.	00014	
0.00014	0.	000100	0.	000100	0.	00009	0.	00009	0.	00009	
0.00009	0.	000080	0.	000080	0.	00007	0.	00007	0.	00007	
0.00007	0.	000060	0.	000060	0.	00005	0.	00005	0.	00005	
0.00005	0.	000040	0.	000040	0.	00003	0.	00003	0.	00003	
0.00003	0.	000020	0.	000020	0.	00001	0.	00001	0.	00001	
0.00001	0.	000000	0.	000000	0.	00000	0.	00000	0.	00000	

ORATIO OF SCATTERING TO SCATTERING PLUS PAIR PRODUCTION ATTENUATION COEFFICIENTS
 ORATIO OF SCATTERING TO SCATTERING PLUS PAIR PRODUCTION ATTENUATION COEFFICIENTS

0.000158 0.000158 0.000158 0.000158 0.000158 0.000158 0.000158 0.000158 0.000158 0.000158 0.000158
 0.00292 0.00292 0.00292 0.00292 0.00292 0.00292 0.00292 0.00292 0.00292 0.00292 0.00292
 0.015819 0.015819 0.015819 0.015819 0.015819 0.015819 0.015819 0.015819 0.015819 0.015819 0.015819
 0.091183 0.091183 0.091183 0.091183 0.091183 0.091183 0.091183 0.091183 0.091183 0.091183 0.091183
 0.587301 0.643989 0.643989 0.643989 0.643989 0.643989 0.643989 0.643989 0.643989 0.643989 0.643989
 1.000000 1.000000 1.000000 1.000000 1.000000 1.000000 1.000000 1.000000 1.000000 1.000000 1.000000



ENERGY SPECTRA OF LATERALLY ESCAPING ELECTRONS
(NUMBER/MEV. NORMALIZED TO ONE INCIDENT PARTICLE)

E (MEV)	27.0000	0.00e+00	99
27.0000	27.0000	0.00e+00	99
24.0000	24.0000	0.00e+00	99
21.0000	21.0000	0.00e+00	99
18.0000	18.0000	0.00e+00	99
15.0000	15.0000	0.00e+00	99
12.0000	12.0000	0.00e+00	99
9.0000	9.0000	0.00e+00	99
6.0000	6.0000	0.00e+00	99
3.0000	1.5000	0.00e+00	99

ANGULAR DISTRIBUTIONS OF TRANSMITTED AND REFLECTED ELECTRONS

E (MEV)	PHI (DEG) = 0.000	THETA (DEG) = 180.000	0
0.0000	18.0000	3.25e+00	0
18.0000	36.0000	4.07e-04	0
36.0000	54.0000	8.63e-05	13
54.0000	72.0000	9.71e-06	25
72.0000	90.0000	1.03e-06	67
90.0000	108.0000	2.04e-09	76
108.0000	126.0000	2.30e-09	50
126.0000	144.0000	1.18e-09	71
144.0000	162.0000	0.00e+00	99
162.0000	180.0000	0.00e+00	99

ANGULAR DISTRIBUTIONS OF LATERALLY ESCAPING ELECTRONS

E (MEV)	PHI (DEG) = 0.000	THETA (DEG) = 180.000	0
0.0000	18.0000	0.00e+00	99
18.0000	36.0000	0.00e+00	99
36.0000	54.0000	0.00e+00	99
54.0000	72.0000	0.00e+00	99
72.0000	90.0000	0.00e+00	99
90.0000	108.0000	0.00e+00	99
108.0000	126.0000	0.00e+00	99
126.0000	144.0000	0.00e+00	99
144.0000	162.0000	0.00e+00	99
162.0000	180.0000	0.00e+00	99

ENERGY SPECTRA AND ANGULAR DISTRIBUTIONS OF ELECTRONS TRANSMITTED AND REFLECTED
AZIMUTHAL INTERVAL IS 0.0000 TO 180.0000 DEGREES

E (MEV)	THETA = 0.000	18.000	36.000	54.000	72.000	90.000	108.000	126.000	144.000	162.000
0.0000	27.0000	1.03e+00	0.00e+00	99.0.00e+00	99.0.00e+00	99.0.00e+00	99.0.00e+00	99.0.00e+00	99.0.00e+00	99.0.00e+00
27.0000	24.0000	1.20e-03	3.0.00e+00	99.6.60e-11	99.1.93e-11	99.0.00e+00	99.0.00e+00	99.1.63e-10	99.0.00e+00	99.0.00e+00
24.0000	21.0000	6.27e-04	3.3.60e-10	94.0.00e+00	99.0.00e+00	99.0.00e+00	99.0.00e+00	99.0.00e+00	99.0.00e+00	99.0.00e+00
21.0000	18.0000	4.03e-04	5.2.16e-10	85.0.00e+00	99.0.00e+00	99.0.00e+00	99.0.00e+00	99.0.00e+00	99.0.00e+00	99.0.00e+00
18.0000	15.0000	2.91e-04	5.4.91e-10	87.0.00e+00	99.0.00e+00	99.0.00e+00	99.0.00e+00	99.0.00e+00	99.0.00e+00	99.0.00e+00
15.0000	12.0000	2.03e-04	8.2.66e-10	99.4.15e-10	99.0.00e+00	99.0.00e+00	99.0.00e+00	99.0.00e+00	99.0.00e+00	99.0.00e+00
12.0000	9.0000	1.93e-04	7.3.75e-07	99.1.2e-07	0.72.0.00e+00	99.0.00e+00	99.0.00e+00	99.0.00e+00	99.0.00e+00	99.0.00e+00
9.0000	6.0000	1.77e-04	7.1.01e-05	24.7.01e-10	99.1.3e-10	97.1.3e-10	99.0.00e+00	99.6.47e-11	99.0.00e+00	99.0.00e+00
6.0000	3.0000	1.22e-04	6.5.61e-05	7.4.81e-07	99.3.48e-10	57.1.3e-10	80.9.07e-11	99.1.3e-10	99.0.00e+00	99.0.00e+00
3.0000	1.6000	6.34e-05	23.1.38e-04	8.5.66e-05	12.6.47e-06	25.6.87e-07	67.8.35e-10	64.1.07e-09	48.0.00e+00	99.0.00e+00

ENERGY SPECTRA AND ANGULAR DISTRIBUTIONS OF ELECTRONS TRANSMITTED AND REFLECTED

0

21.0000 - 18.0000 0.00e+00 .99
18.0000 - 15.0000 0.00e+00 .99
15.0000 - 12.0000 0.00e+00 .99
12.0000 - 9.0000 0.00e+00 .99
9.0000 - 6.0000 0.00e+00 .99
6.0000 - 3.0000 0.00e+00 .99
3.0000 - 0.0100 0.00e+00 .99
0 INTEGRAL (FSR) 0.00e+00 .99

THE NUMBER OF DATA FOR WHICH STATISTICAL ESTIMATES HAVE BEEN PROVIDED IS 568

ECHO 1
TITLE
...100.0 MEV TEST PROGRAM

ELECTRONS
ENERGY 100.0
* DEFAULT SOURCE PHASE SPACE PARAMETERS
* POSITION 0.0 0.0 0.0
* SOURCE-RADIUS 0.95250
* NONDIRECTIONAL 2 AXES

HISTORIES 1000000
BATCHES 10
CUTOFFS 0.05 0.001

ELECTRON ESCAPE
NBINE 10
NBINT 10
PHOTON-ESCAPE
NBINE 10
NBINT 10
ELECTRON-FLUX 1 1
NBINE 10
PHOTON-FLUX 1 1

GEOMETRY 1
ZL 2R RI RD MAT 12R NZ NR ECUT RICZ
0.0 0.00297 0.0 0.95250 1 1 1 0.0 0.5

```

1 ***** PROGRAM XGEN - DECEMBER 1, 1984 *****
***** VERSION 1.0 *****
***** END OF FILE ON UNIT 5 - XGEN *****
***** SUMMARY OF INPUT DATA *****
***** MAXIMUM CROSS SECTION ENERGY = 1.00000e+02 *****
MATERIAL 1 SOLID/LIQUID
DENSITY 3.9650e+00
DENSITY-RATIO 1.0000e+00
STABDL ATOMIC NUMBER WEIGHT FRACTION
1 0 8 4.7100e-01
2 Al 12 5.2900e-01
0 ***** BEGIN EXECUTING PHOTON CROSS SECTION SUBROUTINE - POPEN *****
***** BEGIN EXECUTING PHOTON SUBROUTINE *****
***** END OF PGEN SUBROUTINE *****
***** BEGIN EXECUTING ELECTRON CROSS SECTION SUBROUTINE - DATPAC *****
***** BEGIN EXECUTING ELECTRON CROSS SECTION SUBROUTINE - DATPAC *****
***** 100.0 MEV CROSS SECTIONS SAPPHIRE *****
***** ELECTRON CROSS SECTIONS FOR MATERIAL NUMBER 1 *****
***** 0 11RM 12IP 1SGN 1SUB 1NEL 1CYC NMIX EMAX *****
***** 8 0 1 40 1 1 8 64 1.00000e+02 *****
***** INPUT DATA TAPE IDENTIFICATION *****
***** DATAPAC-2 (REGISTER-ALIGNER PH-RAD CORR). 54 STERNHEIMER SETS. 30 JANE 6 *****
***** ODETOUR DENSITY *****
***** 7.31000e-01 3.96500e+00 *****
***** ORANGE TABLE *****
0 EMAX NCYC EFAC NMAX T(NMAX+1) NCAL Y(NCAL)
0 1.00000e+02 8 9.17000e-01 64 3.96625e-01 134 9.89410e-04
0 JMAX LMIX
0 2
0 0 2 A M
0 15.00000 15.99839 0.47100
0 15.00000 26.98148 0.52300
0 P1 P1D
0 121.89239 121.89239
0 ***** PARAMETERS FOR DENSITY EFFECT *****
P1 C B DM X1 X0
121.89239 -3.22059 0.10475 3.00000 3.00000 0.20000
121.89239 -3.22059 0.10475 3.00000 3.00000 0.20000
***** ELECTRON RESULTS *****
0 EFFECTIVE Z/A = 0.49039 EFFECTIVE MEAN IONIZATION POTENTIAL = 121.89 EV CRITICAL ENERGY = 59.572 MV
0 ENERGY STOPPING POWER RANGE RADIATION CORR DRAINF DIFFID
0 N COLLISION RADIATION TOTAL RADIATION YIELD CORR MEV CM2/G MEV CM2/G g/CM2/G

```

134	9.8941e-04	8.7626e+01	7.4626e+03	8.7838e+01	5.646e-06	0.0000e+00	3.861e-03	0.0000e+00	8.517e-05	5.646e-06	0.0000e+00
135	1.0790e-03	8.3461e+01	7.4588e+03	8.3471e+01	6.6533e-06	7.242e-06	4.210e-03	0.0000e+00	8.935e-05	1.077e-06	7.814e-09
136	1.1755e-03	7.540e+01	7.4536e+03	7.940e+01	7.893e-06	1.424e-05	4.589e-03	0.0000e+00	9.381e-05	2.000e-06	8.946e-09
137	1.2705e-03	7.5443e+01	7.5443e+03	7.5443e+01	9.270e-06	2.105e-05	5.0039e-03	0.0000e+00	9.875e-05	1.376e-06	1.026e-09
138	1.3982e-03	7.4588e+01	7.4524e+03	7.4588e+01	1.059e-05	2.772e-05	5.454e-03	0.0000e+00	1.040e-04	5.91e-06	1.177e-08
139	1.5259e-03	6.7866e+01	7.4352e+03	6.7866e+01	1.261e-05	3.488e-05	5.946e-03	0.0000e+00	1.095e-04	1.02e-06	1.352e-08
140	1.6640e-03	6.4266e+01	7.4288e+03	6.4266e+01	1.478e-05	4.078e-05	6.481e-03	0.0000e+00	1.168e-04	2.02e-06	1.555e-08
141	1.8168e-03	6.080e+01	7.420e+03	6.080e+01	1.717e-05	4.725e-05	6.965e-03	0.0000e+00	1.221e-04	2.410e-06	1.789e-08
142	1.9788e-03	5.1474e+01	7.411e-03	5.1474e+01	1.935e-05	5.375e-05	7.400e-03	0.0000e+00	1.290e-04	2.700e-06	2.061e-08
143	2.1579e-03	5.4227e+01	7.4026e+03	5.4227e+01	2.162e-05	6.030e-05	7.836e-03	0.0000e+00	1.364e-04	3.208e-06	2.316e-08
144	2.3522e-03	5.1224e+01	7.3916e+03	5.1224e+01	2.386e-05	6.854e-05	8.393e-03	0.0000e+00	1.443e-04	3.706e-06	2.741e-08
145	2.5622e-03	4.8306e+01	7.2815e+03	4.8306e+01	2.615e-05	7.568e-05	8.969e-03	0.0000e+00	1.522e-04	4.203e-06	3.164e-08
146	2.7955e-03	4.5522e+01	7.151e+03	4.5522e+01	2.845e-05	8.295e-05	9.617e-03	0.0000e+00	1.619e-04	4.955e-06	3.654e-08
147	3.0518e-03	4.2887e+01	7.0556e+03	4.2887e+01	4.184e-05	8.779e-05	1.184e-03	0.0000e+00	1.715e-04	5.755e-06	4.223e-08
148	3.3205e-03	4.0358e+01	6.9517e+03	4.0358e+01	4.348e-05	9.117e-05	1.290e-03	0.0000e+00	1.819e-04	6.633e-06	4.881e-08
149	3.6222e-03	3.7956e+01	6.7324e+03	3.7956e+01	4.717e-05	9.475e-05	1.392e-03	0.0000e+00	1.930e-04	7.599e-06	5.615e-08
150	3.9576e-03	3.5691e+01	6.5030e+03	3.5691e+01	5.174e-05	9.811e-05	1.501e-03	0.0000e+00	2.047e-04	8.527e-06	6.531e-08
151	4.3588e-03	3.3544e+01	6.2904e+03	3.3544e+01	5.620e-05	1.018e-04	1.668e-03	0.0000e+00	2.173e-04	1.036e-05	7.559e-08
152	4.7065e-03	3.1510e+01	6.151e+03	3.1510e+01	6.151e-05	1.191e-04	1.817e-03	0.0000e+00	2.308e-04	1.202e-05	8.751e-08
153	5.1242e-03	2.9584e+01	6.0250e+03	2.9584e+01	6.725e-05	1.045e-04	1.310e-04	0.0000e+00	2.451e-04	1.356e-05	1.013e-07
154	5.6399e-03	2.7285e+01	5.8755e+03	2.7285e+01	7.425e-05	9.055e-05	1.466e-04	0.0000e+00	2.603e-04	1.621e-05	1.174e-07
155	6.1055e-03	2.5058e+01	5.7055e+03	2.5058e+01	8.005e-05	8.577e-05	1.555e-04	0.0000e+00	2.775e-04	1.884e-05	1.360e-07
156	6.6320e-03	2.3436e+01	5.5426e+03	2.3436e+01	8.648e-05	8.048e-05	1.647e-04	0.0000e+00	2.940e-04	2.160e-05	1.560e-07
157	7.2533e-03	2.2191e+01	5.3791e+03	2.2191e+01	9.291e-05	7.570e-05	1.751e-04	0.0000e+00	3.121e-04	2.597e-05	1.761e-07
158	7.9133e-03	2.1479e+01	5.1318e+03	2.1479e+01	9.936e-05	7.135e-04	1.895e-04	0.0000e+00	3.295e-04	3.471e-05	2.854e-07
159	8.6177e-03	2.0124e+01	4.9010e+03	2.0124e+01	1.049e-04	2.480e-04	2.012e-04	0.0000e+00	3.475e-04	4.072e-05	3.298e-07
160	9.4129e-03	1.8855e+01	4.7070e+03	1.8855e+01	1.104e-04	2.848e-04	2.188e-04	0.0000e+00	3.751e-04	4.728e-05	3.900e-07
161	1.0255e-02	1.7668e+01	4.5070e+03	1.7668e+01	1.178e-04	3.298e-04	2.368e-04	0.0000e+00	3.991e-04	5.410e-05	4.610e-07
162	1.1130e-02	1.6554e+01	4.3060e+03	1.6554e+01	1.254e-04	3.755e-04	2.547e-04	0.0000e+00	4.241e-04	6.105e-05	5.260e-07
163	1.2075e-02	1.5496e+01	4.1050e+03	1.5496e+01	1.321e-04	4.214e-04	2.741e-04	0.0000e+00	4.513e-04	6.786e-05	5.924e-07
164	1.3012e-02	1.4519e+01	3.9060e+03	1.4519e+01	1.387e-04	4.783e-04	2.938e-04	0.0000e+00	4.793e-04	7.371e-05	6.423e-07
165	1.4047e-02	1.3558e+01	3.7070e+03	1.4047e+01	1.454e-04	5.359e-04	3.130e-04	0.0000e+00	5.093e-04	8.954e-05	7.117e-07
166	1.5171e-02	1.2720e+01	3.5080e+03	1.5171e+01	1.523e-04	5.932e-04	3.315e-04	0.0000e+00	5.428e-04	1.046e-04	8.020e-07
167	1.6323e-02	1.1910e+01	3.3100e+03	1.1910e+01	1.592e-04	6.524e-04	3.516e-04	0.0000e+00	5.772e-04	1.248e-04	9.300e-07
168	1.7566e-02	1.1510e+01	3.1110e+03	1.1510e+01	1.662e-04	7.181e-04	3.708e-04	0.0000e+00	6.138e-04	1.436e-04	1.078e-06
169	2.0550e-02	1.0740e+01	2.9120e+03	1.0740e+01	1.732e-04	7.852e-04	4.124e-04	0.0000e+00	6.527e-04	1.597e-04	1.251e-06
170	2.2070e-02	1.0159e+01	2.7130e+03	1.0159e+01	1.803e-04	8.522e-04	4.512e-04	0.0000e+00	6.912e-04	1.798e-04	1.412e-06
171	2.3512e-02	9.5180e+00	2.5140e+03	9.5180e+00	1.873e-04	9.212e-04	4.914e-04	0.0000e+00	7.393e-04	2.171e-04	1.612e-06
172	2.5053e-02	8.9350e+00	2.3150e+03	8.9350e+00	1.944e-04	9.892e-04	5.313e-04	0.0000e+00	7.893e-04	2.563e-04	1.813e-06
173	2.6694e-02	8.4460e+00	2.1160e+03	8.4460e+00	2.015e-04	1.059e-03	5.795e-04	0.0000e+00	8.492e-04	3.054e-04	2.213e-06
174	2.8335e-02	7.9670e+00	1.9170e+03	7.9670e+00	2.086e-04	1.130e-03	6.275e-04	0.0000e+00	8.932e-04	3.654e-04	2.613e-06
175	3.0076e-02	7.5100e+00	1.7180e+03	7.5100e+00	2.157e-04	1.201e-03	6.756e-04	0.0000e+00	9.432e-04	4.254e-04	3.213e-06
176	3.1817e-02	7.0940e+00	1.5190e+03	7.0940e+00	2.230e-04	1.272e-03	7.237e-04	0.0000e+00	9.932e-04	4.854e-04	3.813e-06
177	3.3658e-02	6.6780e+00	1.3190e+03	6.6780e+00	2.303e-04	1.343e-03	7.718e-04	0.0000e+00	1.042e-03	5.454e-04	4.413e-06
178	3.5599e-02	6.2620e+00	1.1190e+03	6.2620e+00	2.376e-04	1.414e-03	8.200e-04	0.0000e+00	1.102e-03	6.053e-04	5.053e-06
179	3.7630e-02	5.8550e+00	9.1900e+03	5.8550e+00	2.449e-04	1.485e-03	8.681e-04	0.0000e+00	1.162e-03	6.653e-04	5.653e-06
180	3.9761e-02	5.4480e+00	7.1700e+03	5.4480e+00	2.522e-04	1.556e-03	9.162e-04	0.0000e+00	1.221e-03	7.251e-04	6.251e-06
181	4.1902e-02	5.0410e+00	5.1500e+03	5.0410e+00	2.595e-04	1.627e-03	9.643e-04	0.0000e+00	1.281e-03	7.851e-04	6.851e-06
182	4.4043e-02	4.6340e+00	3.1300e+03	4.6340e+00	2.668e-04	1.700e-03	1.015e-03	0.0000e+00	1.341e-03	8.451e-04	7.451e-06
183	4.6284e-02	4.2270e+00	1.1100e+03	4.2270e+00	2.741e-04	1.771e-03	1.096e-03	0.0000e+00	1.401e-03	8.951e-04	7.951e-06
184	4.8525e-02	3.8190e+00	6.9900e+03	3.8190e+00	2.814e-04	1.842e-03	1.177e-03	0.0000e+00	1.461e-03	9.451e-04	8.451e-06
185	5.1063e-02	3.4120e+00	5.8700e+03	3.4120e+00	2.887e-04	1.913e-03	1.258e-03	0.0000e+00	1.521e-03	9.951e-04	8.951e-06
186	5.3604e-02	3.0050e+00	4.7500e+03	3.0050e+00	2.960e-04	1.984e-03	1.339e-03	0.0000e+00	1.581e-03	1.045e-03	9.451e-06
187	5.6145e-02	2.5980e+00	3.6300e+03	2.5980e+00	3.033e-04	2.055e-03	1.410e-03	0.0000e+00	1.641e-03	1.105e-03	9.951e-06
188	5.8786e-02	2.2910e+00	2.5000e+03	2.2910e+00	3.106e-04	2.126e-03	1.481e-03	0.0000e+00	1.701e-03	1.165e-03	1.055e-06
189	6.1427e-02	1.9840e+00	1.3800e+03	1.9840e+00	3.177e-04	2.200e-03	1.552e-03	0.0000e+00	1.761e-03	1.225e-03	1.115e-06
190	6.4168e-02	1.6770e+00	1.2600e+03	1.6770e+00	3.248e-04	2.271e-03	1.623e-03	0.0000e+00	1.821e-03	1.285e-03	1.175e-06
191	6.7010e-02	1.3700e+00	1.1400e+03	1.3700e+00	3.319e-04	2.342e-03	1.694e-03	0.0000e+00	1.881e-03	1.345e-03	1.235e-06
192	7.0052e-02	1.0630e+00	1.0200e+03	1.0630e+00	3.390e-04	2.413e-03	1.765e-03	0.0000e+00	1.941e-03	1.405e-03	1.295e-06
193	7.3293e-02	7.5660e+00	9.0000e+03	7.5660e+00	3.461e-04	2.484e-03	1.836e-03	0.0000e+00	1.991e-03	1.465e-03	1.355e-06
194	7.6534e-02	4.5590e+00	7.8000e+03	4.5590e+00	3.532e-04	2.555e-03	1.907e-03	0.0000e+00	2.051e-03	1.525e-03	1.415e-06
195	8.0075e-02	1.5520e+00	7.5000e+03	1.5520e+00	3.603e-04	2.626e-03	1.978e-03	0.0000e+00	2.111e-03	1.585e-03	1.475e-06
196	8.3616e-02	2.5450e+00	7.2000e+03	2.5450e+00	3.674e-04	2.697e-03	2.049e-03	0.0000e+00	2.161e-03	1.645e-03	1.535e-06
197	8.7257e-02	3.5380e+00	6.9000e+03	3.5380e+00	3.745e-04	2.768e-03	2.120e-03	0.0000e+00	2.211e-03	1.705e-03</	

71	2.3527e-01	2.167e+00	7.711e-03	2.174e+00	6.872e-02	0.093e-03	5.274e-01	0.000e+00	3.555e-03	8.704e-03	6.635e-05
70	2.3529e-01	2.096e+00	7.702e-03	2.093e+00	6.851e-02	0.221e-03	5.530e-01	0.000e+00	3.781e-03	9.646e-03	7.685e-05
69	2.3521e-01	2.020e+00	8.126e-03	2.028e+00	6.963e-02	0.381e-03	6.787e-01	0.000e+00	4.024e-03	1.122e-02	8.912e-05
68	3.021e-01	1.957e+00	8.126e-03	1.963e+00	6.942e-02	0.509e-03	6.042e-01	0.000e+00	4.256e-03	1.034e-02	1.034e-04
67	3.248e-01	1.900e+00	8.676e-03	1.908e+00	6.163e-01	0.2668e-03	6.295e-01	0.000e+00	4.565e-03	1.059e-02	1.201e-04
66	3.5220e-01	1.848e+00	8.676e-03	1.856e+00	6.163e-01	0.321e-01	6.544e-01	0.000e+00	4.669e-03	1.579e-02	1.398e-04
65	3.9633e-01	1.803e+00	9.376e-03	1.812e+00	6.488e-01	0.315e-03	6.788e-01	0.000e+00	5.200e-03	1.767e-02	1.628e-04
64	4.299e-01	1.762e+00	9.795e-03	1.774e+00	6.655e-01	0.188e-03	7.026e-01	0.000e+00	5.555e-03	1.971e-02	1.894e-04
63	4.653e-01	1.724e+00	1.027e-03	1.734e+00	6.915e-01	0.437e-01	7.256e-01	0.000e+00	5.958e-03	2.192e-02	2.208e-04
62	6.058e-01	1.687e+00	1.081e-02	1.698e+00	7.160e-01	0.250e-01	7.478e-01	0.000e+00	7.895e-03	2.451e-02	2.581e-04
61	5.523e-01	1.654e+00	1.181e-02	1.665e+00	7.433e-01	0.380e-01	7.691e-01	0.000e+00	8.118e-03	2.698e-02	3.030e-04
60	6.023e-01	1.626e+00	1.209e-02	1.638e+00	7.738e-01	0.188e-03	7.894e-01	0.000e+00	8.309e-03	2.928e-02	3.558e-04
59	6.595e-01	1.601e+00	1.283e-02	1.614e+00	7.986e-01	0.071e-01	8.456e-02	0.000e+00	8.555e-03	3.255e-02	4.188e-04
58	7.141e-01	1.573e+00	1.373e-02	1.593e+00	8.442e-01	0.315e-03	8.267e-01	0.000e+00	8.794e-03	3.708e-02	4.931e-04
57	7.8125e-01	1.561e+00	1.470e-02	1.571e+00	8.851e-01	0.188e-03	8.788e-01	0.000e+00	9.194e-03	4.198e-02	5.119e-04
56	8.596e-01	1.545e+00	1.570e-02	1.561e+00	9.302e-01	0.500e-03	8.594e-01	0.000e+00	9.508e-03	4.508e-02	5.408e-04
55	9.207e-01	1.532e+00	1.701e-02	1.549e+00	9.788e-01	0.7919e-03	8.741e-01	0.000e+00	9.795e-03	4.959e-02	6.130e-04
54	1.0328e-00	1.5224e+00	1.839e-02	1.540e+00	1.040e-01	0.313e-01	8.876e-01	0.000e+00	1.008e-02	5.446e-02	9.635e-04
53	1.1049e-00	1.5144e+00	1.939e-02	1.534e+00	1.040e-01	0.500e-01	8.884e-01	0.000e+00	1.119e-02	5.676e-02	1.143e-03
52	1.2049e+00	1.5084e+00	2.1868e-02	1.6868e-02	5.929e-01	0.2050e-01	7.439e-03	0.000e+00	1.219e-02	6.0726e-02	1.358e-03
51	1.3139e+00	1.5039e+00	2.382e-02	1.5278e-02	5.308e-01	0.0514e-01	7.169e-03	0.000e+00	1.219e-02	6.643e-02	1.616e-03
50	1.4328e+00	1.5016e+00	2.712e-02	1.5228e-02	5.228e-01	0.0514e-01	7.268e-03	0.000e+00	1.219e-02	7.131e-02	1.920e-03
49	1.5225e+00	1.5016e+00	2.822e-02	1.5231e-02	5.218e-01	0.0514e-01	7.268e-03	0.000e+00	1.219e-02	7.190e-02	1.929e-03
48	1.7039e+00	1.5016e+00	3.094e-02	1.5311e-02	5.313e-01	0.0514e-01	7.309e-03	0.000e+00	1.219e-02	7.828e-02	1.942e-02
47	1.8561e+00	1.5016e+00	3.400e-02	1.535e-02	5.338e-01	0.081e-00	7.119e-03	0.000e+00	1.219e-02	8.458e-02	2.078e-02
46	2.0533e+00	1.5016e+00	3.708e-02	1.541e-02	5.416e-01	0.136e-00	7.195e-03	0.000e+00	1.219e-02	9.733e-02	2.108e-02
45	2.2957e+00	1.5016e+00	4.117e-02	1.549e-02	5.494e-01	0.3158e-00	7.319e-03	0.000e+00	1.219e-02	1.040e-01	2.731e-02
44	2.4949e+00	1.5016e+00	4.530e-02	1.557e-02	5.557e-01	0.434e-00	7.450e-03	0.000e+00	1.219e-02	1.286e-01	3.571e-02
43	2.6788e+00	1.5016e+00	5.178e-02	1.562e-02	5.621e-01	0.583e-00	7.583e-03	0.000e+00	1.219e-02	1.518e-01	4.238e-02
42	2.8956e+00	1.5016e+00	5.822e-02	1.5628e-02	5.628e-01	0.693e-00	7.628e-03	0.000e+00	1.219e-02	1.790e-01	4.929e-02
41	3.1951e+00	1.5016e+00	6.188e-02	1.561e-02	5.619e-01	0.852e-00	7.648e-03	0.000e+00	1.219e-02	2.058e-01	5.638e-02
40	3.4078e+00	1.5016e+00	6.786e-02	1.560e-02	5.604e-01	0.2756e-00	7.696e-03	0.000e+00	1.219e-02	2.364e-01	6.165e-03
39	3.7163e+00	1.5016e+00	7.482e-02	1.554e-02	5.581e-01	0.2686e-00	7.268e-03	0.000e+00	1.219e-02	2.485e-01	6.933e-03
38	4.0226e+00	1.5016e+00	8.290e-02	1.531e-02	6.193e-01	0.4732e-00	7.419e-03	0.000e+00	1.219e-02	2.668e-01	8.631e-03
37	4.4194e+00	1.5016e+00	9.176e-02	1.551e-02	6.515e-01	0.4732e-00	7.148e-03	0.000e+00	1.219e-02	2.838e-01	1.050e-03
36	4.9594e+00	1.5016e+00	1.016e-01	1.661e-02	6.651e-01	0.5376e-00	7.937e-03	0.000e+00	1.219e-02	3.130e-01	1.398e-03
35	5.2556e+00	1.5016e+00	1.125e-01	1.686e-02	6.785e-01	0.3176e-00	8.197e-03	0.000e+00	1.219e-02	3.434e-01	1.512e-03
34	5.7133e+00	1.5016e+00	1.247e-01	1.709e-02	6.922e-01	0.3477e-00	8.718e-03	0.000e+00	1.219e-02	3.738e-01	1.617e-03
33	6.2500e+00	1.5016e+00	1.381e-01	1.731e-02	7.159e-01	0.2075e-00	9.093e-03	0.000e+00	1.219e-02	4.088e-01	1.717e-03
32	6.8157e+00	1.5016e+00	1.541e-01	1.748e-02	7.268e-01	0.2686e-00	9.545e-03	0.000e+00	1.219e-02	4.484e-01	1.816e-03
31	7.4235e+00	1.5016e+00	1.694e-01	1.780e-02	7.378e-01	0.4526e-00	9.875e-03	0.000e+00	1.219e-02	4.845e-01	1.951e-03
30	8.1052e+00	1.5016e+00	1.870e-01	1.807e-02	7.426e-01	0.6260e-00	9.828e-03	0.000e+00	1.219e-02	5.238e-01	2.1373e-03
29	8.8388e+00	1.5016e+00	2.070e-01	1.826e-02	7.476e-01	0.806e-00	9.688e-03	0.000e+00	1.219e-02	5.648e-01	2.4098e-03
28	9.6378e+00	1.5016e+00	2.377e-01	1.847e-02	7.527e-01	0.6464e-00	9.255e-03	0.000e+00	1.219e-02	6.048e-01	2.798e-03
27	1.0511e+01	1.5016e+00	2.543e-01	1.866e-02	7.562e-01	0.1376e-00	9.564e-03	0.000e+00	1.219e-02	6.454e-01	3.121e-03
26	1.1633e+01	1.5016e+00	2.816e-01	1.876e-02	7.626e-01	0.1705e-00	9.719e-03	0.000e+00	1.219e-02	6.864e-01	3.422e-03
25	1.2500e+01	1.5016e+00	3.112e-01	1.971e-02	7.158e-01	0.4266e-00	9.924e-03	0.000e+00	1.219e-02	7.272e-01	3.722e-03
24	1.3531e+01	1.5016e+00	3.1919e-01	2.105e-02	7.205e-01	0.1034e-00	9.951e-03	0.000e+00	1.219e-02	7.671e-01	4.137e-03
23	1.4685e+01	1.5016e+00	3.4016e-01	2.060e-02	7.323e-01	0.3298e-00	9.986e-03	0.000e+00	1.219e-02	8.079e-01	4.537e-03
22	1.6210e+01	1.5016e+00	4.203e-01	2.058e-02	7.058e-01	0.1034e-00	9.996e-03	0.000e+00	1.219e-02	8.489e-01	4.934e-03
21	1.7778e+01	1.5016e+00	4.643e-01	2.043e-02	6.867e-01	0.1042e-00	1.010e-03	0.000e+00	1.219e-02	8.872e-01	5.329e-03
20	1.9778e+01	1.5016e+00	5.127e-01	2.028e-02	6.906e-01	0.1166e-00	1.166e-03	0.000e+00	1.219e-02	9.3078e-01	5.730e-03
19	2.1022e+01	1.5016e+00	5.653e-01	2.016e-02	7.020e-01	0.1166e-00	1.300e-03	0.000e+00	1.219e-02	9.759e-01	6.1471e-03
18	2.2225e+01	1.5016e+00	6.245e-01	2.006e-02	7.158e-01	0.1189e-00	1.406e-03	0.000e+00	1.219e-02	1.0229e-01	6.5229e-03
17	2.3500e+01	1.5016e+00	6.886e-01	2.000e-02	7.249e-01	0.2165e-00	1.5188e-03	0.000e+00	1.219e-02	1.0996e-01	6.996e-03
16	2.7053e+01	1.5016e+00	7.595e-01	1.986e-02	7.526e-01	0.1475e-00	1.757e-03	0.000e+00	1.219e-02	1.2778e-01	7.5755e-03
15	3.2721e+01	1.5016e+00	8.274e-01	1.977e-02	7.577e-01	0.1927e-00	1.997e-03	0.000e+00	1.219e-02	1.4769e-01	8.2615e-03
14	3.8355e+01	1.5016e+00	9.762e-01	1.971e-02	7.617e-01	0.2377e-00	2.198e-03	0.000e+00	1.219e-02	1.7761e-01	9.0435e-03
13	4.4555e+01	1.5016e+00	1.169e+00	1.969e+00	7.659e+00	0.1016e+00	2.178e+03	0.000e+00	1.219e+00	2.056e+00	1.295e+00
12	5.1095e+01	1.5016e+00	1.3777e+00	1.977e+00	7.733e+00	0.3007e+00	2.198e+03	0.000e+00	1.219e+00	2.358e+00	1.391e+00
11	5.8545e+01	1.5016e+00	1.4117e+00	1.977e+00	7.813e+00	0.4046e+00	2.238e+03	0.000e+00	1.219e+00	2.456e+00	1.491e+00
10	6.5550e+01	1.5016e+00	1.4926e+00	1.977e+00	7.846e+00	0.4046e+00	2.238e+03	0.000e+00	1.219e+00	2.491e+00	1.501e+00
9	7.2900e+01	1.5016e+00	1.6202e+00	1.977e+00	7.871e+00	0.2304e+00	2.810e+03	0.000e+00	1.219e+00	2.924e+00	1.8139e+00
8	8.0000e+01	1.5016e+00	1.641e+00	1.977e+00	7.891e+00	0.2304e+00	2.810e+03	0.000e+00	1.219e+00	3.146e+00	1.8106e+00

```

7 5.946e+01 1.807e+00 1.804e+00 3.611e+00 2.444e+01 2.982e-01 9.999e-01 4.818e-01 9.980e-01 1.400e+00 2.410e+00
6 5.484e+01 1.814e+00 1.982e+00 3.797e+00 2.589e+01 3.152e-01 8.999e-01 4.910e-01 1.092e+00 1.453e+00 2.750e+00
5 7.071e+01 1.822e+00 2.178e+00 3.999e+00 2.740e+01 3.340e-01 9.999e-01 5.063e-01 1.195e+00 1.506e+00 3.131e+00
4 7.711e+01 1.830e+00 2.392e+00 4.221e+00 2.895e+01 3.524e-01 1.000e+00 5.186e-01 1.308e+00 1.557e+00 3.557e+00
3 8.408e+01 1.838e+00 2.656e+00 4.462e+00 3.055e+01 3.711e-01 1.000e+00 5.310e-01 1.430e+00 1.608e+00 4.033e+00
2 9.1700e+01 1.845e+00 2.989e+00 4.768e+00 3.222e+01 3.900e-01 1.000e+00 5.445e-01 1.564e+00 1.657e+00 4.562e+00
1 1.000e+02 1.850e+00 3.180e+00 5.163e+00 3.014e+00 3.392e+01 4.092e-01 1.000e+00 5.560e-01 1.710e+00 1.705e+00 5.151e+00
END OF DATAPC SUBROUTINE
END OF PROGRAM XGFM

```

AD-A165 589

ELECTRON INDUCED CONDUCTIVITY OF AL203 AS PERTAINING TO 2/2
THERMIONIC INTEGRATED CIRCUITS(C) NAVAL POSTGRADUATE
SCHOOL MONTEREY CA P J PETERSON DEC 85

UNCLASSIFIED

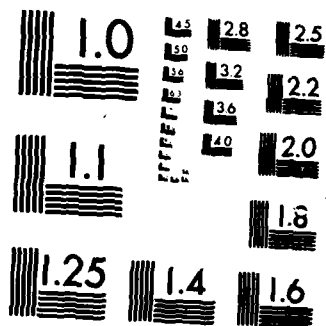
F/G 9/5

NL

END

FRAMED

STIC



MICROCOPY RESOLUTION TEST CHART
NATIONAL BUREAU OF STANDARDS 1963-A

PROGRAM ITS - DECEMBER 16, 1964

VERSION 1.0

CYLTRAN

NUMBER OF MATERIALS

GAMMA RAY CROSS SECTION DATA FOR MATERIAL NUMBER 1

OMP/PAIR	NTAB	NTAB	MAX	25	2	47	3
ENERGIES (MEV)				1000.00000	800.00000	600.00000	500.00000
1000.00000	800.00000	600.00000	500.00000	400.00000	300.00000	200.00000	100.00000
200.00000	150.00000	100.00000	80.00000	60.00000	50.00000	40.00000	30.00000
40.00000	30.00000	20.00000	15.00000	10.00000	8.00000	6.00000	5.00000
8.00000	5.00000	4.00000	3.00000	2.00000	1.50000	1.00000	1.00000
1.00000	0.80000	0.60000	0.50000	0.40000	0.30000	0.20000	0.10000
0.20000	0.15000	0.10000	0.08000	0.06000	0.04000	0.02000	0.01000
0.04000	0.03000	0.02000	0.015000	0.01000	0.005000	0.002000	0.001000
0.001500	0.001000	0.000500	0.000200	0.000100	0.000050	0.000020	0.000010
0.000050	0.000030	0.000020	0.000010	0.000005	0.000003	0.000002	0.000001
0.02859	0.02896	0.02930	0.02963	0.02996	0.03029	0.03063	0.03096
0.02322	0.02350	0.02376	0.02412	0.02438	0.02463	0.02488	0.02513
0.01964	0.01982	0.01994	0.01994	0.01998	0.02003	0.02013	0.02013
0.02638	0.02645	0.02650	0.02650	0.02650	0.02650	0.02650	0.02654
0.002385	0.002384	0.002384	0.002384	0.002385	0.002385	0.002385	0.002385
0.12130	0.13200	0.13287	0.13292	0.13297	0.13301	0.13305	0.13309
0.389203	0.710205	0.710205	0.710205	0.710205	0.710205	0.710205	0.710205
72.111572	232.956118	521.813988	521.813988	521.813988	521.813988	521.813988	521.813988
839.180485	934.813988	2713.430684	2713.430684	2713.430684	2713.430684	2713.430684	2713.430684
ORATIO OF SCATTERING PLUS PAIR PRODUCTION TO TOTAL ATTEN. COEFFICIENTS							
1.000000	1.000000	1.000000	1.000000	1.000000	1.000000	1.000000	1.000000
0.999999	0.999998	0.999998	0.999997	0.999997	0.999997	0.999995	0.999999
0.999999	0.999999	0.999999	0.999998	0.999998	0.999998	0.999997	0.999994
0.999998	0.999998	0.999998	0.999997	0.999997	0.999997	0.999996	0.999993
0.999997	0.999997	0.999997	0.999996	0.999996	0.999996	0.999995	0.999992
0.999996	0.999996	0.999996	0.999995	0.999995	0.999995	0.999994	0.999989
0.999995	0.999995	0.999995	0.999994	0.999994	0.999994	0.999993	0.999988
0.999994	0.999994	0.999994	0.999993	0.999993	0.999993	0.999992	0.999986
0.999993	0.999993	0.999993	0.999992	0.999992	0.999992	0.999991	0.999985
0.999992	0.999992	0.999992	0.999991	0.999991	0.999991	0.999990	0.999984
0.999991	0.999991	0.999991	0.999990	0.999990	0.999990	0.999989	0.999982
0.999990	0.999990	0.999990	0.999989	0.999989	0.999989	0.999988	0.999981
0.999989	0.999989	0.999989	0.999988	0.999988	0.999988	0.999987	0.999979
0.999988	0.999988	0.999988	0.999987	0.999987	0.999987	0.999986	0.999978
0.999987	0.999987	0.999987	0.999986	0.999986	0.999986	0.999985	0.999977
0.999986	0.999986	0.999986	0.999985	0.999985	0.999985	0.999984	0.999976
0.999985	0.999985	0.999985	0.999984	0.999984	0.999984	0.999983	0.999975
0.999984	0.999984	0.999984	0.999983	0.999983	0.999983	0.999982	0.999974
0.999983	0.999983	0.999983	0.999982	0.999982	0.999982	0.999981	0.999973
0.999982	0.999982	0.999982	0.999981	0.999981	0.999981	0.999980	0.999972
0.999981	0.999981	0.999981	0.999980	0.999980	0.999980	0.999979	0.999971
0.999980	0.999980	0.999980	0.999979	0.999979	0.999979	0.999978	0.999969
0.999979	0.999979	0.999979	0.999978	0.999978	0.999978	0.999977	0.999968
0.999978	0.999978	0.999978	0.999977	0.999977	0.999977	0.999976	0.999967
0.999977	0.999977	0.999977	0.999976	0.999976	0.999976	0.999975	0.999966
0.999976	0.999976	0.999976	0.999975	0.999975	0.999975	0.999974	0.999965
0.999975	0.999975	0.999975	0.999974	0.999974	0.999974	0.999973	0.999964
0.999974	0.999974	0.999974	0.999973	0.999973	0.999973	0.999972	0.999963
0.999973	0.999973	0.999973	0.999972	0.999972	0.999972	0.999971	0.999962
0.999972	0.999972	0.999972	0.999971	0.999971	0.999971	0.999970	0.999961
0.999971	0.999971	0.999971	0.999970	0.999970	0.999970	0.999969	0.999960
0.999970	0.999970	0.999970	0.999969	0.999969	0.999969	0.999968	0.999959
0.999969	0.999969	0.999969	0.999968	0.999968	0.999968	0.999967	0.999958
0.999968	0.999968	0.999968	0.999967	0.999967	0.999967	0.999966	0.999957
0.999967	0.999967	0.999967	0.999966	0.999966	0.999966	0.999965	0.999956
0.999966	0.999966	0.999966	0.999965	0.999965	0.999965	0.999964	0.999955
0.999965	0.999965	0.999965	0.999964	0.999964	0.999964	0.999963	0.999954
0.999964	0.999964	0.999964	0.999963	0.999963	0.999963	0.999962	0.999953
0.999963	0.999963	0.999963	0.999962	0.999962	0.999962	0.999961	0.999952
0.999962	0.999962	0.999962	0.999961	0.999961	0.999961	0.999960	0.999951
0.999961	0.999961	0.999961	0.999960	0.999960	0.999960	0.999959	0.999950
0.999960	0.999960	0.999960	0.999959	0.999959	0.999959	0.999958	0.999949
0.999959	0.999959	0.999959	0.999958	0.999958	0.999958	0.999957	0.999948
0.999958	0.999958	0.999958	0.999957	0.999957	0.999957	0.999956	0.999947
0.999957	0.999957	0.999957	0.999956	0.999956	0.999956	0.999955	0.999946
0.999956	0.999956	0.999956	0.999955	0.999955	0.999955	0.999954	0.999945
0.999955	0.999955	0.999955	0.999954	0.999954	0.999954	0.999953	0.999944
0.999954	0.999954	0.999954	0.999953	0.999953	0.999953	0.999952	0.999943
0.999953	0.999953	0.999953	0.999952	0.999952	0.999952	0.999951	0.999942
0.999952	0.999952	0.999952	0.999951	0.999951	0.999951	0.999950	0.999941
0.999951	0.999951	0.999951	0.999950	0.999950	0.999950	0.999949	0.999940
0.999950	0.999950	0.999950	0.999949	0.999949	0.999949	0.999948	0.999939
0.999949	0.999949	0.999949	0.999948	0.999948	0.999948	0.999947	0.999938
0.999948	0.999948	0.999948	0.999947	0.999947	0.999947	0.999946	0.999937
0.999947	0.999947	0.999947	0.999946	0.999946	0.999946	0.999945	0.999936
0.999946	0.999946	0.999946	0.999945	0.999945	0.999945	0.999944	0.999935
0.999945	0.999945	0.999945	0.999944	0.999944	0.999944	0.999943	0.999934
0.999944	0.999944	0.999944	0.999943	0.999943	0.999943	0.999942	0.999933
0.999943	0.999943	0.999943	0.999942	0.999942	0.999942	0.999941	0.999932
0.999942	0.999942	0.999942	0.999941	0.999941	0.999941	0.999940	0.999931
0.999941	0.999941	0.999941	0.999940	0.999940	0.999940	0.999939	0.999930
0.999940	0.999940	0.999940	0.999939	0.999939	0.999939	0.999938	0.999929
0.999939	0.999939	0.999939	0.999938	0.999938	0.999938	0.999937	0.999928
0.999938	0.999938	0.999938	0.999937	0.999937	0.999937	0.999936	0.999927
0.999937	0.999937	0.999937	0.999936	0.999936	0.999936	0.999935	0.999926
0.999936	0.999936	0.999936	0.999935	0.999935	0.999935	0.999934	0.999925
0.999935	0.999935	0.999935	0.999934	0.999934	0.999934	0.999933	0.999924
0.999934	0.999934	0.999934	0.999933	0.999933	0.999933	0.999932	0.999923
0.999933	0.999933	0.999933	0.999932	0.999932	0.999932	0.999931	0.999922
0.999932	0.999932	0.999932	0.999931	0.999931	0.999931	0.999930	0.999921
0.999931	0.999931	0.999931	0.999930	0.999930	0.999930	0.999929	0.999920
0.999930	0.999930	0.999930	0.999929	0.999929	0.999929	0.999928	0.999919
0.999929	0.999929	0.999929	0.999928	0.999928	0.999928	0.999927	0.999918
0.999928	0.999928	0.999928	0.999927	0.999927	0.999927	0.999926	0.999917
0.999927	0.999927	0.999927	0.999926	0.999926	0.999926	0.999925	0.999916
0.999926	0.999926	0.999926	0.999925	0.999925	0.999925	0.999924	0.999915
0.999925	0.999925	0.999925	0.999924	0.999924	0.999924	0.999923	0.999914
0.999924	0.999924	0.999924	0.999923	0.999923	0.999923	0.999922	0.999913
0.999923	0.999923	0.999923	0.999922	0.999922	0.999922	0.999921	0.999912
0.999922	0.999922	0.999922	0.999921	0.999921	0.999921	0.999920	0.999911
0.999921	0.999921	0.999921	0.999920	0.999920			

ELECTRON CROSS SECTION DATA FROM PROGRAM DAIPAC

NUMBER OF SETS ON DATAPAC TAPE = 1
100.0 MEV CROSS SECTIONS SAPPHIRE

MATERIAL	DENSITY	DEUTERIUM
1	0.39850e+01	0.73100e+00
2	0.80000e+01	0.15998e+02
3	0.15000e+02	0.26981e+02
4	0.26981e+02	0.59300e+00
NSET	17RM 12IP 1SGN 15UB 1NCAL 1CVC	NCYC NMAX
1	5	1 40
2	0	1 84
3	5	33 40
4	0	121 3.39242e+01

O COLLISION / TOTAL D/FX RATIOS FOR DATAPAC SET 1

O CUMULATIVE BREMSTRAHLUNG CROSS SECTIONS FOR DATAPAC SET 1

O CUMULATIVE BREMSTRAHLUNG ANGULAR DISTRIBUTIONS FOR DATAPAC SET 1

O GAUSSIAN - EQUIPROBABLE ENDPOINTS FOR INTERPOLATION

O K-X-RAY PRODUCTION FOR DATAPAC SET 1

O PHOTOELECTRON ANGULAR DISTRIBUTIONS

O PAIR ELECTRON ENERGY DIVISION DISTRIBUTION (LEAD)

O PAIR ENERGY DIVISION DISTRIBUTION (LEAD)

O BEGIN READING INPUT

O TITLE

...100.0 MEV TEST PROGRAM

ELECTRONS

ENERGY 10.0

DEFAULT SOURCE PHASE SPACE PARAMETERS

POSITION 0.0 0.0 0.0

SOURCE-RADIUS 0.95250

WARNING - ILLEGAL COMMAND LINE - INFORMATION IGNORED

>>SOURCE-RADIUS 0.95250

MONODIRECTIONAL 2-AXIS

MONODIRECTIONAL 2-AXIS

MONODIRECTIONAL 2-AXIS

ELECTRON-ESCAPE

HISTORIES 1000000

BATCHES 10

CUTOFFS 0.05 0.001

...OUTPUT OPTIONS

GEOMETRY 1

2L 2R R1 R2 MAT 1ZR NZ NR ECUT PTCZ

O 0.0002810.0 0.95250 1 1 1 0.0 0.5

O EOF ON UNIT 9 BEGIN PROCESSING - INPUT

O COMPARISON OF STORAGE REQUIREMENTS VS ALLOCATIONS

O NUMBER OF MATERIALS ON CROSS SECTION FILE

O LENGTH OF ELECTRON CROSS SECTION ENERGY GRID

O ELECTRON ENERGY GRID LENGTH FOR SAMPLING BRENS, PHOTON ENERGY

O PHOTON ENERGY GRID LENGTH FOR SAMPLING BRENS, PHOTON ENERGY

O ELECTRON ANGLE GRID LENGTH FOR SAMPLING BRENS, PHOTON SCATTERING ANGLE

O PHOTON ANGLE GRID LENGTH FOR SAMPLING BRENS, PHOTON ANGLE

INMAT	1	1	5
INMAX	-	64	64
INTOP	-	65	65
INTOP	-	49	49
INMAX	-	23	23
INPANG	-	21	21

PHOTON ENERGY GRID LENGTH FOR SAMPLING BRENS. PHOTON ANGLE
 ELECTRON ENERGY GRID LENGTH FOR SAMPLING BRENS. PHOTON ANGLE
 PHOTON ENERGY GRID LENGTH FOR SAMPLING PHOTO-ELECTRON DIRECTION
 ELECTRON ANGLE GRID LENGTH FOR SAMPLING PHOTO-ELECTRON DIRECTION
 PHOTON ENERGY GRID LENGTH FOR SAMPLING PAIR ELECTRON ENERGY
 ELECTRON ENERGY GRID LENGTH FOR SAMPLING PAIR ELECTRON ENERGY
 GAUSSIAN FUNCTION GRID OR SAMPLING ELECTRON ENERGY LOSS STRAGGLING
 MAXIMUM LENGTH OF TABLES OF PHOTON CROSS SECTIONS
 NUMBER OF PHOTON CROSS SECTION TABLE
 NUMBER OF ELECTRON ESCAPE ENERGY BINS
 NUMBER OF PHOTON ESCAPE POLAR ANGLE BINS
 NUMBER OF PHOTON ESCAPE AZIMUTHAL ANGLE BINS
 LENGTH OF SOURCE SPECTRUM ENERGY GRID
 NUMBER OF PULSE INTEGRAL ENERGY BINS
 NUMBER OF ELECTRON FLUX ENERGY BINS
 NUMBER OF PHOTON FLUX ENERGY BINS
 NUMBER OF ELECTRON FLUX ZONES
 NUMBER OF PHOTON FLUX ZONES
 NUMBER OF PHOTON ZONES
 SIZE OF DOUBLY DIFFERENTIAL BRENS DISTRIBUTION
 SIZE OF SIMPLY DIFFERENTIAL BRENS DISTRIBUTION
 SIZE OF GOODSBUILT-SAUNDERSON ANGULAR DISTRIBUTION
 NO. OF ELECTRON ESCAPE AZIMUTHAL ANGLE BINS
 NO. OF PHOTON ESCAPE AZIMUTHAL ANGLE BINS
 NO. OF PHOTON ZONES
 GLOBAL ELECTRON CUTOFF ENERGY BELOW ELECTRON ENERGY LIST. CUTOFF ENERGY HAS BEEN CHANGED TO 0.408302e+00

* GEOMETRY DEPENDENT INPUT *
 * * * * *
 NUMBER OF INPUT ZONES 1
 0 LEFT PLANE (CM) RIGHT PLANE (CM) INNER RADIUS (CM) OUTER RADIUS (CM) ELECTRON CUTOFF (MEV) PHOTON FORCING FRACTION
 1 0.0000e+00 2.9700e-03 0.0000e+00 9.52800e-01 4.083e-01 5.000e-01

* SOURCE INFORMATION *
 * * * * *

SOURCE ELECTRONS
 THE MAXIMUM SOURCE ENERGY IS 100.0000 MEV
 THE GLOBAL ELECTRON CUTOFF ENERGY IS 0.40830 MEV
 THE PHOTON CUTOFF ENERGY IS 0.00100 MEV
 COORDINATES OF THE POINT SOURCE OR THE CENTER OF THE BEAM (DISK) SOURCE ARE
 A = 0.0000e+00 CM V = 0.0000e+00 CM Z = 0.0000e+00 CM

ONE RADIUS OF THE BEAM (DISK) SOURCE IS 0.00000 CM
 DIFFERENCE DIRECTION FOR ANGULAR DISTRIBUTION IS DEFINED BY
 THETA = 0.000 DEGREES PHI = 0.000 DEGREES
 ORTHODIRECTIONAL SOURCE IN REFERENCE DIRECTION
 ONE STANDARD ERROR ESTIMATES ARE BASED ON 10 BATCHES OF 10000 HISTORIES EACH

* OUTPUT OPTIONS *
 * * * * *
 ELECTRON-ESCAPE ENERGY CLASSIFICATIONS (MEV)
 90.0000 70.0000 60.0000 50.0000 40.0000
 80.0000 60.0000 50.0000 40.0000
 70.0000 50.0000 40.0000
 60.0000 40.0000
 ELECTRON-ESCAPE PH ANGLE CLASSIFICATIONS (DEGREES)
 18.00000 36.00000 54.00000 72.00000 90.00000 108.00000
 126.00000 144.00000 162.00000 180.00000
 ELECTRON-ESCAPE AZIMUTH ANGLE CLASSIFICATIONS (DEGREES)
 180.00000
 OPHELON-ESCAPE ENERGY CLASSIFICATIONS (MEV)
 90.00000 70.00000 60.00000 50.00000 40.00000
 80.00000 60.00000 50.00000
 70.00000 50.00000
 60.00000 40.00000
 OPHELON-ESCAPE POLAR ANGLE CLASSIFICATIONS (DEGREES)

18.0000 38.0000 54.0000 72.0000 90.0000 108.0000
 128.0000 144.0000 162.0000 180.0000 198.0000
 OPHTON-ESCAPE AZIMUTH ANGLE CLASSIFICATIONS (DEGREES)
 180.0000
 SELECTRON FLUX ENERGY CLASSIFICATIONS (MEV)
 90.0000 80.0000 70.0000 60.0000 50.0000 40.0000
 30.0000 20.0000 10.0000 0 40.830
 OPHTON-FLUX ENERGY CLASSIFICATIONS (MEV)
 90.0000 80.0000 70.0000 60.0000 50.0000 40.0000
 30.0000 20.0000 10.0000 0 0.0100

1

2

3

4

5

6

7

8

9

0

1

2

3

4

5

6

7

8

9

0

PHYSICAL OPTIONS
 ELECTRON COLLISION AND RADIATION ENERGY LOSS STRAGGLING
 ORNICH-ON ELECTION PRODUCTION
 AND COUPLED INELASTIC SCATTERING DEFLECTIONS
 OBRENS STRAGGLING AND CHARACTERISTIC X-RAY QUANTA FOLLOWED
 OBRENS STRAGGLING INTRINSIC ANGLE OF EMISSION FROM TABULATED DISTRIBUTION
 OPHTON-PRODUCED ELECTRONS FOLLOWED
 MATERIAL NO.
 O ELECTRON RANGE AT MAXIMUM SOURCE ENERGY IS 0.33924e+02 (G/CM⁻²)

1

2

3

4

5

6

7

8

9

0

1

2

3

4

5

6

7

8

9

0

1

2

3

4

5

6

7

8

9

0

1

2

3

4

5

6

7

8

9

0

1

2

3

4

5

6

7

8

9

0

1

2

3

4

5

6

7

8

9

0

1

2

3

4

5

6

7

8

9

0

1

2

3

4

5

6

7

8

9

0

1

2

3

4

5

6

7

8

9

0

1

2

3

4

5

6

7

8

9

0

1

2

3

4

5

6

7

8

9

0

1

2

3

4

5

6

7

8

9

0

1

2

3

4

5

6

7

8

9

0

1

2

3

4

5

6

7

8

9

0

1

2

3

4

5

6

7

8

9

0

1

2

3

4

5

6

7

8

9

0

1

2

3

4

5

6

7

8

9

0

1

2

3

4

5

6

7

8

9

0

1

2

3

4

5

6

7

8

9

0

1

2

3

4

5

6

7

8

9

0

1

2

3

4

5

6

7

8

9

0

1

2

3

4

5

6

7

8

9

0

1

2

3

4

5

6

7

8

9

0

1

2

3

4

5

6

7

8

9

0

1

2

3

4

5

6

7

8

9

0

1

2

3

4

5

6

7

8

9

0

1

2

3

4

5

6

7

8

9

0

1

2

3

4

<p

NUMBER AND ENERGY ESCAPE FRACTIONS
 TRANSMISSION

	ELECTRON ENERGY	COUNTS	NUMBER	PHOTON ENERGY	COUNTS
1.00e+00	0 1.00e+00 0	1003713	3.52e-03	1 3.83e-04 4	7151

NUMBER AND ENERGY REFLECTION

	ELECTRON ENERGY	COUNTS	NUMBER	PIOND ENERGY	COUNTS
7.00e-08	30 3.39e-08 30	10 3.64e 05	1.21e-09	9 2905	

NUMBER AND ENERGY LATERAL ESCAPE

	ELECTRON ENERGY	COUNTS	NUMBER	PIOND ENERGY	COUNTS
0.00e+00 99 0.00e+00 99	0 5.25e-10 85 2.08e-12 88	7			

(NORMALIZED TO ONE INCIDENT PARTICLE)

ENERGY DEPOSITION

	MATERIAL	MASS(GM)	VOLUME(CC)	PRIM	KNOCK	ENERGY DEPOSITION (MEV)	TOTAL
1	1	3.3544e-02	8.4652e-03	1.9749e-02	0 -4.1869e-03	4 -4.0052e-06	4 1.5559e-01

THE ENERGY CONSERVATION FRACTION IS 15

CHARGE DEPOSITION

	MATERIAL	MASS(GM)	VOLUME(CC)	PRIM	KNOCK	ENERGY DEPOSITION (MEV)	TOTAL
1	1	0.1000043575675e+01	0	1.9749e-02	0 -4.1869e-03	4 -4.0052e-06	4 1.5559e-01

(NORMALIZED TO ONE INCIDENT PARTICLE)

ELECTRONS

	ZONE	MATERIAL	ZL	R1	RO	PRIM	KNOCK	G-SEC	TOTAL
1	1	0.000e+00 2.970e-03	0.000e+00 9.525e-01	0.000e+00 9.525e-01	0.000e+00 9.525e-01	2 -4.4030e-03	2 -4.4030e-03	2.6 5528e-03	1

TOTAL

	ZONE	MATERIAL	ZL	R1	RO	PRIM	KNOCK	G-SEC	TOTAL
1	1	0.000e+00 2.970e-03	0.000e+00 9.525e-01	0.000e+00 9.525e-01	0.000e+00 9.525e-01	2 -4.4030e-03	2 -4.4030e-03	2.6 5528e-03	1

IFLUX CALCULATION - ELECTRONS LEFT AT FLUX CUTOFF ENERGY (AMPERE, NORMALIZED TO ONE INCIDENT PARTICLE)

	1.21e-04	9
1	1	1

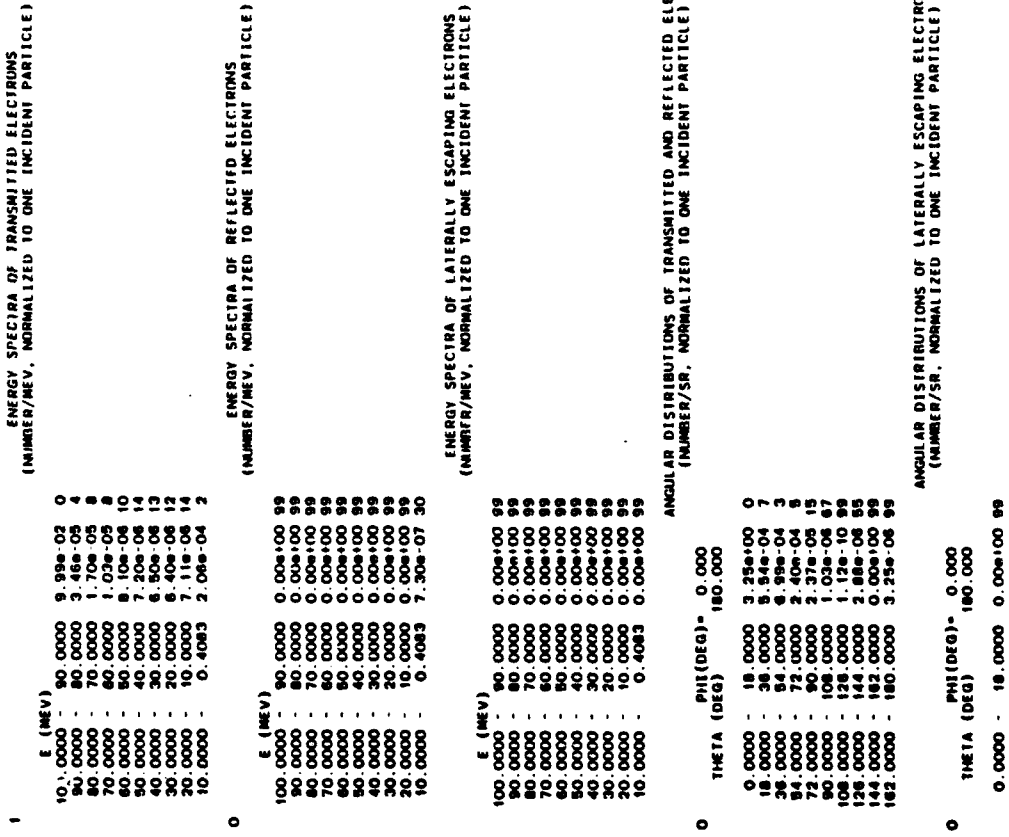
ELECTRON FLUX DISTRIBUTION

(TRACK-LENGTH)/VOLUME-MEV. NORMALIZED TO ONE INCIDENT PARTICLE)

PHOTON FLUX DISTRIBUTION

(TRACK-LENGTH)/VOLUME-MEV. NORMALIZED TO ONE INCIDENT PARTICLE)

	0.00000	1
1	1	1



18.0000	-	38.0000	0.00e+00	99
36.0000	-	54.0000	0.00e+00	99
54.0000	-	72.0000	0.00e+00	99
72.0000	-	90.0000	0.00e+00	99
90.0000	-	108.0000	0.00e+00	99
108.0000	-	126.0000	0.00e+00	99
126.0000	-	144.0000	0.00e+00	99
144.0000	-	162.0000	0.00e+00	99
162.0000	-	180.0000	0.00e+00	99

ENERGY SPECTRA AND ANGULAR DISTRIBUTIONS OF ELECTRONS TRANSMITTED AND REFLECTED

0		0		0	
E (MEV)	THETA	E (MEV)	THETA	E (MEV)	THETA
18.0000	-	38.0000	0.00e+00	99	
36.0000	-	54.0000	0.00e+00	99	
54.0000	-	72.0000	0.00e+00	99	
72.0000	-	90.0000	0.00e+00	99	
90.0000	-	108.0000	0.00e+00	99	
108.0000	-	126.0000	0.00e+00	99	
126.0000	-	144.0000	0.00e+00	99	
144.0000	-	162.0000	0.00e+00	99	
162.0000	-	180.0000	0.00e+00	99	

AZIMUTHAL INTERVAL IS 0.00000 TO 180.00000 DEGREES
(NUMBER/MEV-SR), NORMALIZED TO ONE PARTICLE)

ENERGY SPECTRA AND ANGULAR DISTRIBUTIONS OF ELECTRONS TRANSMITTED AND REFLECTED

0		0		0	
E (MEV)	THETA	E (MEV)	THETA	E (MEV)	THETA
18.0000	-	36.0000	0.00e+00	99	
36.0000	-	54.0000	0.00e+00	99	
54.0000	-	72.0000	0.00e+00	99	
72.0000	-	90.0000	0.00e+00	99	
90.0000	-	108.0000	0.00e+00	99	
108.0000	-	126.0000	0.00e+00	99	
126.0000	-	144.0000	0.00e+00	99	
144.0000	-	162.0000	0.00e+00	99	
162.0000	-	180.0000	0.00e+00	99	

AZIMUTHAL INTERVAL IS 0.00000 TO 180.00000 DEGREES
(NUMBER/MEV-SR), NORMALIZED TO ONE PARTICLE)

ENERGY SPECTRA AND ANGULAR DISTRIBUTIONS OF ELECTRONS LATERALLY ESCAPING

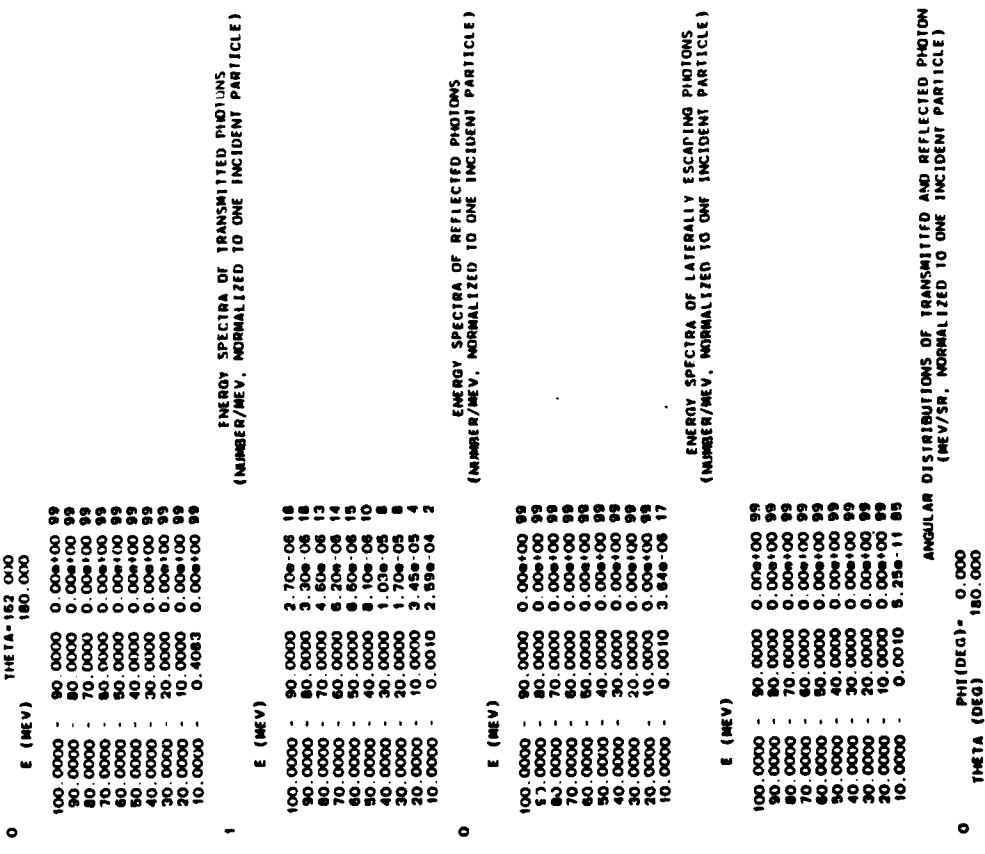
0		0		0	
E (MEV)	THETA	E (MEV)	THETA	E (MEV)	THETA
18.0000	-	36.0000	0.00e+00	99	
36.0000	-	54.0000	0.00e+00	99	
54.0000	-	72.0000	0.00e+00	99	
72.0000	-	90.0000	0.00e+00	99	
90.0000	-	108.0000	0.00e+00	99	
108.0000	-	126.0000	0.00e+00	99	
126.0000	-	144.0000	0.00e+00	99	
144.0000	-	162.0000	0.00e+00	99	
162.0000	-	180.0000	0.00e+00	99	

AZIMUTHAL INTERVAL IS 0.00000 TO 180.00000 DEGREES
(NUMBER/MEV-SR), NORMALIZED TO ONE PARTICLE)

ENERGY SPECTRA AND ANGULAR DISTRIBUTIONS OF ELECTRONS LATERALLY ESCAPING

0		0		0	
E (MEV)	THETA	E (MEV)	THETA	E (MEV)	THETA
18.0000	-	36.0000	0.00e+00	99	
36.0000	-	54.0000	0.00e+00	99	
54.0000	-	72.0000	0.00e+00	99	
72.0000	-	90.0000	0.00e+00	99	
90.0000	-	108.0000	0.00e+00	99	
108.0000	-	126.0000	0.00e+00	99	
126.0000	-	144.0000	0.00e+00	99	
144.0000	-	162.0000	0.00e+00	99	
162.0000	-	180.0000	0.00e+00	99	

AZIMUTHAL INTERVAL IS 0.00000 TO 180.00000 DEGREES
(NUMBER/MEV-SR), NORMALIZED TO ONE PARTICLE)



0.0000	-18.0000	1.24e-01	4
18.0000	-38.0000	3.84e-07	48
36.0000	-54.0000	6.31e-08	5
54.0000	-72.0000	3.75e-08	9
72.0000	-90.0000	1.97e-08	8
90.0000	-108.0000	1.44e-08	16
108.0000	-126.0000	1.90e-08	12
126.0000	-144.0000	2.07e-08	19
144.0000	-162.0000	2.80e-08	14
162.0000	-180.0000	1.91e-08	39

ANGULAR DISTRIBUTIONS OF LATERALLY ESCAPING PHOTON INTENSITY
(MEV/SR. NORMALIZED TO ONE INCIDENT PARTICLE)

0 PHI (DEG) = 0.000
 THETA (DEG) = 180.000

0	0.0000	18.0000	0.00e+00	99
18.0000	-38.0000	0.00e+00	99	
36.0000	-54.0000	0.00e+00	99	
54.0000	-72.0000	0.00e+00	99	
72.0000	-90.0000	0.00e+00	99	
90.0000	-108.0000	7.16e-17	63	
108.0000	-126.0000	1.07e-10	84	
126.0000	-144.0000	0.00e+00	99	
144.0000	-162.0000	0.00e+00	99	
162.0000	-180.0000	0.00e+00	99	

ENERGY SPECTRA AND ANGULAR DISTRIBUTIONS OF PHOTONS TRANSMITTED AND REFLECTED
AZIMUTHAL INTERVAL IS 0.0000 TO 10.0000 DEGREES
(NUMBER/(MEV*SR). NORMALIZED TO ONE PARTICLE)

E (MEV)	THETA	0.0000	18.0000	36.0000	54.0000	72.0000	90.0000	108.0000	126.0000	144.0000	162.0000
100.0000	90.0000	8.78e-06	18.0.00e+00	99.0.00e+00	99.0.00e+00	99.0.00e+00	99.0.00e+00	99.0.00e+00	99.0.00e+00	99.0.00e+00	99.0.00e+00
80.0000	90.0000	1.07e-05	19.0.00e+00	99.0.00e+00	99.0.00e+00	99.0.00e+00	99.0.00e+00	99.0.00e+00	99.0.00e+00	99.0.00e+00	99.0.00e+00
60.0000	70.0000	1.50e-05	13.0.00e+00	99.0.00e+00	99.0.00e+00	99.0.00e+00	99.0.00e+00	99.0.00e+00	99.0.00e+00	99.0.00e+00	99.0.00e+00
40.0000	60.0000	2.02e-05	10.0.00e+00	99.0.00e+00	99.0.00e+00	99.0.00e+00	99.0.00e+00	99.0.00e+00	99.0.00e+00	99.0.00e+00	99.0.00e+00
20.0000	40.0000	2.15e-05	15.0.00e+00	99.0.00e+00	99.0.00e+00	99.0.00e+00	99.0.00e+00	99.0.00e+00	99.0.00e+00	99.0.00e+00	99.0.00e+00
10.0000	0.0010	0.29e-04	2.97e-07	23.9.1e-07	19.7.8e-07	16.1.9e-07	10.1.9e-07	34.1.61e-07	40.5.27e-07	27.7.94e-07	23.1.24e-07
0	INTEGRAL (/SR)	1.13e-02	1.8.71e-06	1.9.14e-06	1.9.7.8e-06	1.9.1.9e-06	1.9.1.61e-06	34.1.61e-06	40.5.27e-06	27.7.94e-06	23.1.24e-06

ENERGY SPECTRA AND ANGULAR DISTRIBUTIONS OF PHOTONS TRANSMITTED AND REFLECTED
AZIMUTHAL INTERVAL IS 0.0000 TO 10.0000 DEGREES
(NUMBER/(MEV*SR). NORMALIZED TO ONE PARTICLE)

E (MEV)	THETA	0.0000	180.000	360.000	540.000	720.000	900.000	1080.000	1260.000	1440.000	1620.000
100.0000	90.0000	9.0.00e+00	99.0.00e+00	99.0.00e+00	99.0.00e+00	99.0.00e+00	99.0.00e+00	99.0.00e+00	99.0.00e+00	99.0.00e+00	99.0.00e+00
80.0000	90.0000	1.07e-05	19.0.00e+00	99.0.00e+00	99.0.00e+00	99.0.00e+00	99.0.00e+00	99.0.00e+00	99.0.00e+00	99.0.00e+00	99.0.00e+00
60.0000	70.0000	1.50e-05	13.0.00e+00	99.0.00e+00	99.0.00e+00	99.0.00e+00	99.0.00e+00	99.0.00e+00	99.0.00e+00	99.0.00e+00	99.0.00e+00
40.0000	60.0000	2.02e-05	10.0.00e+00	99.0.00e+00	99.0.00e+00	99.0.00e+00	99.0.00e+00	99.0.00e+00	99.0.00e+00	99.0.00e+00	99.0.00e+00
20.0000	40.0000	2.15e-05	15.0.00e+00	99.0.00e+00	99.0.00e+00	99.0.00e+00	99.0.00e+00	99.0.00e+00	99.0.00e+00	99.0.00e+00	99.0.00e+00
10.0000	0.0010	0.29e-04	2.97e-07	23.9.1e-07	19.7.8e-07	16.1.9e-07	10.1.9e-07	34.1.61e-07	40.5.27e-07	27.7.94e-07	23.1.24e-07
0	INTEGRAL (/SR)	1.13e-02	1.8.71e-06	1.9.14e-06	1.9.7.8e-06	1.9.1.9e-06	1.9.1.61e-06	34.1.61e-06	40.5.27e-06	27.7.94e-06	23.1.24e-06

E (MEV)	THETA	0.0000	180.000	360.000	540.000	720.000	900.000	1080.000	1260.000	1440.000	1620.000
100.0000	90.0000	9.0.00e+00	99.0.00e+00	99.0.00e+00	99.0.00e+00	99.0.00e+00	99.0.00e+00	99.0.00e+00	99.0.00e+00	99.0.00e+00	99.0.00e+00
80.0000	90.0000	1.07e-05	19.0.00e+00	99.0.00e+00	99.0.00e+00	99.0.00e+00	99.0.00e+00	99.0.00e+00	99.0.00e+00	99.0.00e+00	99.0.00e+00
60.0000	70.0000	1.50e-05	13.0.00e+00	99.0.00e+00	99.0.00e+00	99.0.00e+00	99.0.00e+00	99.0.00e+00	99.0.00e+00	99.0.00e+00	99.0.00e+00
40.0000	60.0000	2.02e-05	10.0.00e+00	99.0.00e+00	99.0.00e+00	99.0.00e+00	99.0.00e+00	99.0.00e+00	99.0.00e+00	99.0.00e+00	99.0.00e+00
20.0000	40.0000	2.15e-05	15.0.00e+00	99.0.00e+00	99.0.00e+00	99.0.00e+00	99.0.00e+00	99.0.00e+00	99.0.00e+00	99.0.00e+00	99.0.00e+00
10.0000	0.0010	0.29e-04	2.97e-07	23.9.1e-07	19.7.8e-07	16.1.9e-07	10.1.9e-07	34.1.61e-07	40.5.27e-07	27.7.94e-07	23.1.24e-07
0	INTEGRAL (/SR)	1.13e-02	1.8.71e-06	1.9.14e-06	1.9.7.8e-06	1.9.1.9e-06	1.9.1.61e-06	34.1.61e-06	40.5.27e-06	27.7.94e-06	23.1.24e-06

E (MEV)		THETA = 162.000		(NUMBER / IMEV.SR). NORMALIZED TO ONE PARTICLE)	
	0	180	000	180	000
100.0000	-	90.0000	0.000000	99	
90.0000	-	80.0000	0.000000	99	
80.0000	-	70.0000	0.000000	99	
70.0000	-	60.0000	0.000000	99	
60.0000	-	50.0000	0.000000	99	
50.0000	-	40.0000	0.000000	99	
40.0000	-	30.0000	0.000000	99	
30.0000	-	20.0000	0.000000	99	
20.0000	-	10.0000	0.000000	99	
10.0000	-	0.000000	0.000000	99	
INTEGRAL (SR)		0.000000		99	

TRUE NUMBER OF DATA FOR WHICH STATISTICAL ESTIMATES HAVE BEEN PROVIDED IS 585

LIST OF REFERENCES

1. Lynn, D. and McCormick, L., et al., "Progress in Radiation Immune Thermionic Integrated Circuits", LA-UR-84-527.
2. Levy, P. W., "Color Centers and Radiation-Induced Defects in Al_2O_3 ", Phys. Rev. V.123, No.4 pp. 1226-1233, 15 August 1961.
3. Muller, R.S. and Kamins, T. I., Device Electronics for Integrated Circuits, pp.152-164, John Wiley and Sons, 1977.
4. Seitz, F., Discussions of the Faraday Society, V.5 p.271, 1949.
5. Arnold, G. W., and Compton, W. D., "Threshold Energy for Lattice Displacement in $\alpha\text{-Al}_2\text{O}_3$ ", Phys. Rev. Lett. V.4, No.2, 15 January 1960.
6. Enge, H. A., Introduction to Nuclear Physics, p.185, Addison-Wesley, 1966.
7. Berger, M. A., and Seltzer, S. M., "Stopping Powers and Ranges of Electrons and Positrons", NBSIR 82-2550 1982.
8. Chaffin R. J., Microwave Semiconductor Devices: Fundamentals and Radiation Effects, John Wiley and Sons, 1957.
9. Dienes, G. J., and Vinyard, G. H., Radiation Effects in Solids, Interscience Publishers, 1957.
10. Rudie, N. J., Principals and Techniques of Radiation Hardening, 2d ed., V.1, pp. 2-1,2-42, Western Periodicals, 1980.
11. Askeland, D. R., The Science and Engineering of Materials, p. 586, Brooks/Cole Engineering Division, 1984.
12. Rothwarf A., "Plasmon Theory of Electron-Hole Pair Production: Efficiency of Cathode Ray Phosphors", J. Appl. Phys. V.44, No.2, pp. 752-760, February 1973.

13. van Lint, V. A. J., Harrity, J. W. and Flanagan, T. M., "Scaling Laws for Ionization Effects in Insulators", IEEE Trans. Nucl. Sci., NS. 15, pp. 194-204, 1968.
14. Berard, R. W., and Traverso, T. J., Neutron Form Factors from Elastic Electron-Deuteron Scattering Ratio Experiments at Very Low Momentum Transfers, Masters thesis, Naval Postgraduate School, Monterey California, June 1973.
15. Anderson, R. A., "Mechanism of Fast Surface Flashover in Vacuum", Appl. Phys. Let. V.24, No.2, pp. 54-56, 15 January 1974.
16. Criss, J. D., and Srivastava, K. D., "High Speed Photography of Surface Flashover of Solid Insulators Under Impulse Voltages in Vacuum", Appl. Phys. Let. V. 21, No. 11, pp. 549-551, 1 December 1972.
17. Face, S. H., Ekland, C. A. and Stringer T. A., "Measurements of Radiation Induced Conductivity for Hardened Cable Dielectric Materials at High Fluence", IEEE Trans. Nuc. Sci., NS. 30, No.6, pp. 4450-4456, December 1983.
18. Pomerantz, M. A., Shatas, R. A. and Marshall, J. F., "Electrical Conductivity Induced in MgO Crystals by 1.3-MeV Electron Bombardment", Phys. Rev. V. 99, No. 2, pp. 489-490, 15 July 1955.
19. Arguello, W. R., The Radiation Effects of High Energy Electrons upon Thermionic Integrated Circuits, Masters thesis, Naval Postgraduate School, Monterey California, December 1985.

INITIAL DISTRIBUTION LIST

	No. Copies
1. Defense Technical Information Center Cameron Station Alexandria, Virginia 22304-6145	2
2. Library, Code 0142 Naval Postgraduate School Monterey, California 93943-5100	2
3. Prof. F. R. Buskirk, Code 61Bs Department of Physics Naval Postgraduate School Monterey, California 93943-5100	6
4. Prof. J. R. Neighbours, Code 61Nb Department of Physics Naval Postgraduate School Monterey, California 93943-5100	1
5. Lt. P. J. Peterson 11945 Cottonmill Drive Woodbridge, Virginia 22192	2
6. Mr. H. L. Peterson 4858 N. Swan Road Milwaukee, Wisconsin 53225	1
7. Dr. D. Lynn E-11 Division Los Alamos National Laboratory Los Alamos, New Mexico 87545	1
8. D. Snyder, Code 61 Department of Physics Naval Postgraduate School Monterey, California 93943-5100	1

END

FILMED

4-86

DTIC